Sede Amministrativa: Università degli Studi di Padova

Dipartimento di MEDICINA MOLECOLARE

CORSO DI DOTTORATO DI RICERCA IN: MEDICINA MOLECOLARE

CURRICOLO: MEDICINA RIGENERATIVA

CICLO 32

In vitro modeling of patient-specific susceptibility to neurotropic flavivirus infection by using induced pluripotent stem cells

Coordinatore: Ch.mo Prof. Stefano Piccolo

Supervisore: Ch.mo Prof. Luisa Barzon

Co-Supervisore: Ch.mo Prof.ssa Marta Trevisan

Dottorando : Silvia Riccetti

"There are more things in Heaven and Earth, Horatio,
than are dreamt of in your philosophy."

— William Shakespeare, Hamlet

Contents

ABSTRACT

Background: A characteristic feature of many infections is that only a portion of exposed individuals develop clinical disease. These include mosquito-borne flaviviruses such as West Nile virus (WNV), Zika virus (ZIKV) and Usutu virus (USUV) infections, which generally cause mild illness or asymptomatic infections in humans. Nonetheless, WNV can cause serious neuroinvasive diseases in less than 1% of infected patients, mainly elderly and immunocompromised subjects; ZIKV may cause fetal microcephaly in about 5% of infections acquired during pregnancy and 1 in 10,000 infected adults develop Guillain-Barré syndrome; USUV seems less pathogenic than WNV and most human infections described so far were asymptomatic, with rare cases of encephalitis or meningitis.

Aim of the study: The different infection outcomes or progression to severe disease can be partly explained by host genetic variations, but the genetic traits associated with susceptibly to severe infection remain poorly understood. Aim of this study was to develop a patient-specific *in vitro* platform, based on human induced pluripotent stem cells (hiPSCs), to investigate the mechanisms of variations in human susceptibility to severe flavivirus infection.

Methods: iPSCs were generated from erythroblasts of two blood donors with asymptomatic WNV infection (controls) and from two patients who developed WNV encephalitis but had no co-morbidity or other risk factors (cases). Patient-specific iPSCs were differentiated into neural stem cells (NSCs) and infected with WNV lineage 1 (GU011992), ZIKV Asian lineage (KU853013), and USUV lineage Europe 1 (AY453411) at different MOIs. Time course experiments were performed to evaluate viral replication kinetics in infected NSCs, cell viability and cell death following infection, and expression of genes involved in antiviral innate immunity. Next-generation sequencing of 2,600 genes related to immune system in iPSCs of cases and controls was performed to detects mutations potentially associated with increased susceptibility to neuroinvasive disease.

Results: USUV and WNV replicated more efficiently, yielding 10 and 100-fold higher viral load and inducing 40% and 70% higher cell mortality, respectively, in NSCs derived from cases than in NSCs derived from controls. WNV induced 3-fold higher caspase 3 activity in infected NSC derived from encephalitis patients than in NSCs derived from asymptomatic donors. Several genes involved in the antiviral IFN pathway were significantly upregulated after USUV, ZIKV

and WNV infection (in particular, type 3 IFNs genes), but the general trend indicated an attenuated response in NSCs derived from WNV encephalitis cases, which showed significantly lower mRNA levels of IFN pathway regulators such as *TLR3*, *MAVS* and *IRF7*. Exome sequencing analysis identified heterozygous inactivating mutations in the *PSIP1* and *DDX58* genes of cases, but not in controls, as polymorphism in other genes that could play a role in disease susceptibility.

Conclusions: Patient-specific iPSCs are useful tools to model individual susceptibility to viral infectious diseases and allowed to demonstrate that WNV and USUV and, to a lesser extent, ZIKV, replicated more efficiently and induced more cell death and apoptosis in NSCs derived from patients with WNV encephalitis than in cells derived from blood donors with asymptomatic infection. This increased susceptibility to neurotropic flaviviruses was associated with a significantly attenuated innate antiviral response. Exome sequencing revealed inactivating mutations in genes that represent good candidates for further investigation.

1. INTRODUCTION

1.1 Introduction to arthropod-borne viruses (Arboviruses)

Hematophagous arthropod vectors of viral disease include mosquitoes, biting flies and ticks that transmit to vertebrate hosts arthropod-borne viruses (arboviruses) that belong to different families and orders of RNA viruses such as *Flaviviridae*, *Togaviridae, Bunyaviridales*, *Reoviridae*, and *Rhabdoviridae* (Weaver and Reisen, 2010). Four major viral genera are responsible of the majority arboviral disease: *Flavivirus* (e. g., yellow fever, Japanese encephalitis, West Nile, Zika and dengue viruses), *Alphavirus* (e. g., chikungunya virus and equine encephalitis viruses), *Orthobunyavirus* (e. g., California encephalitis and Toscana encephalitis virus) and *Phlebovirus* (e. g. Rift Valley fever and sandfly fever viruses) (Lequime S et al., 2014). Arboviruses are transmitted in a climate-dependent manner. In tropical areas, viruses circulate throughout the year, while in temperate climates, viruses are transmitted between the vector and vertebrate host species only during the warmer months (Hollidge BS et al., 2010). Vector-borne viruses replicate in the body of the arthropod vector prior to be vertically transmitted from an infected female vector to female or male offspring or transmitted horizontally by venereal means, from a vertically infected male to a female vector, or by oral means from a female vector to a vertebrate host via saliva during blood co-feeding (Go YY et al., 2014). Different vertebrates, including birds, rodents, bats, horses, or human and non-human primates, may serve as amplifying hosts (Hubálek Z et al., 2014).

Arboviruses represent a relevant infectious cause of neurological disease in humans worldwide (Salimi H et al., 2016). Following a subcutaneous bite of the arthropod vector, arboviruses replicate in peripheral tissues, produce viremia and viruses enter the CNS, where they replicate and spread throughout neural and non-neural populations, causing neurological diseases including encephalitis, meningitis, myelitis, encephalomyelitis, neuritis, and myositis (Griffin DE et al., 2004). Several symptoms like fatigue, malaise, fever, headache, rash, vomiting/diarrhea and nausea usually precede the neurologic manifestation and occur within days after arthropod bite, however disease severity varies among individuals. In fact, a virus causing severe neurologic abnormalities or death in one individual may cause little or no disease in another. There is no specific treatment for arbovirus diseases. Effective human vaccines are available for prophylaxis of yellow fever virus (YFV), Japanese encephalitis virus (JEV), and tick-borne encephalitis virus (TBEV).

Human vaccine for dengue virus (DENV) is available but with limited efficacy against all serotypes and safety concerns (Dighe SN et al., 2019). Although several vaccines are in the development stage, no vaccines have been approved for human use so far to prevent West Nile Virus (WNV) infection, a relevant cause of encephalitis and death in many countries worldwide (Silva JVJ Jr.et al., 2018). Treatments are supportive and the most efficient preventive measure is the use of mosquito repellent and community-based mosquito control programs (Ferguson NM, 2018). Human behaviour influences emergence and re-emergence of arboviral diseases. Composition and dynamics of host and vector population, but also environmental factors and viral genetics, may substantially affect natural systems, leading to amplification of these arboviruses to epidemic levels. Modern travel and trade have facilitated the spread of arboviruses and anthropophilic mosquitoes throughout the globe (Wilder-Smith A et al., 2017). The geographic distribution and the frequency of the epidemic outbreaks of vector-borne viral infections have expanded across the world and today, they account for significant global public health problems (Kraemer MUG et al., 2019).

1.2 Flaviviruses

1.2.1 Introduction to Flaviviruses

The genus *Flavivirus* belongs to the *Flaviviridae* family, which includes other three virus genera: *Pestivirus, Hepacivirus* and *Pegivirus* (Huang YJ et al., 2014). The term *Flaviviridae* originated from the word “flavus” meaning yellow in Latin, for the hallmark jaundice in victims caused by the infection with yellow fever virus. The family encompasses more than 70 recognized arboviruses and vector-unassociated single-stranded and positive-sense RNA viruses, many of them are the most clinically important arboviruses world-wide. In addition to YFV, some of them includes JEV, WNV, DENV, Zika virus (ZIKV), TBEV (Cleton N et al., 2012; Best SM, 2016) and several other viruses responsible for extensive morbidity and mortality in humans (Gould EA and Solomon T,2008). Flaviviruses are maintained in nature in transmission cycles involving a mosquito or tick vector and mammalian or bird amplification hosts, with humans generally serving as dead-end incidental hosts. Flaviviruses can be classified into eight antigenic complexes by cross-neutralization assays with polyclonal hyperimmune sera (Calisher CH et al., 1989). The most medically relevant antigenic complexes are the tick-borne encephalitis virus complex, the Japanese encephalitis virus complex, the dengue virus complex, and the yellow fever virus complex.

Phylogenetic analyses of the Flavivirus genus was performed to explore the genetic relationship among flaviviruses and several clades defined by their epidemiology and disease associations have been recognized. These phylogenies identified mosquito-borne, tick-borne and no-known-vector virus clades, which could be further subdivided according to their principal vertebrate host (Gaunt MW et al., 2001). The mosquito-borne flaviviruses encloses two groups epidemiologically associated: (i) the neurotropic viruses, often associated with encephalitic disease in humans, transmitted by the *Culex* species vector and amplified in bird reservoirs and (ii) the non-neurotropic viruses, associated with haemorrhagic disease in humans, associated with the *Aedes* species vector and primate hosts (Fig 1.1). The first group includes the emerging or re-emerging human pathogenic JEV, WNV, St Louis encephalitis virus (SLEV), Murray Valley encephalitis virus (MVEV) and Usutu virus (USUV). They are primarily associated with ornithophilic *Culex* species mosquitoes that are active during the night in summer season. The habitats of *Culex* mosquitoes include sewage, stagnant water, waste tires and drainage systems. Their geographical dispersion is strongly influenced by the birds that they infect, and migratory birds can carry these viruses for long distances. They are not transmitted from-animal-to-person or person-to-person by casual contacts and thus, humans represent dead-end hosts (Rizzoli A et al., 2015).

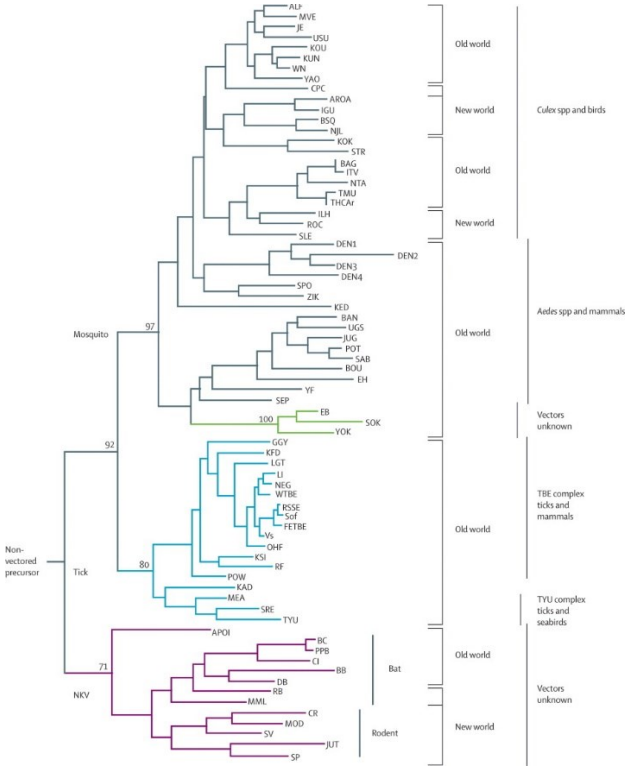

Fig 1.1 Phylogenetic tree showing the association of the groups of related viruses with their invertebrate vectors, vertebrate hosts, and geographic distribution (Gould EA and Solomon T, 2008)

The second group is represented by the human pathogenic *Aedes*-species-associated flaviviruses which includes YFV, DENV serotypes 1, 2, 3, and 4 and ZIKV. Aedes species mosquitoes may breed in tree holes and other forms of vegetation and/or in man-made environments including houses, plant pots, discarded car tyres and bottles. They are active in early morning or late afternoon (*A. Aegypti*) or during full sunlight (*A. Albopictus*: the Asian "tiger mosquito"). Eggs can survive cold winters and other adverse climate conditions by supporting long periods of drying. They feed primarily on available non-human mammals (sylvatic/enzootic cycle) but depending on the local habitat, they tend to feed aggressively on humans (Alonso-Palomares LA et al., 2018). Carried viruses can sustain transmission between humans without having to depend on their natural reservoir forest cycle (e.g. DENV and YFV). Additionally, non-vector-borne transmission in the form of maternofoetal, sexual and post-transfusion have also been associated with ZIKV infection (Moreira J et al., 2016). Different species can transmit the same pathogens (e.g. DENV can be transmitted by *A. aegypti* or *A. albopictus* in Asia and Africa) or the same species can transmit different pathogens (e.g. *A. aegypti* transmits DENV, ZIKV and YFV).

1.2.2 Genome of Flaviviruses

Flaviviruses have a non-segmented, single-stranded, positive-sense RNA genome of about 10 to 12 kb, that is complexed with multiple copies of the capsid C protein (C), which is surrounded by a lipid bilayer containing the envelope (E) protein and the membrane (M) protein (Villordo SM et al., 2016). Mature virions are spherical and icosahedral of about 40 nm in diameter (Sirohi D et al., 2016) and contain the M protein, produced by the cleavage of the membrane precursor protein (prM) by the host furin-like protease, located in the trans-Golgi (Wang A et al., 2017) and the E protein that represents the major virion surface protein (Faye O et al., 2014). E protein is involved in host cell binding and membrane fusion and is also the main antigenic protein of the virus (Pierson TC and Diamond MS, 2012).

The genome of flaviviruses has a single open reading frame (ORF) flanked by 5'- and 3'-untranslated regions (UTRs); the 5'- end terminates with a type 1 cap, and the 3'- end is not polyadenylated and terminates in a conserved CUOH motif (Ng WC et al., 2017). All flavivirus genomes include two conserved RNA elements that are essential for viral RNA synthesis: the Y shape stem-loop A structure (SLA) at the 5' end, and the small hairpin 3' stem-loop (sHP-3'SL) at the 3' end (Yu L et al., 2008).

The single open reading frame encodes for a single polyproteins that is co- and post-translationally processed into three structural proteins (capsid [C], membrane [prM/M] and envelope [E]) and seven non-structural (NS) proteins NS1, NS2A, NS2B, NS3, NS4A, NS4B and NS5, by cellular and viral protease. All the non-structural proteins have been implicated in viral RNA synthesis or protein processing (Murray CL et al., 2008). NS3 and NS5 proteins have known enzymatic activities. NS3 is a trypsin-like serine protease with a nucleic acid helicase activity in the C-terminal domain (Li K et al., 2014). NS5 comprises an N-terminal S-adenosyl-L-methionine (SAM)-dependent methyltransferase (MTase) domain and an RNA-dependent RNA polymerase (RdRP) domain at the C-terminus (Egloff MP et al., 2002; Lu G and Gong P, 2013).

1.2.3 Flavivirus replication cycle

The viral anchoring to the host cell surface is mediated by a first interaction of the viral E glycoprotein with host attachment factors that include glycosaminoglycans like heparan sulphate or the dendritic cell-specific intercellular adhesion molecule-3 grabbing nonintegrin (DC-SIGN) expressed in dendritic cells and macrophages, which are key target cells of flavivirus infection. Further specific interactions during flavivirus entry involve secondary receptors represented by phosphatidylserine receptors of the TIM (T-cell immunoglobulin and mucin domain) and TAM (Tyro3, Axl,and Mer) families (Perera-Lecoin M et al., 2013; Smit JM et al., 2011). Viruses bind to these receptors through phospholipids exposed on their surface and exploit the transduced signals that induce phagocytosis by immune cells to promote infection (Sirohi D et al., 2017). After clathrin-mediated endocytosis (Jemielity S et al., 2013), the viral E glycoproteins undergo conformational rearrangements induced by the low pH into the endosome, that allow fusion between viral and endosomal membranes, resulting in the release of the viral nucleocapsid into the cytosol (Gollins S et al., 1986). Ribosomes translate viral genome into a single polyprotein, which is processed by host proteases and the viral NS2B-NS3 protease (Markoff L et al., 1994). Viral NS proteins orchestrate genome RNA synthesis that occurs in replication organelles (ROs) at the endoplasmic reticulum membrane and the nascent genome RNAs could function as templates for transcription and translation, and as substrates for encapsidation (Neufeldt CJ et al., 2018). After budding from the endoplasmic reticulum, the assembled progeny viral particles maturate in the trans-Golgi network, where E glycoprotein undergoes irreversible conformational changes and the cellular serine

protease furin cleaves prM into mature membrane protein M. Mature virions are finally exocytosed via secretory vesicles (García LL et al., 2017).

1.3 Neuropathogenesis of flavivirus infection

Several members of the genus *Flavivirus* represents important human pathogens able to alter the homeostasis of the central nervous system (CNS) (Huang YJ et al., 2014). Neurotropic viruses can induce neurological dysfunction and may result in serious inflammatory disease leading to disruption of the CNS architecture and leaving the patient with a poor or fatal prognosis. Flaviviruses such as WNV, JEV, TBEV, USUV and the newly emerging ZIKV share the ability to enter the CNS, infect neural cells and establish acute or persistent infections. Clinical symptoms range from mild fever and malaise to fatal encephalitis or haemorrhagic manifestations (Mukhopadhyay S et al., 2005). Except for ZIKV, mosquito-borne flaviviruses are scarcely associated to post-natal encephalitis and they are rarely responsible for congenital brain malformations (Tang H et al., 2016; O'Leary DR et al., 2006; Mathur A et al., 1982). Otherwise, ZIKV infection, especially during the first trimester of pregnancy, can results in microcephaly and other foetal anomalies defined congenital Zika syndrome (CZS, 6-15% of infections in the first trimester) and foetal demise (Schuler-Faccini L et al, 2016). In addition, during the recent epidemics, ZIKV infection was associated with severe neurological complications in adults including meningitis and encephalitis (Carteaux G et al., 2016) and Guillain-Barré syndrome (GBS,<0,0025% of infections) (Dirlikov E et al., 2018).

The dynamic dissemination of neurotropic flavivirus infections is still largely unknown. Following a subcutaneous bite of a mosquito, the viruses firstly infects the resident dendritic cells (Wu SJ et al., 2000; Welte T et al., 2009) or epidermal keratinocytes (Lim PY et al., 2011), which migrate to local lymph nodes where further replication in monocyte lineage cells takes place. Viremia occurs and the virus is transported to visceral and peripheral organs including the brain. Once in the brain, the virus may induce CNS disease in the host (Samuel MA and Diamond MS, 2006; Dumpis U et al., 1999).

Flaviviruses can penetrate the blood-brain barrier through various mechanisms. Infection of microvascular pericytes in the brain can induce or amplify neuroinflammation caused by JEV infection (Chang CY et al., 2017) and inflammatory chemokine osteopontin (OPN) can impair the blood-brain barrier in mice and promote WNV nerve invasivion (Paul AM et al., 2017).

An undamaged immune system is vital to prevent neuroinvasion by WNV and JEV (Chan-Tack KM et al., 2005; Misra UK and Kalita J, 2010). Inflammation assists the entry of flaviviruses and allows them to infect brain tissues. Interferon (IFN) signalling has a key role in the regulation of permeability of the blood-brain barrier after WNV infection (Daniels BP et al., 2017), while WNV can impair the activation of the JAK-STAT pathway by reducing the steady-state level of tyrosine phosphorylation, antagonizing the IFN immune response (Guo JT et al., 2005). The apoptotic pathway induces a process that might damage barrier cells and besides causing inflammation it can increase its effects (Tu YF et al., 2011) magnifying the resulting neuropathies induced by high JEV loads. JEV can subvert host cell apoptosis by deactivating proapoptotic proteins (Al-Obaidi MMJ et al., 2017). Some studies found that DENV affects the structure and function of the blood-brain barrier and activates endothelial cells which promote immune cell migration to benefit the virus (de Souza KP et al., 2013; Velandia-Romero ML et al., 2016). After infection of endothelial cells that comprise the blood-brain barrier, flaviviruses recruit inflammatory cytokines and open TH17/TH9-controlled gates that destroy close connections between endothelial cells, so that immune cells and immune factors can penetrate the barrier causing inflammation and allowing the virus to enter the brain (Hunsperger EA and Roehrig JT, 2006). Additional mechanisms may assist the passive transport of the virus to the CNS. WNV, for example, infects olfactory nerves and spreads to olfactory bulbs, entering through a “Trojan horse mechanism” (Paul AM et al., 2017). While infected immune cells transport the virus to the CNS across the blood brain barrier or by passive diffusion, the infected neurons are relayed to other neurons by retrograde transport (Hunsperger EA et al., 2006).

Although ZIKV generally does not cause fatal disease in adults, mortality has been described in case who develop Guillain–Barré syndrome (Dirlikov E et al., 2018). Guillain–Barré syndrome is an acute inflammatory immune-mediated polyneuropathy that typically presents paresthesia, weakness and pain but can progress in paralysis and even death. The pathological mechanism of ZIKV-associated GBS remains largely unknown, however hypotheses include the direct infection and injury of peripheral nervous system or immunopathology mediated by B or T-cell due to viral antigen mimicry (Yuki N, 2001). Considerable effort has been made to define ZIKV ability to invade the developing brain of foetuses (Brasil P et al., 2016; Cauchemez S et al., 2016; Shapiro-Mendoza CK et al., 2017). Vertical transmission requires ZIKV to spread to the foetus, where maternal-foetus

interaction occur. The *Placental villous* form a physical barrier against infection and have active roles in antiviral immunity by Type III IFN and microRNAs production (Bayer A et al., 2016 and 2018). Cell culture studies demonstrated that ZIKV targets several placental villous core cells including trophoblasts and structure beneath (Szaba FM et al., 2018; Richard AS et al., 2017; Quicke KM et al., 2016). While human trophoblast cells isolated early during pregnancy propagated ZIKV to high levels (Sheridan MA et al., 2017), those cells obtained later during gestation supported less ZIKV infection, and this probably reflects pregnancy stage-dependent effects of trophoblast differentiation and immunological maturation (Bayer A et al., 2016). Infection of trophoblasts and injury to the placenta were also found after inoculation of human placental explants or pregnant mice with the related West Nile and Powassan viruses (Platt DJ et al., 2018), suggesting that this tropism of ZIKV may not be unique among flaviviruses.

Differences in amino acids of flaviviruses are associated with differences in virus recognition of and attachment to receptors on host cells (Sirohi D et al., 2016; Lin HH et al., 2018). As E glycoprotein is involved in flavivirus host cell binding and entry, substitution in E protein results in altering cellular uptake and glycosylation of E envelope protein represents the main determinant of a neuroinvasive phenotype (Beasley DW et al., 2004; Muylaert IR et al., 1996). In most ZIKV strains, E protein is modified by a single N-linked glycan at position E154 and some pre-epidemic ZIKV strains lack this modification and are less neuroinvasive (Annamalai AS et al., 2017). 50% of E protein is conserved among ZIKV and DENV strains, and the DENV E protein is characterized by glycosylation at a close site (Asn153) that is important for virion release (Lee E et al., 2010). Another glycosylation at Asn67 characterizes E protein of DENV and this is important for the interaction with DC-SIGN receptor (Pokidysheva E et al., 2006). Similarly, the glycosylation of WNV E protein enhances virus neurovirulence of North American WNV strains compared with other Old-World lineage 1 strains (Beasley DW et al., 2005). The region surrounding this glycosylated site varies among flaviviruses and represents an important determinant for antibody specificity (Fernandez E et al., 2017).

1.4 West Nile virus

West Nile virus (WNV) is a *Culex* mosquito-transmitted flavivirus closely related to JEV, USUV and MVEV and within the genus Flavivirus; it is second to DENV in the extent of its global distribution. The ancestral WNV lineage emerged in Africa and was dispersed by

birds taking north and north east migratory routes into Europe. Based on nucleotide sequence data, WNV strains are phylogenetically classified into at least five genetic lineages, but only lineages 1 and 2, which have a nucleotide sequence identity of about 75%, have been associated with major epidemics. Lineage 1 is primarily distributed throughout North Africa, Central/Southern Europe, North America and Sub-Saharan Africa, while lineage 2 covers Central/Eastern Europe and Greece (Barzon L et al., 2015). The awareness of WNV rised with the emergence of West Nile encephalitis in humans, in birds and horses in New York in 1999 (Lanciotti RS et al., 1999), followed by the rapid dispersal of the virus throughout Canada and Mexico (Gubler DJ, 2007). Since 1999 WNV has become the most widespread flavivirus that causes neurological disease globally (Chancey et al., 2015) and nearly 44,000 human cases of clinically apparent WNV infections were recorded in the US by August 2016 (Gould E et al., 2017). Today, WNV is endemic in some regions in Europe, Asia, and Africa, where it caused sporadic outbreaks (Sambri et al., 2013).

WNV infection in humans is asymptomatic in about 80% of cases and associated with a flu-like illness in about 20% of cases. In less than 1% of individuals infected by WNV, mostly elderly and immunocompromised, experience a neurological disease characterized by encephalitis, meningoencephalitis, meningitis, or, rarely, flaccid paralysis (Tsai et al., 1998; Chowers et al., 2001; Mostashari et al., 2001; Gould EA and Solomon T, 2008). Mortality due to WNV encephalitis and meningitis ranges between 10% and 17% (Petersen LR et al., 2013).

1.4.1 Epidemiology of WNV in Italy

In Europe, the presence of WNV was first detected in 1958 when specific antibodies were detected in two Albanians (Bardos V et al., 1959). In Italy, the first human outbreak occurred in 2008 in north-eastern Italy, in wetland areas surrounding the Po River. Five cases of asymptomatic WNV infection and seven patient who developed fever, aseptic encephalitis and meningitis were reported (Barzon L et al., 2009). During the summer of 2009 other 18 cases of neuroinvasive disease due to WNV were diagnosed in the same areas and Lombardia region (Rizzo C et a., 2009). The WNV strain that caused these two outbreaks was found to belong to the lineage 1 and was termed Po River strain. During the following years, cases of severe disease in humans were reported also in the Friuli-Venezia Giulia Region and Sardinia Island (Magurano F et al., 2012). Only WNV lineage 1

was detected until 2011, when the first human cases of autochthonous WNV lineage 2 infection were reported in Marche and Sardinia Regions. Interestingly, in 2011, two new WNV lineage 1 strains, the Piave and the Livenza strains, spread throughout the Veneto region, whereas the Po River strain simultaneously disappeared (Barzon L et al., 2012 and 2013). A large outbreak caused by lineage 1 Livenza was reported in 2012 with a total of 42 human cases of neuroinvasive disease and fever (Barzon L et al., 2012). In 2013, 40 cases of WNV infection were reported, associated with both lineages 1 and 2, in Veneto and Emilia-Romagna regions (Barzon L et al., 2013). According to data from the European Centre for Disease Prevention and Control (ECDC), the transmission season of 2018 has represented the largest WNV outbreak described in Europe so far and Italy was the most affected country with 577 human cases (230 neuro-invasive diseases, 279 WNFs and 68 blood donors). A higher number of cases were reported compared with transmission seasons in previous years and the total number of reported autochthonous infections in 2018 exceeded, by far, the total number from the previous seven years. Compared to the previous transmission season in 2017, there was a 7.2-fold increase. WNV transmission in endemic provinces in Italy began early with higher human case counts of confirmed infection compared with previous years. A possible hypothesis is that the warmer temperatures and the higher cumulative rainfall reported during the Spring 2018 created favourable conditions for mosquito survival and abundance, which led to an anticipation and an overall longer duration of WNV transmission season. Since the beginning of June 2019, 19 confirmed human cases of West Nile infection Virus have been reported in Italy, including 8 neuro-invasive forms, of which 2 deceased; 8 cases of confirmed WNV fever, all reported in Veneto region, and 3 cases identified in blood donors. EU Member States and EU neighbouring countries reported a total of 241 human infections, suggesting that the current can be defined a normal transmission season.

1.4.2 WNV mechanisms to subvert host immune evasion

In order to establish a productive infection, the virus requires evasion, inhibition, or subversion of innate immune responses. Therefore, improvement of our understanding of viral factors and mechanisms that mediate host immune evasion may facilitate novel strategies of therapeutic discovery for the cure and prevention of WNV infection. Viruses counteract IFN responses by inhibiting IFN production and its signalling cascade and by suppressing the activity of IFN-induced antiviral enzymes (Szretter KJ et al., 2012). Several

studies have identified viral factors that mediate immune evasion, but the mechanisms underlying these evasion strategies need to be fully defined (Bossert B et al, 2003; Foy E et al., 2003; He B et al., 2002; Heim MH et al., 1999; Poole E et al., 2002). WNV evades detection of RLRs by sequestering and accumulating viral RNA in ER membrane vesicles during viral replication (Fredericksen BL et al., 2004). Membrane structures of the viral replication machinery induced during flavivirus infection provide protection from the antiviral activity of the IFN-stimulated MxA protein (Hoenen A et al., 2007). Both structural and NS proteins of WNV are implicated in antagonism of type 1 IFN signalling cascade, albeit with different mechanisms and relative suppressive activity can differ between virulent and attenuated virus strains (Suthar MS et al., 2012; Evans JD and Seeger C, 2007; Liu WJ et al., 2005). Several non-structural proteins of WNV inhibit JAK-STAT signalling by preventing JAK1 and Tyk2 activation (Evans JD et al., 2011; Keller BC et al., 2006) or STAT1 and STAT2 phosphorylation. This block prevents downstream signalling including nuclear localization of STAT1 and STAT2 as well as ISG expression (Evans JD and Seeger C, 2007; Liu WJ et al., 2005; Muñoz-Jordán JL et al., 2005; Laurent-Rolle M et al., 2010; Perwitasari O, et al., 2011). An example includes WNV NS5 that functions as IFN antagonist, not just using its 2'-O-methylation activity to evade the antiviral effects of IFIT1 (Szretter KJ et al., 2012), but also blocking IFN-dependent STAT1 phosphorylation or degrading STAT2 (Laurent-Rolle M et al., 2010). Another mechanism by which WNV counteracts the JAK-STAT signalling pathway is the modulation of cellular cholesterol biosynthesis and its redistribution to sites of viral replication complexes by the synergic action of HMGCR enzyme and viral NS4A (Mackenzie JM et al., 2006). Indeed, compounds that target cholesterol biosynthesis and/or HMGCR activity may provide candidate antiviral treatments. In addition to blocking the IFN signalling cascade, viral NS2A protein is implicated in the suppression of IFN production and inhibits the IFN-beta promoter-driven transcription [Liu WJ et al., 2004 and 2006). RNA-based evasion mechanisms have only recently begun to be identified and are not yet known, however subgenomic flavivirus RNA (sfRNA) has been shown to inhibit the antiviral activity of IFN-α/β (Szretter KJ et al., 2012; Roby JA et al., 2014). Like the innate system, the adaptive system, which includes both humoral immunity and cell-mediated immunity, are essential components of the immune response to flaviviruses and antigenic variation in the E protein may be relevant to humoral immune evasion. In cell culture experiments indeed, mutations in domain III of the WNV E protein enable viral escape from neutralizing antibodies (Beasley DW et al.,

2002). However, its relevance *in vivo* remains to be confirmed. Activation of the complement pathway can directly suppress viral infection and programme adaptive immune responses. Currently, flavivirus factors able to impair complement function have not been defined. Nonetheless, preliminary data shows that secreted WNV NS1 protein attenuates activation of the complement alternative pathway and speculation have been made on the possible role of NS1 in enabling WNV to evade complement-dependent control mechanisms (Chung KM et al., 2006). Taken together, these studies begin to delineate potential mechanisms of flavivirus resistance to IFN and adaptive immunity and have direct implications for design of antiviral drugs or vaccine adjuvants by serving to stimulate 'virus-specific' innate immune signatures that drive enhanced adaptive immune responses and immune protection design. Possibly, new classes of drugs that alter production of sfRNA in infected cells, for example, could make flaviviruses susceptible to the innate antiviral effects of type I IFN.

1.5 Usutu virus

Among emerging viruses, only recently Usutu virus (USUV) has attracted the attention of the scientific community due to its extensive spread in Europe. USUV belongs to the Japanese encephalitis virus serocomplex and is phylogenetically close to MVEV and WNV, and JEV. USUV emerged at the beginning of 16th century in Africa, where it was detected in different bird and mosquito species. According to phylogenetic studies based on the nucleic acid sequence of the NS5 gene, USUV strains can be divided into eight lineages: three African and five European (Cadar D et al., 2017), and the level of genetic relatedness of each lineage depends on the geographical origin and on the host from which viruses have been isolated. The first circulation of USUV in Europe is suggested to go back to 1950s when, along an eastern Atlantic migratory route of *Culex* mosquitoes from Africa, the virus was introduced in Spain (Engel D et al., 2016) followed by a unique introduction in Central Europe in the 1980s along a Black Sea/Mediterranean migratory route (Weissenböck H et al., 2013). Retrospective analysis of archived tissue samples from dead Eurasian blackbirds in Tuscany (Italy) indeed, discovered that USUV had circulated in northern Italy since 1996 or earlier (Manarolla G et al., 2010). However, the earliest evidence of USUV in Europe emerged in 2001 in Austria, where it caused deaths of several species of resident birds (Weissenböck H et al., 2002). In the following years, USUV was found in birds, mosquitoes, bats and horses in 12 European countries including Hungary, Switzerland, Spain, Czech

Republic, Germany, Belgium, Italy, France, Austria, Croatia, Greece and Serbia (Ashraf U et al., 2015; Kemenesi G et al., 2018; Scheuch DE et al., 2018; Eiden M et al., 2018). During the summer of 2016, a major USUV epidemic affecting birds was evidenced in Northern Europe, and equines in Slovakia and in Poland (Rijks JM et al., 2016; Csank T et al., 2018; Bażanów B et al., 2018). In 2018, USUV spread rapidly in Western Europe. In Italy, eight human cases of USUV infection were reported, one of them developed neuro-invasive disease, six had WNF and one was a viraemic blood donor. In eastern Austria, the same year, 18 USUV infections among blood donors were detected, representing the highest number of human infections reported since the emergence of USUV in Austria in 2001. Symptoms of USUV infection in humans vary from moderate (i.e. rash, fever, headache) to severe sign of infection (i.e. neurological complications). Among the USUV-infected patients who developed neurological disorders, all were immunocompromised individuals with the exception for three Italian patients with acute meningoencephalitis, whose cerebral spinal fluid (CSF) were collected between 2008 and 2009 (Cavrini F et al., 2018) and a French patient with acute facial paralysis whose CSF was collected in 2016 (Simonin Y et al., 2018). During the 2018 transmission season, *Culex pipiens form pipiens* was the principal vector of USUV in Europe. A recent study speculated that the invasive mosquito *Ae. j. japonicus* might be involved in epizootic transmission of USUV in Europe (Camp JV et al., 2019). According to this study, multiple introductions of the virus into Europe have occurred and the population in central Europe is highly expanding in range and local abundance. In regions where WNV is endemic, USUV and WNV have been observed to co-circulate in an avian-mosquito transmission cycle (Zannoli S and Sambri V, 2019). Given that USUV and WNV are genetically, antigenically and epidemiologically closely related, the cocirculation of WNV and USUV warrants increased laboratory support and awareness of possible virus misidentification. In addition, reliable data on the geographic spread of the virus is critical to informing clinicians of the risk so that they can include USUV infection in their differential diagnosis. Whether USUV will continue to expand geographically in Europe or elsewhere remains to be seen, but, considering the increasing numbers of bird deaths and the recent observations of human USUV infections in northern Italy, USUV appears to be emerging as a significant avian and human pathogen in both northern and southern Europe.

1.6 Zika virus

The *Aedes*-species-associated ZIKV is a close relative of DENV and YFV. It was mostly restricted to the African continent and later it was reported in South East Asia (1980). Two geographically overlapping lineages of ZIKV, West African and East African have been recently defined (Faye O et al., 2014) and a descendant Asian lineage was firstly identified in 1969 in Malaysia (Marchette NJ et al., 1969). This Asian lineage has been associated to the epidemic outbreaks which occurred throughout the tropical Western Hemisphere. In 2007, ZIKV caused an epidemic which involved 73% of the population on Yap Island in Micronesia (Duffy MR et al., 2009). Until 2007, only fourteen cases of ZIKV fever had been reported worldwide (Korzeniewski K et al., 2016). ZIKV infection was associated with only mild illness prior to the large French Polynesian outbreak in 2013 and 2014, when severe neurological complications such as Guilliam-Barre syndrome were reported, and non-vector-borne transmission of ZIKV first emerged (Musso D et al., 2014). The virus continued to disperse across the Pacific Ocean reaching the tropical and sub-tropical regions of the Americas during 2015-2016 (Pettersson JH et al., 2016). Following the emergence in Brazil of a dramatic increase in severe congenital malformations (microcephaly) suspected to be associated with ZIKV, the World Health Organization declared ZIKV as a "Public Health Emergency of International Concern" (Musso D and Gubler DJ, 2016). From April 2007 to March 2017, 84 countries across the world have been involved in the transmissions of ZIKV (Baud D et al., 2017). As of July 2019, a total of 87 countries and territories have had evidence of autochthonous mosquito-borne transmission of ZIKV distributed across four of the six WHO Regions (African Region, Region of the Americas, South-East Asia Region, and Western Pacific Region). In 2018, Ethiopia was the only new country added to the list of countries with evidence of autochthonous, mosquito-borne transmission (Mengesha Tsegaye M et al., 2018). The clinical syndrome caused by ZIKV in humans was usually reported as a mild influenza-like illness that occurred in approximately 20% of infected individuals, who recovered within a few days (Duffy MR et al., 2009). In addition to the already described neurological complications and teratogenic effects, ZIKV infection has been associated, although very rarely, with multi-organ failure (Swaminathan S et al., 2016), and thrombocytopenia (Karimi O et al., 2016). Even if ZIKV generally does not cause death in adults, mortality has been described in children with sickle cell disease, adults with cancer (Swaminathan S et

al., 2016) and those cases who develop Guillain–Barré syndrome (Dirlikov E et al., 2018). During the recent epidemic, evidences of ZIKV ability to persist in multiple organs have been described and an apparent broadening of its cellular tropism came to view. Several case reports demonstrated that ZIKV persists in whole-blood for 60–100 days long after serum became negative (Murray KO et al., 2017; Mansuy JM et al., 2017) and in immune-sanctuary sites. ZIKV can replicate persistently within cells of the eye (Miner JJ et al., 2016), which causes optic neuritis and blindness in newborns and conjunctivitis and uveitis in adults. Persistence of ZIKV in the eye is speculated to be a means of direct transmission. Another target site of ZIKV is the male sperm and semen where persistent ZIKV RNA has been detected in humans for months (Mansuy JM et al., 2016). Studies in mice have demonstrated that ZIKV infection of the testis, including spermatogonia, Sertoli cells and Leydig cells was responsible to destruction of testicular architecture, reduction in sperm counts, lower levels of sex hormones and reduced fertility (Govero J et al., 2016; Ma W et al., 2017).

In the last decades, the emergence or resurgence of epidemic arboviruses such as DENV, CHIKV, and WNV has been dramatic (Gubler DJ, 2002; Failloux AB, 2019). Global population growth, urbanization, globalization, and a lack of effective vector control represent the principal drivers for this emergence and changing epidemiology (Gubler DJ, 2011). There is good evidence that new clinical patterns and new modes of transmission were associated to this phenomenon (Marfin AA and Gubler DJ, 2001; Chandak NH et al., 2009; Renault P et al., 2007). Virus genetic changes have been responsible for phenotypic changes of emerging arboviruses influencing their virulence and epidemic potential (Tsetsarkin KA et al., 2007; Bennett SN et al., 2003; Brault AC et al., 2007). ZIKV has essentially the same epidemiology and mosquito vectors in urban areas as DENV and CHIKV and humans are the principal vertebrate host in urban and peri urban areas. The potential impact of climatic change on the spread of ZIKV in unknown but human connection greatly increases and the risk of global spread via infected humans to areas where mosquito control has failed is high. It was suggested indeed, that ZIKV will likely follow the path of DENV and CHIKV and become a global public health problem and considering the severe disease associated with ZIKV in French Polynesia and Brazil, this virus will become a very serious issue (Musso D et al.,2015).

1.7 Individual susceptibility to flavivirus infection

There is clear evidence that some individuals respond differently to infectious agents compared to others. Epidemiological studies have highlighted the role of host genetic factors as determinants of this spectrum of clinical phenotypes. Since the early 1940s, twin studies have demonstrated that infectious diseases such as tuberculosis, leprosy, malaria and pneumonia have a heritable component (Comstock GW, 1978; Misch EA, 2010; Herndon CN & Jennings RG, 1951), making the basis for further studies to identify the specific genes involved (Murray K et al., 2006). Recently, unbiased whole-genome approaches have revealed robust associations between genetic markers and susceptibility to disease (Yudin NS et al., 2018). Many individuals exhibit flavivirus-specific antibodies, suggesting that infection with these viruses may be mild or even unapparent and revealing that a sort of adaptation between the virus and its host has occurred. In some other cases, however, flaviviruses can cause human epidemic outbreaks and infected individuals may develop symptoms, ranging from transient febrile illness to life-threatening haemorrhagic fever (yellow fever and dengue fever), meningoencephalitis syndromes (Japanese encephalitis and West Nile fever), Guillain-Barré syndrome (caused by Zika virus) and other neurological complications. The different outcomes or progression to severe disease can be partly explained by human genetic variations but this genetic basis remains poorly understood. Old age and immunodeficiency are the most important risk factors for severe neuroinvasive disease. Younger patients are more susceptible to aseptic meningitis, but elderly patients are at greater risk of developing severe encephalitis with poor prognosis. For the elderly, the risk is most likely related to a compromised immune system or pre-existing medical conditions, such as diabetes, obesity and autoimmune diseases, which increase accessibility of the CNS to infection (Murray K et al., 2006). Considering that no other acquired risk factors have been identified so far, the hypothesis of the existence of genetic predisposition to WNND is increasingly taking hold. One of the central questions in the search for therapeutic targets for the treatment of flavivirus neurological syndromes is whether these diseases are induced by virus-mediated cytolysis, immune-pathological responses to virus infection, or a combination of both. Mouse models have permitted temporal analysis of the progressive dissemination of virus infection within the CNS and have revealed important details regarding the innate and adaptive immune responses to viral infections (Wang T and Fikrig E, 2004; Lim SM et al., 2011). In addition, *in vivo* studies

have favoured the detection of genetic loci that predispose to flavivirus infectious diseases. As far back as in the 1920s, Webster and coll. demonstrated that mice innate resistance to flavivirus-induced morbidity had monogenic and autosomal dominant inheritance (Webster LT, 1923). Most lines of laboratory mice were susceptible to flavivirus infection, while homozygous wild mice were resistant to flavivirus, but susceptible to other types of viruses. The higher susceptibility to flavivirus infection of laboratory mice was associated to higher detected virus titres, especially in the brain, compared to resistant animals. The alleles that determined resistance and susceptibility were designated *Flv*^{r} and *Flv*^{s}, respectively. This allele was later identified as mouse 2'-5'-oligoadenylate synthetase 1B (Oas1b) (Perelygin AA et al., 2002). Oas1a is an enzymatically active synthetase that upon binding to viral dsRNA synthetizes 2'-5'-oligoadenylates (2–5A) from ATP that activate the latent endonuclease RNase L, which in turn degrades both cellular and viral single-stranded RNAs (Samuel CE, 2001). This gene is induced by the canonical IFN-mediated pathway and during the activation of alternative anti-viral mechanisms (Pulit-Penaloza JA et al., 2012). An interaction with ATP-binding cassette transporter 3 (ABCF3) protein is involved in the mechanism by which the Oas1b protein selectively decreases the replication of flaviviruses in the target tissues (Courtney SC et al., 2012). The specific variant that was found responsible to mouse predisposition to flaviviruses was a C820T nonsense mutation in exon4 of Oas1b that produces a protein truncated by 30% (Mashimo T et al., 2002; Brinton MA and Perelygin AA, 2003). The high prevalence of subclinical human infections precludes the identification of WNV-infected individuals and subsequent clinical and immune response evaluations, limiting our knowledge of anti-WNV immunity. For this reason, most immunity studies were performed on inbred mouse models of infection, generally using wild-type (WT) and transgenic gene knockout C57BL/6J mice (B6 mice) that, however, do not reproduce the full diversity of clinical symptoms observed in human. Thus, a more efficient mouse model was created by crossing recombinant inbred lines (Graham JB et al, 2015). Newly Collaborative Cross (CC) mouse lines identified three categories of WNV susceptibility: asymptomatic, symptomatic, and asymptomatic with CNS involvement; that reflected the range of disease outcomes in human infection. Studies with CC mouse models underlined the complex genetic interactions that drive the differential initial/innate antiviral responses, as well as the overall control of *in vivo* viral disease responses. The divergent outcomes of CC mouse lines despite sharing *Oas1b* alleles reinforced the notion that the

ISG expression that altered innate immune regulation among hosts can likely contribute to differential outcome of infection and immunity among a population outbreak and that *Oas1b* alone is often not sufficient to completely protect against WNV infection (Graham JB et al, 2015; Green R et al., 2017).

1.7.1 Candidate genes of predisposition to WNV infection

It is widely known that the course and outcome of an infectious disease is driven not only by the properties of the causative agent itself, but also by the host individual immune ability to detect and neutralize the pathogens, which significantly depends on hereditary factors (Khor CC and Hibberd ML, 2012). The identification of specific genetic markers implicated in the course of infectious disease will promote the detection of individuals with an increased risk of the emergence of severe forms and will allow to direct the risk group patients to vaccination or preventive therapy in advance (Mentzer AJ et al., 2015). However, when a specific gene variant is discovered to predispose to a disease, it does not necessarily indicate the direct involvement of the gene or its product in the pathological process. Instead, it is possible that this is a neutral variant that does not influence the phenotype by itself, but it is in linkage disequilibrium with another variant, which directly influences the disease trait. Each polymorphic allele that characterizes specific genes may have alone a little effect on the phenotype, but the total effect during the combination of these alleles can lead to weakening of the immune system (Kumar V et al., 2014). To date, many large-scale associative studies, both genome-wide and focused on the search for individual candidate genes, have been performed leading to significant progress in the genomics of flavivirus infectious diseases. Most of the studies on the human hereditary predisposition to West Nile fever was mainly executed among the residents of the United States.

The main candidate genes that have been associated with severe WNV neurological disease include *OAS* cluster genes (that consists of four genes, *OAS1, OAS2, OAS3* and *OASL*), *CCR5* chemokine receptor gene, HLA system antigens, the IFN type 1-mediator genes *TLR3* and *IRF3*, and the *MX1* gene. The human leukocyte antigen (HLA) system encodes the major histocompatibility complex (MHC) and functions in the presentation of foreign antigens to circulating leukocytes. Most of the research on the association between HLA expression and flavivirus disease has been performed with dengue viruses. A few studies have indirectly implicated HLA alleles in modulating the severity of WNV

infections (De Groot AS et al., 2001; Kim Set al., 2010). In 2011, a comparison of allele distributions across groups of WNV-infected subjects with different infection outcomes revealed higher frequencies of the allele HLA-A*68, HLA-C*08, and HLA-DQB1*05 in patients who developed neuroinvasive diseases and these alleles were designated as "susceptible". Conversely, the alleles HLA-B*40 and HLA-C*03 were present at higher frequencies in the group of asymptomatic WNV-infected individuals than in the group of WNV symptomatic subjects (Lanteri MC et al., 2015). Previously, it was demonstrated (Mashimo T et al., 2002; Brinton MA and Perelygin AA, 2003) that the nonsense mutation in the Oas1b gene predisposes the susceptibility on inbred mouse lines to WNV. Studies on human OAS genes revealed 23 single nucleotide polymorphisms (SNPs) including a synonymous SNP in OASL exon 2 (rs3213545 C/T (Leu136Leu) SNP) in which the reference allele occurred at a higher frequency in case patients (Yakub I et al., 2005). As the C allele is part of the potential SF2/ASF splicing factor binding site (ctctCgt), it was suggested that the rs3213545 SNP can affect the development of different protein isoforms. Two other SNPs associated with the increased risk of developing West Nile fever were also identified in the *OAS1* gene: the rs34137742 SNP in the second intron of the gene, and the rs10774671 (A/G) SNP associated with WNV infection in Caucasians from the United States (Lim JK et al., 2009). The former was associated with increased risk of the development of encephalitis and paralysis during WNV infection (Bigham AW et al., 2011), and the latter allele influences the alternative splicing of the *OAS1* gene transcripts in mononuclear cells of peripheral blood (Bonnevie-Nielsen V et al., 2005). Similar effects of the *OAS1* gene variability on hereditary predisposition to WNF was also detected in horses (Rios JJ et al., 2010).

A loss-of-function mutation in *CCR5* corresponded to an increased severity in WNV infection, though it was not associated with increased susceptibility. A deletion of 32-base-pair in the gene encoding for the chemokine receptor CCR5 that produces a truncated form of the protein, which eliminates its surface expression, has been associated with severe disease following flavivirus infection (Glass WG et al., 2006). However, CCR5 deficiency does not seems to be a risk factor for WNV infection per se, but rather seems a risk factor for both early and late clinical manifestations after infection. CCR5Δ32 homozygous individuals, indeed, had early clinical presentation of the disease and a higher frequency of multisystem symptoms such as lymphadenopathy, neurological deficits and

gastrointestinal complications (Lim JK et al., 2010). Similar results were obtained for TBEV (Kindberg E et al., 2008).

The Toll-like receptor 3 (TLR3) modulates the immune response by recognition of dsRNA and induces the production of IFN type I and the subsequent induction of the pro-inflammatory cytokine TNF-α. This gene has been studied as a genetic risk factor for TBEV and WNV infection (Kindberg E et al., 2011; Kong KF et al., 2008). High levels of TLR3 result in an increase of cytokine levels and may contribute to the increased permeability of the blood-brain barrier. This implication has been observed in elderly individuals and suggested another possible mechanism for the increased severity of WNV infection (Kong KF et al., 2008).

Significant associations between WNV infection and SNPs in the *IRF3* and *MX1* innate immune response and effector genes have also been reported (Bigham AW et al., 2011). MX1 belongs to the MX (myxovirus resistance) family of interferon-induced proteins that are GTPases with antiviral functions (Sadler AJ and Williams BR, 2008). During the penetration of the virus into the cell, the MxA (the human equivalent of mouse Mx1) binds to the nucleocapsid and prevents its transportation to the cell nucleus. Both SNPs are in the gene intron and none is in strong linkage disequilibrium with known functional variants in their respective genes. Each of these loci is involved in either an interferon regulatory pathway or is an effector of the interferon response. To sustain the positive correlations of Mx1 in susceptibility of WNV infection, an additional rs7280422 SNP in the *MX1* gene intron were detected among Ashkenazi Jewish patients with symptomatic WNV infection (Danial-Farran N et al., 2015). All these evidences suggest that genetic variations in the interferon (IFN) response pathway appear to correlate with the risk of symptomatic WNV infection in humans, however further investigation is needed to better define how these polymorphisms alter protein expression and function during WNV infection. Fig 1.2 shows some cellular processes activated in response to flavivirus infection and mainly associated with severe disease (Yudin NS et al., 2018).

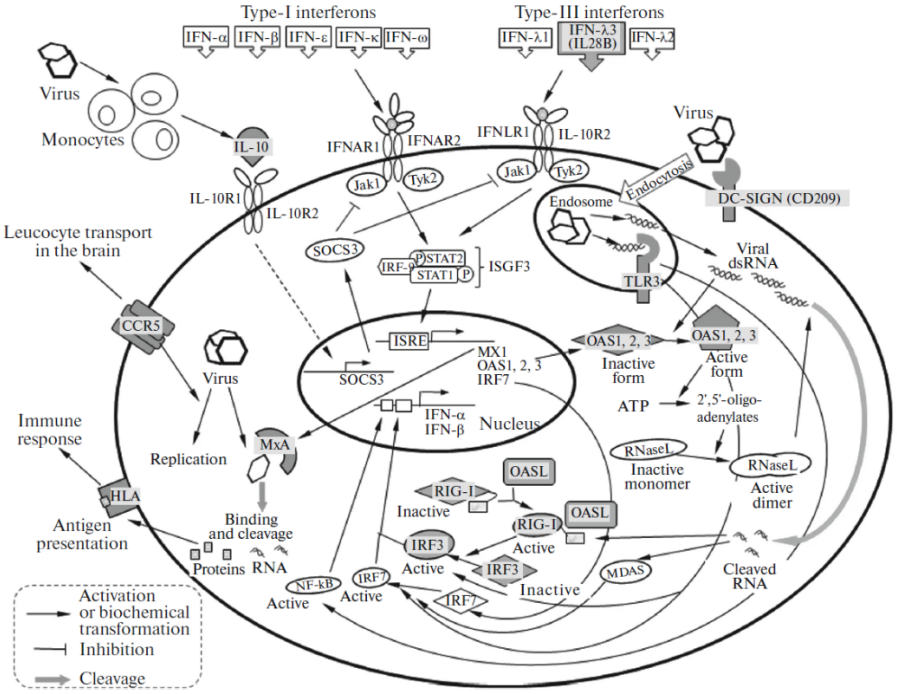

Fig 1.2 Cellular processes activated in response to flavivirus infection. Protein products that control signalling pathways mainly associated with the emergence of flavivirus severe disease are highlighted in grey (Yudin NS et al., 2018).

1.8 Infectious disease modelling using Induced Pluripotent Stem Cells (iPSCs)

Mouse models have been fundamental in determining the molecular basis of developmental, cellular and structural immunology (Lim SM et al., 2011; Graham JB et al, 2015). They have contributed to key discoveries in host defence and have determined primary and tertiary structures of a growing number of molecules involved in antiviral signalling pathways that are increasingly well described. Infections of conditional knockout mice will provide irreplaceable information that is not available in human and surely, they will be crucial in future studies of immunity to infection. However, mouse models lack the genetic diversity present in human populations. The marked genetic diversity of humankind is now amenable to genetic examination, while most mice model consist of a small collection of inbred strains that have only a few natural mutations (Wade CM et al, 2002). Human pathogens affect patient health through a complex interplay with the host, but *in vitro* model systems to study the host-pathogen interactions are limited because of tissue scarcity and challenges in primary culture. The breakthroughs on cell reprogramming and generation of human induced pluripotent stem cells (hiPSCs) (Takahashi K and Yamanaka S, 2006) could overcome the problem of genetic diversity and tissue insufficiency. In 2006, it was demonstrated that cells with embryonic stem cell

features could be derived from mouse fibroblasts by ectopic expression of four stem cell transcription factors (i.e., Oct4, Sox2, Klf4, and c-Myc) (Takahashi K and Yamanaka S, 2006). In the following year, iPSCs have been generated for the first time from human somatic skin cells by using similar reprogramming protocols (Takahashi K et al., 2007; Yu J et al., 2007). The human iPSCs, like embryonic stem cells (i.e., pluripotent cells derived from preimplantation stage embryos), replicate indefinitely and differentiated into a variety of cells, but they do not require embryos or somatic cell nuclear transfer to be conceived. So far, different methods have been set up for generation of iPSCs and efficient and standardized protocols are now available (Schlaeger TM et al., 2014). The first methods exploited integrating retroviral vectors for the delivery of reprogramming factors, but they may induce insertional mutagenesis and/or transgene reactivation thus, other efficient and safe non-integrating methods have been subsequently developed. These included approaches based on the use of Sendai viral vectors, episome plasmid vectors, synthetic mRNAs and small molecules and are now widely applied in stem cell laboratories (Schlaeger TM et al., 2014). The biological characteristics of human iPSCs resemble those of embryonic stem cells (i.e., pluripotent cells derived from preimplantation stage embryos) such as the potential to differentiate into all somatic cell types of the body. Several protocols are available for the differentiation of iPSCs into a variety of cell types, including keratinocytes, neurons, cardiomyocytes, hepatocytes and hematopoietic cells (Sterneckert JL et al., 2014). There are three general approaches to initiate differentiation: the first method exploits the formation of EBs, i.e., 3D cellular aggregates obtained by withdrawal of undifferentiating stimuli such as adhesion and b-FGF (Imamura T et al., 2004). In the second approach, pluripotent cells are grown directly on stromal cells, and differentiation takes place in contact with these cells (Nakano T et al.,1994). The third protocol starts with cells growing in a uniform monolayer on extracellular matrix proteins (Carpenter L et al., 2012). hiPSCs represent versatile, non-invasive, ethically sustainable, cruelty-free, and patient-specific models for the investigation of host-pathogen interactions. The availability of human iPSC-derived differentiated cells holds immense promise for the development of easy to handle cell systems for the investigation of interaction with the human host, viral tropism, pathogenesis, latency and reactivation (Trevisan M et al., 2015). iPSCs indeed, offer the possibility to set up *in vitro* cultures of normal human cells for viruses that are strictly species-specific or that can grow only in specific human cell types, sometimes inaccessible.

Among the first reports of using iPSCs-derived systems, we can find models of infectious disease to study hepatitis B (HBV) (Shlomai A et al.,2014) and hepatitis C (HCV) (Sa-Ngiamsuntorn K et al., 2016) viruses, which can be grown in hepatocytes; human citomegalovirus (HCMV) (D'Aiuto L et al., 2012), which can be propagated in human neural cells; the neurotropic alphaviruses herpes simplex virus (HSV) (Lee KS et al., 2012); varicella zoster virus (VZV) (D'Aiuto L et al., 2014) and recently the flaviviruses ZIKV and USUV (Caires-Júnior LC et al., 2018; Salinas S et al., 2017).

1.8.1 Modeling individual susceptibility to infectious diseases

Genome-wide association studies (GWAS) have identified several polymorphisms, as well as human genetic variations in innate and adaptive antiviral-immunity or encoding viral receptors associated with common diseases (Sancho-Shimizu V et al., 2011). However, very large sample sizes are required to generate enough statistical power to detect true disease associations (McCarthy MI et al., 2008) and may be unrealistic for the study of less-common infectious disease. Therefore, multiple causative rare variants were hypothesized to be the major responsible of the individually large effects and were considered a likely source of the 'missing heritability' of common disease. For this reason, next-generation sequencing studies focused at identifying rare variants are widely expected to become a dominant approach in human disease genetics (Cirulli ET and Goldstein DB, 2010). Some examples in which GWAS led to identification of genetic variants associated to infectious diseases include studies on HIV-1 and HCV infections (Fellay J et al., 2007; Rauch A et al., 2010); HSV-1 encephalitis (Zhang SY et al., 2013) and influenza (Ciancanelli MJ et al.,2015). In common with other major infectious diseases, susceptibility to HIV and the clinical outcome after infection has marked inter-individual variation. Host genetic studies based on candidate-genes and genome-wide strategies have examined various phenotypes, including susceptibility to HIV-1 acquisition, viral load following infection, and disease progression. Candidate-gene studies showed that individuals who are heterozygous for a 32 base-pair deletion in C-C chemokine receptor type 5 gene (known as CCR5Δ32) progress more slowly to AIDS (Dean M et al., 1996) and homozygous individuals for CCR5Δ32 (~1% of the European population) are also highly resistant to acquiring HIV-1 infection (Liu R et al., 1997). Interestingly, in an early GWAS the association with CCR5Δ32 was not observed probably because of the rarity of the homozygous state (Fellay J et al., 2007). A central role in HIV-1 infection and progression was confirmed also for the HLA class I region

through both candidate and genome-wide approaches (Fellay J et al., 2007). Taken together, GWASs have confirmed the major roles of polymorphisms in the CCR5–CCR2 locus and in HLA class I loci in the pathogenesis of HIV infection, that explain approximately 23% of the observed variability in HIV-1 control (The International HIV Controllers Study, 2010). However, additional major susceptibility loci for phenotypes studied have not yet been identified but may reflect the combined effect of multiple host genetic variants that are individually rare but induce large sequels. Other GWASs focused on hepatitis C virus (HCV), the causative agent of cirrhosis and hepatocellular carcinoma, which infects millions of individuals worldwide. Initial studies reported strong associations between SNPs in interleukin-28B gene (IL28B) and the response to IFNα treatment of HCV (Ge D et al., 2009), and these SNPs were later attributed to spontaneous clearance of HCV (Rauch A et al., 2010). The mechanisms underlying the association between *IL28B* polymorphism and HCV treatment response and clearance remain unrevealed. However, the anti-HCV activity *in vitro* of IFNα and IL-28B (also known as IFNλ3) by distinct but complementary mechanisms is widely recognized (Marcello T et al., 2006). The key role of IFNλ signalling in the host control of HCV infection raised the hypothesis to combine the use of IFNα and IFNλ as therapeutic application. The interest in the role of individually rare and large-effect variants in susceptibility to common disease was particularly relevant to infectious disease, as it parallels the description of an increasing number of single-gene defects underlined specific infectious-disease phenotypes. A famous example is represented by herpes simplex virus-1 (HSV-1) infection that is widespread in children, but the life-threatening complication herpes simplex encephalitis (HSE) develops in only a small minority of individuals. Zhang SY et al. in 2013 demonstrated that HSE may result from single-gene inborn errors of TLR3-mediated immunity in some children with homozygous or heterozygous mutations of genes belonging to the TLR3 pathway (such as *TLR3*, *TRIF*, *TRAF3*, *UNC93B1* and *TBK1*). As TLR3 was expressed on CNS cells that were permissive for HSV-1 infection, its association with HSE was phenotypically analysed by using patient-specific iPSC (Lafaille FG et al., 2012). High susceptibility to HSV-1 infection in patient-specific iPSC–derived UNC-93B- and TLR3-deficient neurons and oligodendrocytes was demonstrated. Impaired CNS–intrinsic TLR3–dependent interferon (IFN)-α/β and IFN-λ immunity to HSV-1 was therefore linked to HSE in children with TLR3 pathway deficiencies. Surprisingly, human patients with inborn errors of TLR3 immunity (that acts against many viruses), who suffered from HSE, remained normally resistant to other common viruses

(Zhang SY et al., 2007). A further example of the using of iPSCs as a model to study the individual genetic susceptibility to infectious diseases was the study of life-threatening influenza during primary infection, performed in 2015 by Ciancanelli MJ et al. The pathogenesis of most cases of life-threatening influenza among children remains largely unexplained. However, as monogenic inborn errors in genes involved in immunity against a few other viruses may underlie life-threatening, isolated diseases in otherwise healthy children (Casanova JL and Abel L, 2013), they hypothesized that severe influenza affecting healthy children may also result from single-gene inborn errors of immunity. They firstly performed whole-exome sequencing (WES) in a 7-year-old girl who have developed influenza in the course of primary infection with pandemic H1N1 (pH1N1) 2009 influenza A virus (IAV) at the age of 2.5 years, prior to any influenza vaccination. The analysis reported compound heterozygous null mutations in transcription factor interferon regulatory factor 7 (IRF7), whose role in amplify interferon (IFN) production in response to viruses was well-known (Honda K et al., 2005). Considering that IAVs in humans firstly target the entire respiratory tract, especially pneumocytes, they generated patient-specific pulmonary epithelial cells (PECs) from induced pluripotent stem cells (iPSCs) reprogrammed from primary fibroblasts of the young girl patient, in order to confirm phenotypically the genetic causative trait. Patient-specific iPSCs–derived pulmonary epithelial cells produced reduced amounts of type I IFN and displayed increased influenza virus replication, suggesting that amplification of type I and III IFNs was strictly dependent on IRF7 and was required for protection against primary infection by influenza virus in humans.

Although the studies based on iPSCs reported in the literature are very few in comparison with the numerous applications for other inherited and degenerative diseases, the results achieved in virology are remarkable. Considering moreover all the clinical observations of the high variability of infectious disease phenotypes in different individuals, it is believable that host genetic background plays a crucial role in the outcome of many infections and that the spectrum of genetic polymorphisms and mutations associated with viral disease phenotypes is larger than currently known. As iPSCs carry the same genotype as donor individuals, they provide a potentially valuable tool for understanding the genetic basis and the mechanisms of individual susceptibility or resistance to infectious disease and can be used to derive relevant cell types to model virus–human cell interactions and patient-specific viral disease outcome.

2. RATIONALE

The observation that some infectious diseases seem to have an inherited component is not new, since many infections induce clinical diseases only in a proportion of exposed individuals. The different outcomes, such as the resolution of infection, clinical worsening to severe disease or progression from acute to persistent infection that occur following viral infection, can be at least partly explained by human genetic variations. Large-scale screening on gene function, performed *in vitro* or in animal models, have been done to identify candidate genes related to innate immunity and infection susceptibility (Petrova E et al., 2019; Kenney AD et al., 2017; Manet C et al., 2018). Some phenotype-association studies have been done on blood cells (Lee MN et al., 2014), but this approach cannot be applied to diseases whose phenotype is restricted to specific tissues or organs that can't be easily accessed *in vivo* (brain, heart, liver). Susceptibility of CNS cells to viral infection is a major determinant to clinical outcome, but little is known about the molecular factors involved in this vulnerability. Neurotropic viruses use different mechanisms to infect and spread among different subtypes of neural cells, to establish acute or persistent infection, and to cause neural cell injury (Chen T et al., 2019). A comprehensive understanding of viral infection in neural cells and cellular response to viral infection might be useful to identify shared and virus-specific mechanisms of neural injury and to identify potential molecular targets for therapy. Mosquito-borne flaviviruses, such as West Nile virus (WNV), Zika virus (ZIKV) and Usutu virus (USUV), which generally cause mild illness or asymptomatic infections in humans, can cause serious neuroinvasive diseases in a small percentage of infected individuals. WNV may cause meningoencephalitis or acute flaccid paralysis in less than 1% of infected patients; ZIKV may cause fetal microcephaly in about 5% of infections acquired during pregnancy and 1 in 10,000 infected adults develop Guillain-Barré syndrome; and the emerging USUV may rarely cause human encephalitis or meningitis.

Aim of this research project is to develop a patient-specific *in vitro* platform, based on human induced pluripotent stem cells (hiPSCs), to model and investigate the mechanisms of variations in human susceptibility and innate immune restrictions to neurotropic WNV, ZIKV and USUV infections (Trevisan M et al., 2015). WNV infection provide a good model for the study of phenotypic variations since many studies in animal models have already identified a set of candidate genes involved in host restriction of WNV infection, that could be studied in human cell models (Clark DC et al., 2012).

For these purposes, two categories of WNV-infected individuals were analysed: blood donors with asymptomatic infection and young and immunocompetent patients who developed West Nile encephalitis without co-morbidity. Patient-specific hiPSCs were generated by Sendai virus-based cell reprogramming and then differentiated into neural stem cells (NSCs), which are one of viral target cells *in vivo*. These patient-specific models were applied to study the correlations between infection outcomes (neuroinvasive disease vs asymptomatic, or persistent vs acute infection), gene expression (with particular focus on innate immunity pathways), and genetic background (related to the innate immune response).

3. MATERIALS AND METHODS

3.1 Cell lines

3.1.1 Vero cells

African green monkey (also known as *Cercopithecus aethiops*) kidney (Vero) cells were maintained at 37°C in Dulbecco's modified Eagle medium (DMEM, Thermo Fisher Scientific, Waltham, USA) supplemented with 10% Fetal Bovine Serum (FBS, Gibco, Thermo Fisher Scientific).

3.1.2 Peripheral blood mononuclear cells (PBMCs)

Human peripheral blood mononuclear cells (hPBMCs) are circulating cells such as monocytes, macrophages and lymphocytes, characterized by having a round nucleus. Once isolated from the whole blood, mononuclear cells were cultured in suspension with the erythroblast proliferation culture medium (Expansion medium, EM, see table 3.1), in order to select erythroblasts population. Blood from two healthy donors with asymptomatic WNV infection and two patients who developed WNV-related encephalitis was collected and processed.

3.1.3 Irradiated CF1 Mouse Embryonic Fibroblast (MEFs)

CF1 Mouse embryonic fibroblasts (MEFs, Thermo Fisher Scientific) were employed as feeder cells to support the culture of human induced pluripotent stem cells (hiPSCs), as they are able to maintain their naïve pluripotent state by secreting growth factors, including leukemia inhibitory factor (LIF), fibroblast growth factor (FGF), and bone morphogenetic protein (BMP) (Eiselleova et al., 2008; Talbot et al., 2012, Llames et al., 2015;). MEFs are isolated from outbred CF1 mice, expanded for up to three passages and mitotically inactivated via gamma irradiation. Before plating MEFs, the surface of each culture vessels was coated with porcine gelatin 0,1% (Merck Millipore, Darmstadt, Germany) and left to polymerize for 30 minutes at 37°C, after this incubation, gelatin solution was removed and replaced with MEF medium (see table 3.2). The cryovial containing inactivated MEFs was removed from liquid nitrogen and rapidly thawed in a water bath at 37°C and centrifuged at 1100 rpm for 5 minutes at room temperature (RT). The supernatant was aspirated, and cell pellet was resuspended in pre-warmed MEF medium. MEFs were then plated in gelatin-coated 6-wells plates at a concentration of approximately $1,5x10^5$ cells/well and incubated at 37°C and 5% CO_2. They were ready to use after 24 hours.

3.1.4 Human Induced Pluripotent Stem Cells (hiPSCs)

Human induced pluripotent stem cells (iPSCs) were generated by cell reprogramming using vectors based on Sendai virus (see paragraph 3.2.2). iPSCs colonies were grown on MEF-feeder layer with iPS medium (see paragraph 3.1.3 and Table 3.3) or on extracellular matrix, such as Matrigel substrate (Corning Inc., Tewksbury, USA) with serum-free StemMACS iPS-Brew XF medium (Miltenyi Biotec, Bergisch Gladbach, Germany) supplemented with 1% Penicillin/Streptomycin (Thermo Fisher Scientific) (see paragraph 3.1.4.2).

3.1.4.1 Culture of hiPSCs on MEF feeder

To maintain and expand hiPSC colonies, cells were cultured with iPS medium (see table 3.3), with a daily medium change. To expand colonies, cells were detached from the feeder using Collagenase IV enzyme (Gibco), isolated from *Clostridium histolyticum*. Collagenase IV is a protease able to degrade, at physiological temperature and pH, the triple-helical native collagen fibrils commonly found in many tissues. After a wash with Dulbecco's phosphate buffer saline (DPBS, Thermo Fisher Scientific) 1 mg/ml of Collagenase IV was added to the cells and incubated at 37°C for 10 minutes, then the enzyme was discarded and 1 ml of iPS medium without basic fibroblast growth factor (b-FGF, ORF Genetics, Kopavogur, Iceland) was added. Cells were then scraped to detach the clumps from the well; the medium containing the cell suspension was then aspirated and centrifuged at 1100 rpm for 5 minutes at RT to allow the removal of supernatant. Clumps were then resuspended in iPS medium with 10 ng/ml of b-FGF and plated at the desired concentration in MEFs pre-coated multi-wells plates.

3.1.4.2 Culture of iPSCs clones on Matrigel

Matrigel (Corning Inc, USA) is an extracellular matrix, which replace animal-derived MEF feeder, which retain the xenogeneic components that may contaminate iPSC cultures *in vitro* (Martin et al., 2005; Villa-Diaz, 2013). Matrigel is a soluble form of basement membrane purified from Engelbreth-Holm-Swarm (EHS) mouse sarcoma (Xu et al.,2001) and it is composed of approximately 60% laminin, 30% collagen IV, 8% entactin that acts as a bridge between laminin and collagen IV, heparan sulfate proteoglycan (perlecan), TGFβ, epidermal growth factor, insulin growth factor, fibroblast growth factor, tissue plasminogen activator, other growth factors and residual matrix metalloproteinases, which occur naturally in the EHS tumor. Matrigel was stored at -80°C and, when necessary, it was thawed overnight at 4°C, resuspended in DMEM/F12 at a concentration of 10µl/ml, and then plated into the multi-well

plate. After one hour DMEM/F12 was replaced with StemMACS iPS-Brew XF medium (Miltenyi Biotec), which was employed to culture hiPSC on Matrigel matrix. This medium has the advantage of being serum-free and containing bovine albumin that helps cells in their metabolic and biosynthetic activity, proliferation, and survival. It allows an efficient expansion of iPSCs over multiple passages while maintaining a pluripotent phenotype as well as pluripotent differentiation potential.

Two enzymatic methods were used to expand hiPSC on Matrigel, including Dispase II enzyme (Gibco) and StemPro Accutase enzyme (Gibco). Dispase II was used for routine passages of hiPSC growing in clumps. hiPSC colonies were washed with DPBS, then covered with 2 U/ml of pre-warmed Dispase solution and incubated at 37°C. After 5 minutes, the amino-endo peptidase was discarded and colonies were detached from the well using a scraper. Cells were pelleted by centrifugation, then resuspended in fresh StemMACS medium and plated on Matrigel pre-coated wells.

Single hiPSCs were obtained and maintained by StemPro Accutase cell dissociation reagent. hiPSC colonies were washed once with DPBS, then covered with the enzyme and incubated for 10 minutes at 37°C until individual single cells start to round up. 5 volumes of DPBS were added to the plate surface and cell suspension was collected and pelleted by centrifugation. StemMACS medium supplemented with 10µM ROCK Inhibitor (StemMACS™ Y27632, Miltenyi Biotec) was used to resuspend the cells that could be plated on Matrigel-coated wells. From the day after, medium had to be changed daily.

3.1.4.3 Freezing and thawing of iPSC clones

To freeze the iPSCs, cells were detached using the desired enzymatic method, as previously described, and resuspended in 1 ml of freezing solution, composed by 50% of iPS medium without b-FGF and 40% of filtered FBS and 10% of dimethyl sulfoxide (DMSO; Sigma-Aldrich). Cells were aliquoted into cryovials and placed into a cooler at -80°C. After 24 hours, cryovials were moved into liquid nitrogen at - 200°C for long time storage.

In order to thaw the iPSCs, cells were recovered from liquid nitrogen and rapidly thawed at 37°C, then resuspended in iPS medium to dilute DMSO, centrifuged for 5 minutes at 1100 rpm at 4°C and resuspended in iPS medium with 10 ng/ml of b-FGF , then plated on MEF coated wells. The overnight treatment with the ROCK inhibitor Y27632 at a final concentration of 10 µM is also required at the time of plating to prevent cell death.

3.2 Reprogramming of erythroblasts

3.2.1 Isolation of circulating mononuclear cells

Venous blood was collected from patients and healthy donors in 0,129 M trisodium citrate to avoid platelet aggregation. PBMCs were separated from other blood components (plasma, erythrocytes, platelets) using Ficoll-Paque Plus (Merck Millipore). Whole blood was first mildly centrifuged at 1000 rpm for 10 minutes at RT without brake to separate platelet-rich plasma (PRP) from other blood components. The blood sample was diluted with PBS and carefully stratified onto the Ficoll-Paque media solution to avoid mixing the two phases, then centrifuged 30 minutes at 1800 rpm at RT (brake should be turned off) in order to separate PBMCs from red blood cells (RBCs) and granulocytes. The thin mononuclear cell layer at the interface was collected and diluted with PBS in a sterile tube, then centrifuged at 1500 rpm at RT for 10 minutes to recover the cell isolate. After two PBS washes the mononuclear cells were resuspended in erythroblast proliferation culture medium (Expansion medium, see table 3.1). Culture medium was changed every 3 days and after 8-10 days most of the cells reached the erythroblast stage.

3.2.2 Reprogramming with Sendai virus

hiPSC colonies were generated by transduction of erythroblasts population with recombinant non-integrating Sendai viral vectors. Transduction was performed with CytoTune-iPS Sendai Reprogramming Kit (Thermo Fisher Scientific), that provided four vectors, each expressing one of the four Yamanaka factors (Oct3/4, Sox2, Klf4 and c-Myc). The vials contained about 100 µl of the reprogramming vectors at a concentration of about $\geq 3\times10^7$ cell infectious units/ml (CIU/ml). Reprogramming protocol published by Yang et al., 2012 was applied with some modification.

After 8 days of PBMCs culture in Expansion Medium (EM), a large population of erythroblasts was obtained and transduction with Sendai virus vectors was performed. $2x10^5$ cells were transduced with the four viral vectors at a multiplicity of infection (MOI) of 10. After addition of viral vectors, cells were plated in 6-well plates with EM and spinoculated at 2250 rpm for 90 minutes at RT to support gene delivery, and then incubated for 2 hours at 37°C. After the incubation, cells were centrifuged at 1500 rpm for 10 minutes at RT to eliminate the excess viral vectors, resuspended into EM and plated on MEF coated wells. The plate was centrifuged at 500 rpm for 30 minutes at RT in order to enhance cells adhesion and finally incubated at

37°C, 5% CO_2. Two days after transduction, EM was substituted with FBS-iPS medium (see table 3.4) with the addition of growth factors included in the expansion medium (see table. 3.1). On the fourth day post transduction (p.t.), growth factors were withdrawn and at the 6th day pt., medium was switched with 1:1 FBS-iPS and iPS media. After 8 days pt, cells were fed only with iPS medium with 10 ng/ml of b-FGF (see table 3.3) and changed daily. When colonies started to emerge (usually after 15/20 days pt.), they were picked with a pipette, plated into a MEF-coated 6 well with iPS medium with the addiction of b-FGF at 10 µM final concentration and ROCK Inhibitor at 10µM final concentration and then expanded. Fig. 3.1 summarize the main steps of the reprogramming protocol.

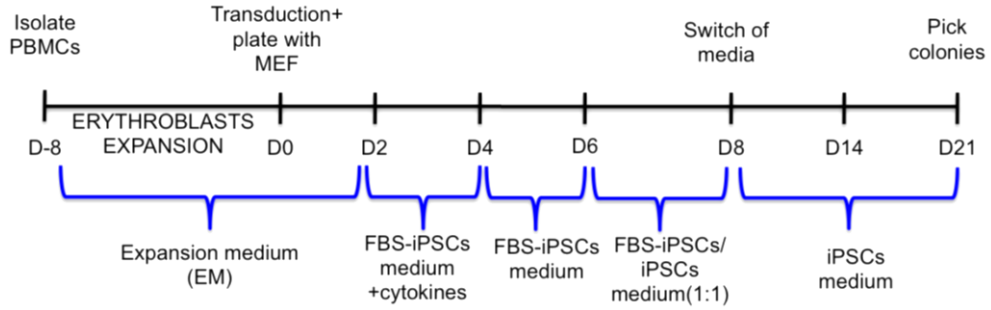

Fig 3.1 Reprogramming steps.

3.3 Differentiation of hiPSC into Neural Stem Cells

When hiPSC clumps on Matrigel substrate reached a confluency of 15-25%, the spent medium was aspirated to remove the non-attached cells and 2.5 mL of pre-warmed complete PSC Neural Induction Medium (see table 3.5) were added to each well of the 6-well plates. On day 1 of neural induction, the morphology of the cells was checked for its homogeneity to proceed with the differentiation, otherwise all unwanted colonies were removed by using a Pasteur glass pipette to aspirate the cells from the marked colonies. Cells were then maintained with an every-other-day medium change of 2.5mL/well on 6-well plates, for 7 days. On day 7, neural stem cells (NSCs) (P0) were ready to be harvested and expanded. The PSC Neural Induction Medium was removed from the well and after a washing with 1 ml of DPBS, cells were detached in single cells using StemPro Accutase enzyme (Thermo Fisher Scientific) and incubated for 10 minutes at 37°C until most cells detach from the surface of the culture vessels. 5 volumes of DPBS were then added on each well to dilute the enzyme and then the cells were collected and centrifuged for 5 minutes at 1200 rpm at RT. After a washing with DPBS, supernatant was discarded and the NSCs were resuspended in pre-warmed Neural

Expansion Medium (see table 3.6). Cells were counted and diluted to plate the cells at a density of 0.5×10^5–1×10^5 cells/cm^2 on wells previously coated with Geltrex matrix (Thermo Fisher Scientific). ROCK inhibitor Y27632 was added to the cell suspension to a final concentration of 5 µM and after overnight incubation, the medium was changed to complete Neural Expansion Medium to eliminate the ROCK inhibitor Y27632. Thereafter, the Neural Expansion Medium was exchanged every other day without ROCK inhibitor. Usually NSCs reached confluency on days 4–6 after plating and when NSCs reached confluency, they can be further expanded in complete Neural Expansion Medium, cryopreserved or differentiated into specific neural cell types. The overnight treatment with the ROCK inhibitor Y27632 at a final concentration of 5 µM is required to avoid apoptosis until passage 4 (P4 NSCs). Below it is reported a schematic representation (Fig. 3.2) of the neural differentiation protocol of hiPSC.

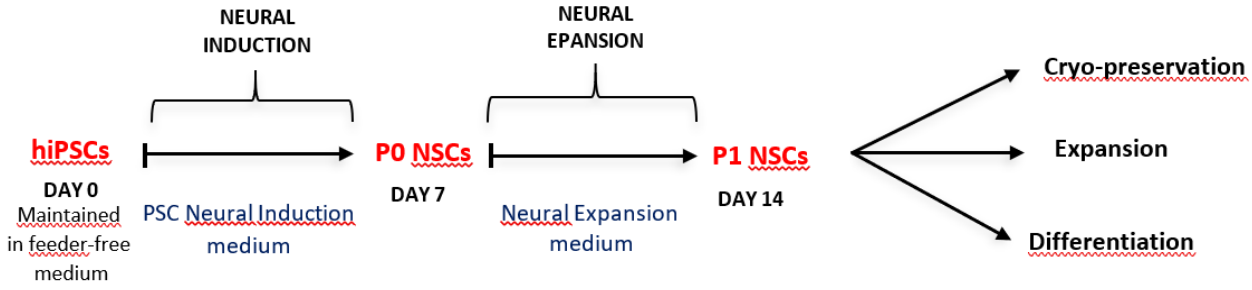

Fig 3.2 Workflow of NSC derivation from hiPSCs.

3.4 Media

3.4.1 Expansion Medium (EM)

EM was used to expand PBMCs towards the erythroblast lineage.

Expansion Medium	Final concentration
Iscove Modified Eagle Medium (Euroclone, Milan, Italy)	
L-Ascorbic Acid (Sigma-Aldrich, Merck Millipore Darmstadt Germany)	50 µg/ml
SCF (Stem Cell Factor, ISOkine, ORF Genetics, Kopavogur, Iceland)	50 ng/ml
IL-3 (Recombinant human Interleukyne 3, R&D Systems, Minneapolis, USA)	10 ng/ml

EPO (Erythropoietin, R&D Systems)	2U/ml
IGF-1 (Human recombinant insulin-like growth factor-1, R&D Systems)	40 ng/ml
Dexamethasone (Merck Millipore)	1µM

Table 3.1 EM medium.

3.4.2 MEF Medium

MEF medium was used to thaw and seed MEFs.

MEF Medium	Final concentration
DMEM (Dulbecco's Modified Eagle Medium, Thermo Fisher Scientific)	
Filtered FBS (Gibco, Thermo Fisher Scientific)	10%
GlutaMax 100x (Gibco)	1%
Penicillin/Streptomycin (Gibco)	1%

Table 3.2 MEF medium.

3.4.3 iPS Medium

IPS medium was employed to grow colonies on MEF feeders.

iPS Medium	Final concentration
DMEM/F-12, GlutaMAX supplement (Gibco)	
KnockOut Serum Replacement (Gibco)	20%
Non-Essential Amino Acids (NEAA, Gibco)	1%
GlutaMax 100x (Gibco)	1%
Penicillin/Streptomycin (Gibco)	1%
β-mercaptoethanol (Merck Millipore)	0.1%

Basic-FGF (ISOkine, ORF Genetics) had to be added daily to avoid it lose its activity, in a concentration of 10 ng/ml.

Table 3.3 iPS medium.

3.4.4 FBS-iPS Medium

FBS-iPS medium was used during the first days after reprogramming.

FBS-iPS Medium	Final concentration
DMEM/F-12, GlutaMAX supplement (Gibco)	
Filtered FBS (Fetal Bovine Serum, Gibco)	20%
Non-Essential Amino Acids (NEAA, Gibco)	1%

GlutaMax 100x (Gibco)	1%
Penicillin/Streptomycin (Gibco)	1%
β-mercaptoethanol (Merck Millipore)	0.1%
b-FGF (ORF Genetics)	10 ng/ml
L-Ascorbic Acid (Merck Millipore)	50 ug/ml

Table 3.4 FBS-iPS medium.

3.4.5 PSC Neural Induction Medium

PSC Neural Induction Medium is a serum-free neural induction medium, which can differentiate human PSCs into NSCs in one week.

PSC Neural Induction Medium	Final concentration
Neurobasal Medium (Gibco)	
Neural Induction Supplement 50X (Gibco)	2%
Penicillin/Streptomycin (Gibco)	1%

Table 3.5 PSC Neural induction medium.

3.4.6 Neural Expansion Medium

Neural Expansion Medium was employed to expand the NSCs.

Neural Expansion Medium	Final concentration
Neurobasal Medium (Gibco)	50%
Advanced DMEM/F-12 (Gibco)	50%
Neural Induction Supplement 50X (Gibco)	2%
Penicillin/Streptomycin (Gibco)	1%

Table 3.6 Neural Expansion medium.

3.5 Characterization of hiPSCs and hiPSC-derived NSCs

3.5.1 Analysis of gene expression by RT-PCR and qRT-PCR

3.5.1.1 RNA extraction, quantification and reverse transcription

Efficient purification of total RNA from cell pellets was obtained by using RNeasy Mini Kit (Qiagen, Netherlands) that combine the stringency of guanidine-isothiocyanate lysis with the speed and purity of silica-membrane purification. Samples were first lysed and then homogenized. Ethanol was added to the lysate to provide ideal binding conditions. The lysate was then loaded onto the RNeasy silica membrane RNA binds (up to 100 µg capacity), thus all

contaminants were efficiently washed away. The pure, concentrated RNA was eluted in 30 µl of water. RNA quantification was assessed with Nanodrop 1000 spectrophotometer (Thermo Fischer Scientific) that allows quantifying RNA concentration starting from 2 µL of sample. A $A_{260/280}$ratio of 1.9–2.1 (measured in 10 mM Tris-·Cl, pH 7.5) was required to proceed with the experiments. To eliminate any residue of DNA that can generate a false positive signal in RT-PCR applications, a DNase treatment of the samples was performed using TURBO DNA-free kit (Ambion, Thermo Fisher Scientific). TURBO™ DNase is a recombinant, engineered form of DNase I that allows the complete digestion of DNA along with the removal of the enzyme and divalent cations post-digestion. After treatment, the concentration of purified RNA was checked through NanoDrop 1000 spectrophotometer.

1 µg of extracted RNA was reverse transcribed using the recombinant RNA-dependent DNA polymerase MuLV Reverse Transcriptase combined with reagents according to table 3.7. All reagents came from Applied Biosystem (Thermo Fisher Scientific).

Reagent	Amount
Buffer 10X	6 µL
MgCl_2 Solution	11 µL
dNTPs	1 µL
Random hexamers	2 µL
RNase inhibitor	1 µL
M-Mulv Reverse Transcriptase	1.25 µL

Table 3.7 Reverse Transcription Reaction Mix

A final volume of 60 µL was reached with the addition of DEPC water. The reaction mix was incubated according to table 3.8.

25°C	48°C	95°C	4°C
10 min	60 min	5 min	∞

Table 3.8 cDNA synthesis reaction temperature and incubation profile

3.5.1.2 RT-PCR analysis

The end-point RT-PCR was performed to evaluate the expression of the specific markers that characterize the reprogrammed iPSCs and the differentiated NSCs:

- Pluripotency genes: OCT4, NANOG, DNMT3B, TERT, REX1 and SOX2;

- Genes of the three embryonic germ layers: The ectoderm (TUBB and PAX6), the mesoderm (PECAM, CDH5, GATA2 and FLK1) and the endoderm (AFP and GATA4);
- Neural Stem Cells genes: NESTIN, PAX6, SOX1, SOX2;

The expression of the housekeeping gene ACTIN was analyzed to normalize the data. 100 ng of cDNA template was combined with 45 µL of the reaction mix, according to table 3.9. All reagents came from Applied Biosystem.

Reagent	Amount
Buffer 10X	5 µL
MgCl_2	3 µL
dNTPs	4 µL
Primer Fw	1 µL
Primer Rw	1 µL
AmpliTaq Gold™ polymerase	0,25 µL
Milli-Q water	30,8 µL

Table 3.9 RT-PCR Reaction mix

The reaction mix was incubated according to table 3.10.

Stage 1	95°C for 10 min
Stage 2 35-40 Cycles	95°C for 30 s (D*enaturation step*) XX°C for 30 s (*Annealing step*) 72°C for 30 s (*Elongation step*)
Stage 3	72°C for 7 min

Table 3.10 RT-PCR reaction temperature and incubation profile

The annealing temperature (XX) and the number of cycles were different according to the type of primers used.

RT-PCR products were resolved by electrophoresis on 1,5% agarose (Lonza, Switzerland) gel and visualized by UV exposition via the GelDoc 2000 (Bio-Rad, CA, USA) device and analyzed with Image Lab 4.1 software.

3.5.1.3 Real-time quantitative PCR

Real-time qPCR analysis was performed using the 7900HT Fast Real-Time PCR System instrument (Applied Biosystem) to study the expression of hiPSC genes OCT3/4, NANOG and SOX2.

For each reaction, 100ng of cDNA were used in a total volume of 25 µL of a mix composed by TaqMan Universal PCR Master Mix (Applied Biosystem), the primer pairs (10 µM) and the associated FAM-MGB probe (5µM) as described in table 3.11.

Reagent	Amount
Universal TaqMan master mix 2X	12,5 µL
Primer Fw	1 µL
Primer Rw	1 µL
Probe	1 µL
Milli-Q water	4,5 µL

Table 3.11 TaqMan real-time qPCR reagent mix

The reaction mix was incubated according to table 3.12. All results were normalized to human ACTIN gene and analyzed using ΔCt method.

Stage 1	50 °C for 2 min 95°C for 10 min (P*olymerase activation*)
Stage 2 *40 cycles*	95 °C for 15 s (D*enaturation phase*) 60 °C for 1 min (A*nnealing and elongation phase*)
Stage 3	Gradient: 60-95 °C for 30 min (M*elting*)

Table 3.12 Real-time qPCR reaction temperature and incubation profile

3.5.2 Indirect Immunofluorescence assays (IIF)

Cells were fixed with 4% paraformaldehyde (PFA; Merck Millipore) in PBS for 20 minutes at RT. To permeabilize the membranes, cells were washed three times with PBS/0.05% Tween 20 (Merck Millipore) and then treated with PBS/0.1% Triton X-100 (Merck Millipore) for 15 minutes at RT. After three washes with PBS/0.05% Tween 20, cells were blocked with 4% Bovine Serum Albumin (BSA, Merck Millipore) in PBS at RT for 1h and incubated with the primary antibodies (diluted in PBS with 4% BSA) at 4°C overnight. To analyze the expression of proteins which characterized hiPSCs, we used primary antibodies specific for Oct4 (goat, 1:200, Santa Cruz Biotechnology), Nanog (mouse, 1:100, Merck Millipore), Ssea4 (mouse,

1:50, Abcam, England), Klf4 (rabbit, 1:50, Santa Cruz Biotechnology) and Sox2 (rabbit, 1:50, Merck Millipore). To characterize hNSCs we used antibodies anti-Pax6 (rabbit, 1:100, Merck Millipore) and anti-Nestin (mouse, 1:100, Abcam) while to evaluate the presence of viral particles we employed a specific antibody for Flavivirus Envelope protein E (clone 4G2, mouse, 1:500, Merck Millipore, USA). To remove the unbounded antibodies, the wells were washed three times with PBS/0.05% Tween 20 and the secondary antibody, diluted in PBS 1X, was added and incubated in the dark at RT for 1h. The secondary antibodies used included the anti-mouse IgG Alexa Fluor-488 (goat, 1:250, Thermo Fisher Scientific) and the anti-rabbit IgG Alexa Fluor-546 (goat, 1:250, Thermo Fisher Scientific). After incubation, the wells were washed three times with PBS/0.05% tween 20 and the cell nuclei were stained with the intercalating 1000x 4',6-diamidino-2-phenylindole (DAPI, 1:1000, Thermo Fisher Scientific) or DRAQ5 Fluorescent probe solution (1:2000, Thermo Fisher Scientific) for a far-red DNA stain. Cells were visualized under a fluorescent microscope (Leica) with 20x magnification or a confocal microscope (Leica) with 20x and 63x magnification.

3.5.3 Embryoid bodies test

The embryoid bodies (EBs) test is an assay that evaluates the ability of iPSC clones to differentiate into the three germ lineages: ectoderm, mesoderm and endoderm. This is achieved through formation of embryoid bodies, i.e. aggregates of pluripotent stem cells that differentiate randomly towards all lineages. The hiPSC clones growing on MEFs were washed with PBS and detached from the well with collagenase IV as previously described. Cell clumps were resuspended in iPS medium without b-FGF to prevent retention of staminality and plated in Ultra Low Attachment Plates (Corning Inc.) to let them grow in suspension. The medium was changed every three days and after seven days, EBs were collected with a pipette and moved to a 6-well plate coated with porcine gelatin 0,1% (Merck Millipore). Briefly, 1 ml per well of porcine gelatin was added to a 6-well plate and let polymerize for 20 minutes at RT. After incubation, gelatin solution was removed and DMEM with 10% FBS was added to the well. Medium was changed every three days. After a week, cells were detached with 0,05% trypsin-EDTA (Gibco) by incubation at 37°C for 5 minutes and then diluted with two volumes of DMEM 10% FBS medium to inactivate the effect of trypsin. Cells were then centrifuged at 1200 rpm for 5 minutes at RT to eliminate the solution, washed with PBS and centrifuged again to obtain a cell pellet. Total RNA was extracted from the pellet as previously described and

reverse transcribed to cDNA. RT-PCR analysis allowed to assess expression of the three germ layers markers: Ectoderm, Mesoderm and Endoderm (see paragraph 3.5.1.2).

3.6 Viral strains

Three neurotropic flaviviruses grown on the permissive Vero cell line were employed for infection experiments: Zika virus, West Nile virus and Usutu virus.

3.6.1 Zika virus

The Zika virus (ZIKV) isolate that was used in experiments belonged to contemporary Asian lineage, strain DOM/2016/PD2 (GenBank KU853013). This strain was isolated from the saliva of a traveler returning from the Dominican Republic to Italy in January 2016 (Barzon et al., 2016). It was adapted in the laboratory and expanded on Vero cells. It gave cytopathic effect (CPE) in cell culture *in vitro*, evidenced by spacing between cells, roundish and non-adherent cells and a period of 5-6 days of incubation was required before the manifestation of the cytopathic effect. A security level of 2 (BSL2) is recommended in handling the virus. A viral titer of 1 x 10^6 50% Tissue Culture Infective Dose (TCID50)/mL was obtained.

3.6.2 West Nile virus

Two reference laboratory-adapted strain of West Nile virus (WNV) were used in the experiments reported below:

- WNV lineage 2 strain AUT/08 (GenBank KF179640) isolated from a goshawk in Austria, 2008 and kindly provided by Prof. N. Nowotny. Viral stocks were produced and titered in the permissive Vero cells. The titer of this virus obtained was 1,7 x 10^7 pfu/mL.
- WNV lineage 1 strain ITA/09 (GenBank GU011992). It was the first human West Nile virus isolated in Italy in 2009 and was expanded on Vero cells reaching a titer of 2 x 10^7 pfu/mL.

A period of 2-3 days of incubation in *in vitro* cell culture was required before the manifestation of the cytopathic effect with cell rounding, progressive degeneration and detachment. A security level of 3 (BSL3) is recommended in handling the virus.

3.6.3 Usutu virus

Usutu virus (USUV) belonged to Europe 1 lineage, strain Vienna 2001 (GenBank AY453411) and was isolated from Eurasian Blackbird (isolate 939/01) from Vienna. It was kindly provided by Prof. N. Nowotny from the University of Vienna. It was adapted in the laboratory and expanded on Vero cells obtaining a viral titer of 3,6 x 10^6 pfu/mL. Vero cells usually started to manifest cytopathic effect (CPE) after 3-4 days of viral incubation. A security level of 3 (BSL3) is recommended in handling the virus.

3.7 Viral Production and determination of viral titer

3.7.1 Production of ZIKV, WNV and USUV viral stocks

To produce concentrated viral stock of ZIKV (such as WNV and USUV), 5 plates of permissive Vero cells at a confluence of 70% were expanded and infected. Cells were preliminarily washed twice with DMEM with antibiotics without FBS, in order to eliminate the FBS used in the culture medium that could hinder the virus from entering the cells. The infection was carried out with 7 mL of the supernatant of the first passage of the virus isolated on Vero and diluted 1:7; subsequently, cells were incubated at 37 ° C in a 5% CO_2 atmosphere for 90 minutes. At the end of the incubation, 8 mL of DMEM were added with antibiotics supplemented with 2% FBS. After 4-5 days, in the presence of a cytopathic effect (CPE) on about 90% of the cell monolayer, the virus was collected and purified. The infected cells were mechanically detached by scraper, collected in sterile 50mL Falcon type tubes and subjected to a thermal shock cycle (they were placed in a freezer at -80 ° C until completely frozen and, then, thawed in a 37 ° C bath, then centrifuged at 3000 rpm for 10 minutes to remove cellular debris. The supernatant containing concentrated virus wss divided into individual 1 mL aliquots in sterile freezing tubes and stored at -80 ° C.

3.7.2 Determination of viral titer

Viral titration was performed on infected Vero cells through 50% Tissue Culture Infective Dose ($TCID_{50}$) assay and Plaque Forming Assay.

3.7.2.1 50% Tissue Culture Infective Dose ($TCID_{50}$)

ZIKV, WNV and USUV viral stock was serially diluted in DMEM with 1% Pen/Strep, in a range between 10^{-3} and 10^{-10}, and inoculated on Vero-P cells seeded in 96 well tissue culture plate ($1,5x10^4$ cells/well). 10 wells were infected with each dilution of viral stock. After an incubation

of 1h 30 minutes at 37 °C in 5% CO2, DMEM with 6% FBS and 1% Pen/Strep was added to each well. When the presence of CPE was evident, usually after 4-5 days depending on the virus, crystal violet fixing/staining solution (Merck Millipore) was added to each well and incubated at RT for 30 minutes. The plate was washed two times in tap water by immersion in a large beaker, and then could air dry at RT. $TCID_{50}$ was assessed by presence or absence of the deep purple color in each well. The viral titer was calculated by *Spearman-Kärber algorithm*.

$$T=10^{1+d(S-0.5)+1}\ TCID_{50}/mL$$

Where *d* represents Log10 of the dilution and *S* is the sum of wells with CPE for a specific dilution factor.

3.7.2.2 Plaque Forming Assay

WNV and USUV viral titer was expressed as Plaque-Forming Units per mL (PFU/mL). Monolayers of Vero cells was seeded in duplicate in 6 well plates and after 24h they were infected with serial 10-fold dilutions of viral stocks and incubated for 1h 30 minutes at 37°C in 5% CO_2. The inoculum was removed and MEM 2X containing 4% FBS and 50% agarose was added to each well and incubated at 37°C. After 72h, MEM 2X containing 4% FBS and 50% agarose with 0.003% Neutral Red Dye (Merck Millipore) was added to each well followed by an incubation at 37°C for 24 h and the plaques were counted.

3.8 Viral infection and analysis of virus replication kinetics

3.8.1 Infection of iPSC-derived NSCs

In order to infect the NSCs at different multiplicity of infection (MOI; ratio of virus to infection target cells) the viral stock was serially diluted in DMEM with 1% Pen/Strep, and a lysate from uninfected Vero-P cells was used as a mock control. hiPSC-derived NSCs growing on Geltrex in serum-free Neural Expansion Medium were infected at MOI of 0.01, 0.1, and 1 with virus diluted in DMEM as previously described, when confluency of 30% was reached. After virus inoculation, cells were incubated at 37°C, with 5% CO_2 for 90 minutes to allow the adsorption of the virus. At the end of the incubation, the viral medium was aspirated and replaced with the respective growth media. The cells were incubated at 37°C, with 5% CO_2. Supernatants of infected cells were collected at different time points and growth media were replaced every day. The supernatants were used for viral titer measurement either by real-time quantitative PCR (qPCR) or TCID50. Infected cells were either detached with StemPro Accutase treatment

for the gene expression studies or fixed with 4% PFA in PBS to perform indirect immunofluorescence (IIF) assay. The same procedure was followed to infect hNSCs with ZIKV, WNV and USUV.

3.8.2 Analysis of virus replication kinetics

The replication kinetics of ZIKV, WNV and USUV were measured on infected hNSCs supernatants and cell lysates collected at different time p.i. by using quantitative real-time RT-PCR (qRT-PCR) and $TCID_{50}$ assay.

3.8.2.1 Quantitative real-time RT-PCR

The supernatants of hNSCs infected with ZIKV, WNV and USUV at different MOIs were collected every day until day 7 p.i. and inactivated by MagNA Pure 96 lysis buffer (Roche Diagnostic, USA). The nucleic acid purification from samples of 200 µL was performed by the Roche MagNA Pure 96 System (Roche Diagnostic) and pipetted into a 96-well processing cartridge. A one-step RT-PCR was subsequently performed through the 7900HT Fast Real-Time PCR System instrument (Thermo Fisher Scientific) using primers and TaqMan-probe sets specific for ZIKV NS5 (Lanciotti et al., 2007), WNV NS5 (Linke et al., 2007) and USUV NS5 (Cavrini et al., 2011). Both nucleic acid purifications and PCR analyzes were performed at least in duplicate to confirm the results and at each run three negative controls containing water were added to verify that there were no contaminations. A sample was considered positive for the presence of viral genomic sequences when all the repeated tests gave concordant positive results. The sensitivity of the real-time PCR assay was estimated to be approximately 5 copies of genome per reaction.

3.8.2.2 50% Tissue Culture Infective Dose ($TCID_{50}$)

Supernatants of hNSCs infected with ZIKV, WNV and USUV at different MOIs were collected at different time points p.i. Scalar dilutions in base 10 in DMEM with antibiotics, were prepared up to 10^{-8}dilution and inoculated on Vero-P cells seeded in 96 well tissue culture plate ($1{,}5x10^4$/well) in triplicate and then the procedure described in section 3.7.2.1 was completely followed

3.9 Real-time quantitative PCR for the analysis of the antiviral innate immune response genes expression

Variations in the expression of some genes involved in the immune and inflammatory reactions were evaluated using real-time quantitative RT-PCR. The pellets of hNSCs infected with ZIKV (MOI 1), WNV (MOI 0.01) and USUV (MOI 1) were collected at 96h pi and the total RNA was isolated from the cells using RNeasy Mini Kit and reverse transcribed to cDNA. The immune response genes analyzed included: *IFIT1, IFIT2, MDA5, RIG-I, TLR2, TLR3, TLR7, TLR8, MAVS, IL-1β, CASP1, CASP3, NF-kβ, TNFα, C-GAS, IRF3, IRF7, VIPERIN, IFN-α, IFN-β, IFNλ1, IFNλ2, IFNλ3* (see table 3.13).

Gene	Primer Fw	Primer Rw	Probe-dye	Exon-exon primer	Lenght (bp)	Ref.
RIG1	ACCAGAGCACTTG TGGACGCT	TGCCGGGAGGGTC ATTCCTGT	sybr green	Yes (exon 13-15)	126	Webster Marketon et al., 2014
MDA5	CAGAAGGAAGTG TCAGCTGCTTAG	TGCTGCCACATTCT CTTCATCT	sybr green	Yes (exon 4-5)	107	Joseph B. Prescott et al.,2007
CGAS	CCTGCTGTAACAC TTCTTAT	TTAGTCGTAGTTGC TTCCT	sybr green	No	148	Yugen Zhang et al., 2014
TLR3	GAAAGGCTAGCA GTCATCCA	CATCGGGTACCTGA GTCAAC	sybr green	Yes (exon1-2)	170	Abrahams VM et al., 2012
TLR7	CTTGGCACCTCTC ATGCTCT	GTCTGTGCAGTCCA CGATCA	sybr green	Yes	227	Yu-Lin Hsu et al., 2016
TLR8	AGTTTCTCTTCTC GGCCACC	GGAACATGTTTTCC ATGTTTCTGT	sybr green	Yes	103	Yu-Lin Hsu et al., 2016

TLR2	GGCCAGCAAATTACCTGTGTG	AGGCGGACATCCTGAACCT	fam-CCATCCCATGTGCGTGG-mgb	No	67	Sha Q et al., 2004
MAVS	AGCAAGAGACCAGGATCGACTG	CGCAATGAAGTACTCCACCCA	sybr green	Yes (exon 2-3)	118	Joseph B. Prescott et al.,2007
NFKB	GCCAACAGATGGCCCATACC	TGCTGGTCCCACATAGTTGC	sybr green	Yes (exon2/3-5)	169	Zong C et al., 2019
IRF3	AGCAGAGGACCGGAGCAA	AGAGGTGTCTGGCTGGGAAA	fam-ACCCTCACGACCCACATAAAATCTACGAGTTTG-tamra	yes (exon3-4)	94	Thornik Reimer et al., 2007
IRF7	TACCATCTACCTGGGCTTCG	AGGGTTCCAGCTTCACCA	sybr green	yes (exon 9-10)	83	Joseph B. Prescott et al.,2007
TNF-alpha	CCAGACCAAGGTCAACCTCC	CCCTCCCAGATAGATGGGCT	sybr green	No	106	Yunfei Qin et al., 2016
IFNA1	AGAATCTCTCCTTTCTCCTG	TCTGACAACCTCCCAGGCAC	sybr green	No	369	Teng TS et al., 2012
IFNB1	GAGCTACAACTTGCTTGGATTCC	CAAGCCTCCCATTCAATTGC	fam-ACAAAGAAGCAGCAATTTTCAGTGTCAGAAGCT-tamra	No	83	Thornik Reimer et al., 2007
IFNλ1	GAGGCCCCCAAAAAGGAGTC	AGGTTCCCATCGGCCACATA	sybr green	Yes (exon4/5-5)?	104	Yu-Lin Hsu et al., 2016

IFNλ2	AATTGTGTTGCCAGTGGGGA	GCGACTGGGTGGCAATAAAT	sybr green	No	84	Yu-Lin Hsu et al., 2016
IFNλ3	AGGGCCAAAGATGCCTTAG	CAGCTCAGCCTCCAAAGC	sybr green	Yes (exon2/3-4)	132	Yu-Lin Hsu et al., 2016
IFIT1	TCTCAGAGGAGCCTGGCTAA	TGACATCTCAATTGCTCCAG	sybr green	Yes (exon 1-2)	118	Yu-Lin Hsu et al., 2013
IFIT2	AAGAGTGCAGCTGCCTGAA	GGCATTTTAGTTGCCGTAGG	sybr green	Yes (exon 1-2)	112	Yu-Lin Hsu et al., 2013
RSAD2	CTTTGTGCTGCCCCTTGAG	TCCATACCAGCTTCCTTAAGCAA	sybr green	No	63	Dill MT et al., 2011
CASP1	AAGACCCGAGCTTTGATTGACTC	AAATCTCTGCCGACTTTTGTTTCC	sybr green	Yes (exon2-4/5)	297	Lianglian g Niu et al., 2015
CASP3	TGCATACTCCACAGCACCTG	TTCTGTTGCCACCTTTCGGT	sybr green	Yes (exon7-8)	154	Nakajim a R et al., 2017; Hai-Bo Xing et al., 2018
IL1B	GAGCAACAAGTGGTGTTCTCC	AACACGCAGGACAGGTACAG	sybr green	Yes (exon5/6-6)	110	Riedmai er I et al., 2009
GAPDH	GAAGGTGAAGGTCGGAGTC	GAAGATGGTGATGGGATTTC	fam-CAAGCTTCCCGTTCTCAGCC-tamra	Yes (exon1-3)	322	Gordon FE et al., 2010

Table 3.13 Sequences of the oligonucleotide primers employed for the immune response analysis.

Genes were amplified with Fast SYBR Green Master Mix (Thermo Fisher Scientific) as described in table 3.14:

Reagent	Amount
Fast SYBR Green Master Mix 2X	12,5 µL
Primer Fw (10 µM)	1 µL
Primer Rw (10 µM)	1 µL
Milli-Q water	10,5 µl

Table 3.14 Fast SYBR Green real-time qPCR reagent mix

The reaction mix was incubated according to table 3.11. and the results were normalized to Human Glyceraldehyde-3-phosphate dehydrogenase (GAPDH) and analyzed using ΔΔCt method (Livak et al., 2011). All assays were performed in triplicate and repeated in three independent experiments.

3.10 Apoptosis assay

The activity of Caspase 3 was measured at 72h and 96h p.i. in mock control and in hNSCs infected with ZIKV and WNV at MOI 1.

Cells were plated in 12 wells tissue culture plates at a density of $7x10^4$ cells/well, in quadruplicate. Infected cells growing on Geltrex substrate were washed with PBS, detached from the wells with StemPro Accutase as previously described (see paragraph 3.3), and fixed with 4% PFA in PBS for 10 minutes at 37°C and 1 minute on ice. PFA was removed and the cells were permeabilized in ice-cold 90% methanol for 30 minutes on ice and stored at -20°C overnight.

The day after, cells were washed twice with incubation buffer (PBS with BSA 0.05%) to remove methanol and then, incubated 1h at RT with anti-cleaved Caspase-3 primary antibody (Cell Signaling Technology, USA) diluted 1:100 in incubation buffer. Cleaved Caspase-3 (Asp175) Antibody detected endogenous levels of the large fragment (17/19 kDa) of activated caspase-3 resulting from cleavage adjacent to Asp175, thus it did not recognize full length caspase-3 or other cleaved caspases. After washing three times with incubation buffer, cells were resuspended in PBS for data acquisition with Becton Dickinson LSR II Flow Cytometer (BD Bioscience, USA). Data analysis was performed using Flowing software.

3.11 MTT assay

The MTT (3-(4, 5-dimethylthiazolyl-2)-2, 5-diphenyltetrazolium bromide) assay is a colorimetric assay for measuring cell metabolic activity (Stockert et al., 2018). It is based on the ability of (NADPH)-dependent cellular oxidoreductase enzymes to reduce the yellow

water-soluble tetrazolium dye MTT to insoluble purple colored formazan crystals which are then quantified by absorbance. This assay therefore measures cell viability in terms of reductive activity as enzymatic conversion of the tetrazolium compound to water insoluble formazan crystals by dehydrogenases occurring in the mitochondria of living cells (Stockert et al., 2012).

Cell survival was evaluated by MTT assay in mock and hNSCs infected with ZIKV, WNV and USUV (MOI 0.1 and 1) plated in 96 well tissue culture plate (at a density of $8x10^3$ cells/well). Freshly dissolved solution of MTT (5mg/mL, AppliChem) in PBS was added to infected cells at 72h and 96h p.i. and after an incubation of 4 hours at 37 °C, a solubilization solution (10% sodium dodecyl sulfate (SDS) and 0.01 M HCl) was added. After an overnight incubation at 37 °C, absorbance was read at 620 nm to assess the production of formazan. All data of mock and infected samples were normalized to blank corresponding to medium without cells. The ratio between infected sample and mock, after normalization, provided the percentage of cell survival.

3.12 Whole-exome sequencing (WES) by NGS

Sequencing by next-generation sequencing (NGS) technology of a panel of 2250 genes involved in innate immunity was performed on DNA extracted from four patient-specific iPSCs. With WES, the protein-coding portion of the genome is selectively captured and sequenced. The exome represents less than 2% of the human genome, but contains most of the known disease-causing variants, making whole-exome sequencing (WES) a cost-effective alternative to WGS (Van Dijk et al., 2014).

DNA extraction was carried out using QIAamp®DNA kit (Qiagen) following manufacturer's instructions. DNA was eluted in a volume of 50 µl and its concentration and purity were measured loading 1 µl of the sample to the NanoDrop 1000 Spectrophotometer. Prior to NGS, target enrichment on DNA samples was conducted with SeqCap custom probes (Roche). Pools of biotinylated oligonucleotide probes specific for exome regions of interest were hybridized to a sequencing library in solution. Next, the biotinylated probe/target hybrids were pulled down by streptavidin-coated magnetic beads to obtain libraries highly enriched for the target regions. Library preparation was done with KAPA DNA Library Preparation Kits (KapaBiosystems, Roche). Library size was determined using Bioanalyzer system (Agilent Technologis, CA, USA) and library quantification using NEBNext Library Quant Kit (BioLabs). Sequencing was conducted using Illumina Miseq and MiSeq Reagent Kit v2-150 bp (Illumina,

USA). A combination of various existing analysis packages (Bamtools, Samtools, Vcftools), various in-house written scripts and database like HG38, dbSNP, Ensembl were used to complete the analysis.

In order to study single nucleotide polymorphisms (SNPs) or mutations found in the analysis, servers such as Mutation Tasting, Mutation Assessor and SIFT have been consulted. These servers predicted whether an amino acid substitution affects protein function based on sequence homology and the physical properties of amino acids. The functional impact was assessed based on evolutionary conservation of the affected amino acid in protein homologs.

3.13 Statistical analysis

Data were presented as mean value ± standard deviation (SD). Statistical analysis was conducted using an unpaired Student's t-test and the statistical significance was defined as $p < 0.05$.

4. RESULTS

4.1 Modelling patient-specific susceptibility to flavivirus infections

Human pathogens cause disease through a complex interplay with the host that involves both pathogen virulence mechanisms and abnormal host responses. *In vitro* model systems to study the interaction between pathogens and human cells and tissues are limited because of tissue scarcity and challenges in the set-up of primary cultures. The induced pluripotent stem cell (iPSC) technology offers the possibility to set up *in vitro* cell cultures derived from normal human cells to grow viruses that can infect only in specific human cell types, sometimes inaccessible, such as neural cells. In addition, the iPSC technology allows generating *in vitro* patient-specific cell cultures, which can be used to investigate the genetic basis and the mechanisms of individual susceptibility or resistance to infectious diseases.

In this study, to investigate the mechanisms of individual susceptibility to severe West Nile virus (WNV) disease, we derived iPSCs from the erythroblasts of individuals who had a previous history of confirmed WNV infection. Study subjects included two blood donors with asymptomatic WNV infection (the derived cell lines were named Asympt 1 and Asympt 2, respectively) and two patients with West Nile neuroinvasive disease (WNND) without comorbidities or risk factors like old age and immunosuppression (the derived cell lines were named WNND 1 and WNND 2, respectively). Demographic and clinical features of study subjects are summarized in table 4.1.

ID	Subject characteristics	Infection	Symptoms
Asympt 1	Healthy male in his late 40s	WNV lineage 2 infection in 2016	asymptomatic
Asympt 2	Healthy male in his late 40s	WNV lineage 2 infection in 2016	asymptomatic
WNND 1	Healthy male in his late 50s	WNV lineage 1 infection in Aug 2012	meningitis, no complete recovery
WNND 2	Healthy male in his late 50s	WNV lineage 2 infection in Sept 2016	severe encephalitis followed by a persistent infection, no complete recovery

Table 4.1 WNV-infected subjects enrolled for the study.

In addition to these individuals, iPSCs were also generated from a patient with symptomatic USUV-infection (USUVsympt cell line): the case was an healthy male in his late 50s, infected with USUV lineage Europe 2 in 2018, who developed arthralgia and myalgia two days after a NAT-positive blood donation.

4.1.1 Generation of human erythroblast-derived iPSC lines using Sendai virus reprogramming system.

Peripheral blood mononuclear cells (PBMCs) were isolated from the peripheral blood of study subjects, expanded and differentiated for 8 days in EM medium in order to obtain a large erythroblast population. Cell reprogramming was performed by transduction of $2x10^5$ erythroblasts with non-integrating Sendai virus vectors expressing the four Yamanaka factors (Oct-3/4, Sox-2, Klf-4 and c-Myc) at a MOI of 10.

The clones obtained from the reprogramming protocol were manually picked and expanded (fig 4.1). For each subject, 10 iPSC clones were collected and frozen for back-up purposes. Among these, 3 clones were characterized for their pluripotency and differentiation potential, and one iPSC clone for each patient was employed in the study.

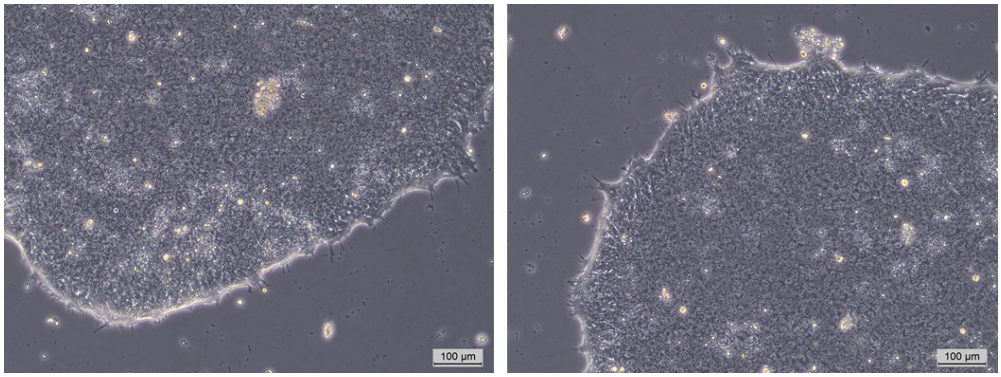

Fig 4.1 hiPSC clones cultured in clumps on feeder-free substrate. The derived hiPSC clones displayed a typical stem cell colony morphology, characterized by a round shape and high nucleus/cytoplasm ratio. Bright light optical microscopy of live, unstained iPSC clones; 10× magnification.

4.2 Characterization of iPSCs clones confirmed the pluripotency status

In order to demonstrate the pluripotency of hiPSC clones, pluripotency tests and *in vitro* differentiation test were performed. These tests included RT-PCR, real-time qPCR, and indirect immunofluorescence (IIF) staining to check for iPSC marker expression, and the embryoid bodies (EBs) assay

4.2.1 Pluripotency tests

After induction of cell reprogramming, distinct markers are sequentially activated or repressed in a fine regulatory system named pluripotency gene regulatory network (PGRN). Differentiation genes are early repressed, while genes essential for pluripotency are activated later. The PGRN receives multiple regulatory inputs in addition to transcriptional regulation. These inputs include translation, post-transcriptional regulation of RNA processing, protein modification and turnover, and epigenetic and metabolic regulation (Li M et al., 2017).

Accordingly, the epigenetic state of somatic donor cells is completely reprogrammed resembling that of embryonic stem cells. Several biochemical and molecular markers have been identified that are specific to hiPSCs; these markers include the nuclear transcription factors Klf-4 and Rex-1, the keratan sulphate antigen Tra-1-60, the glycolipid antigen SSEA4, the human telomerase reverse transcriptase (hTERT) and DNA methyl transferase 3B (Dnmt3b) enzymes. However, only three transcription factors, namely Oct-4, Nanog, and Sox-2, are fundamental to maintain the pluripotent state and proliferative capacity of stem cells and to prevent their differentiation. The highly regulated equilibrium between Oct-4, Nanog and Sox-2 expression represents the core of PGRN (Li M et al., 2017; Ng HH et al., 2011; Nichols J et al., 1998; Masui S et al., 2007; Mitsui K et al., 2003).

4.2.1.1 Expression of iPSC markers in patient-specific clones

In order to test the pluripotent state of patient-specific hiPSCs, clones were seeded onto Matrigel layer (feeder-free substrate) to avoid murine contamination derived from MEF feeder-cells and cultured in StemMACS iPS-Brew XF medium. After 7 days of growth in culture, patient-specific hiPSCs were collected and RNA was extracted, reverse transcribed into cDNA, and amplified by PCR to detect expression of the human pluripotency genes *DNMT3B*, *TERT*, *NANOG*, *OCT4*, *REX1* and *SOX2*, as described in paragraph 3.5.1.1 and 3.5.1.2. Electrophoresis on agarose gel showed the expression of the stemness genes, confirming the pluripotency of each patient-specific iPSC clones (Fig. 4.2).

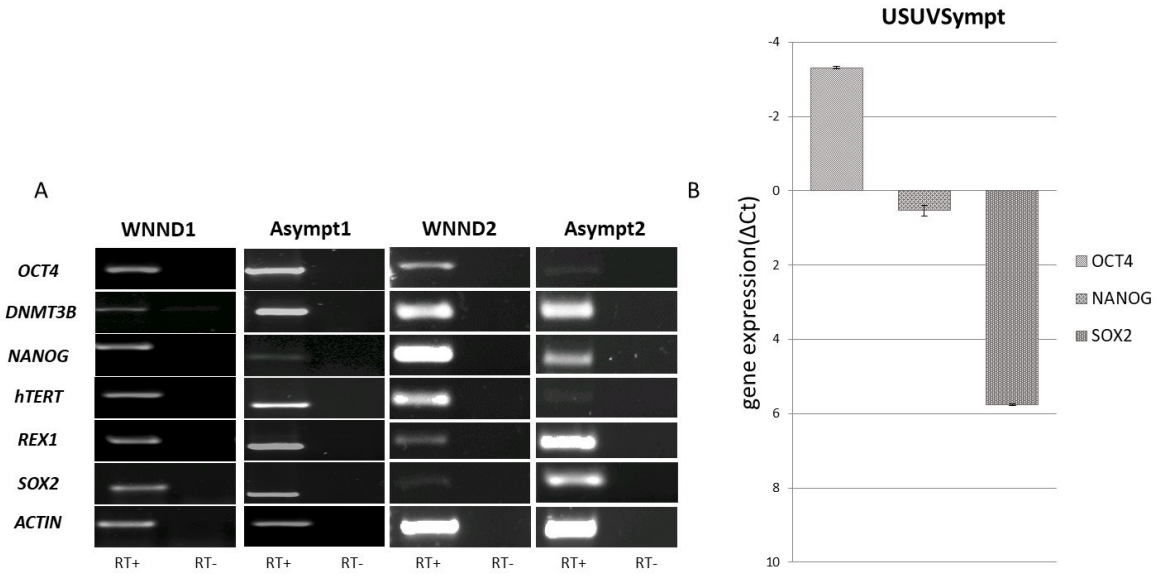

Fig 4.2 RT-PCR products (**A**) and real-time qPCR analysis (**B**) confirmed the expression of pluripotency genes in hiPSC clones derived from two patients with neuroinvasive disease (cell lines WNND1 and WNND2) and two asymptomatic blood donors (cell lines Asympt1 and Asympt2). Real-time qPCR results (Ct values: 24; 27.8; 33 for

the expression of Oct-4, Nanog, and Sox-2, respectively) were normalized on human Actin gene (Ct 27) and expressed as ΔCt. RT: Reverse transcriptase.

The expression of transcription factors Oct-4, Nanog and Sox-2 genes were also confirmed in USUVSympt-derived iPSCs by real-time qPCR (Fig 4.2B), following the methods described in paragraph 3.5.1.3.

Expression of the core transcription factors Oct-4, Sox-2 and Nanog, the nuclear marker Klf-4 and the surface markers Tra-1-60 and SSEA4 was analysed by IIF as described in paragraph 3.5.2. For IIF experiments, patient-specific iPSC lines were grown for 5 days in clumps on MEF-coated 24-well plates (Fig 4.3) and in single-cells on Matrigel substrate (Fig 4.4).
All patient-specific iPSC clones growing on MEF feeder showed intense immunofluorescent staining of pluripotency markers (Fig. 4.3A).

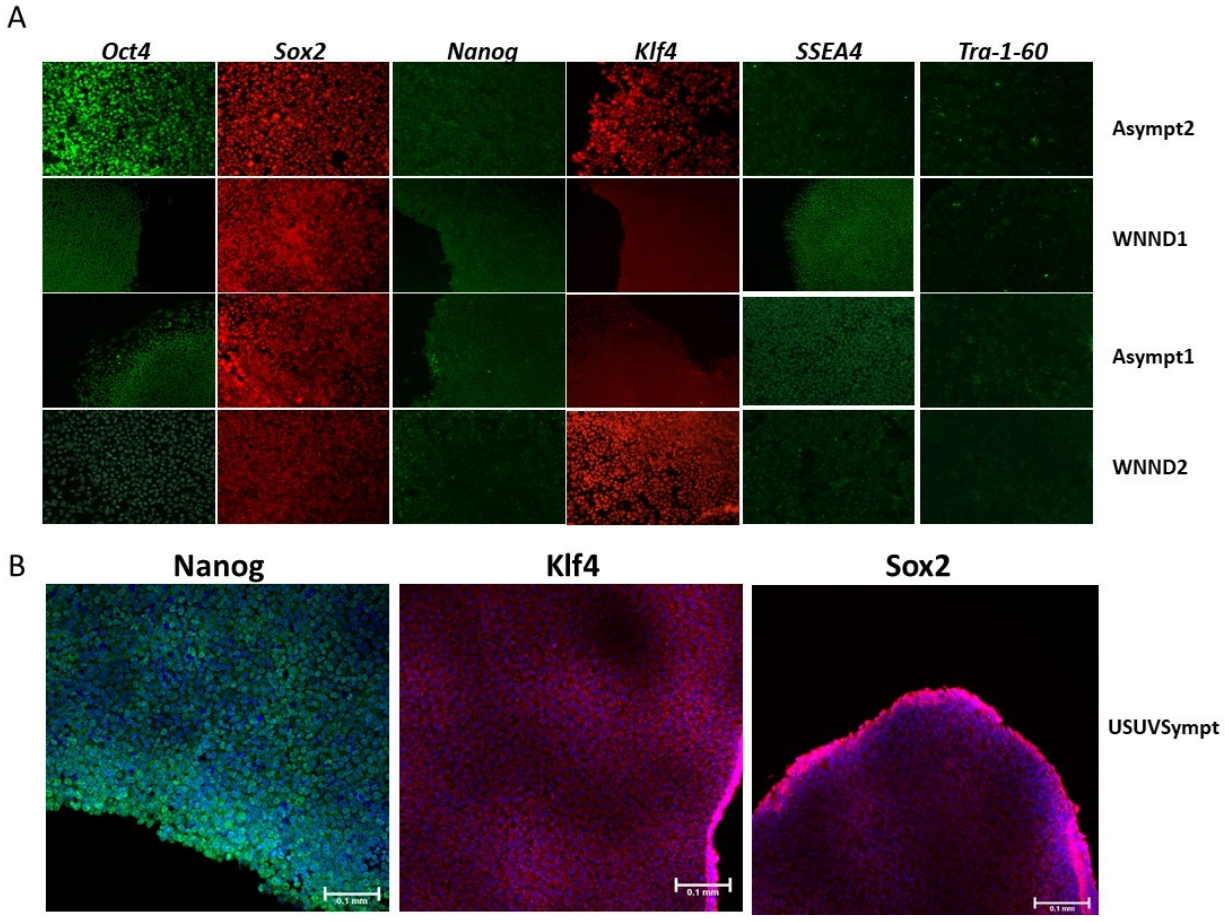

Fig 4.3 IIF analysis of pluripotency markers on patient specific-iPSC clones growing in clumps on MEF feeder. (**A**) Expression of pluripotency markers Oct-4 (green), Sox-2 (red), Nanog (green), Klf-4 (red), SSEA4 and Tra-1-60 (both green) was confirmed in all patient-derived iPSC lines. Nuclei were stained with DAPI (data not shown). Fluorescence microscopy, 10× magnification. (**B**) High fluorescent signals of Nanog, Klf-4 and Sox-2 markers were detected in USUVSympt iPSC line and were represented in the figure as merge with DRAQ5's stained nuclei. Confocal microscopy, 20× magnification.

A similar IIF analysis was performed on patient-specific iPSCs growing as single-cells on Matrigel. By combining primary antibodies of Nanog (mouse) and Sox-2 (rabbit) which were recognized by a goat anti-mouse secondary antibody (Alexa Fluor-488, green) and a goat anti-rabbit secondary antibody (Alexa Fluor-546, red) respectively, the nuclear co-localization of the transcription factors was confirmed. All patient-derived iPSC lines showed a strong immunostaining of Nanog, Sox-2 and Klf-4 (Fig 4.4).

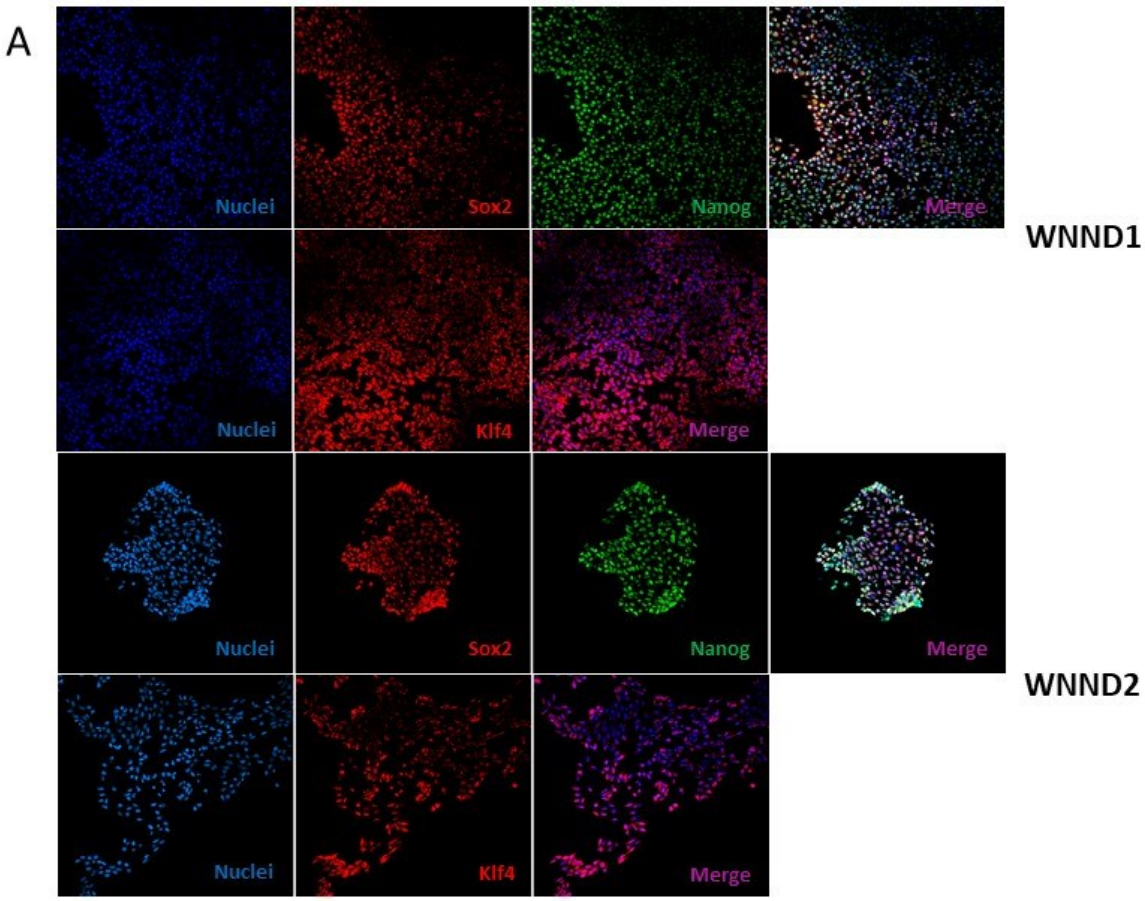

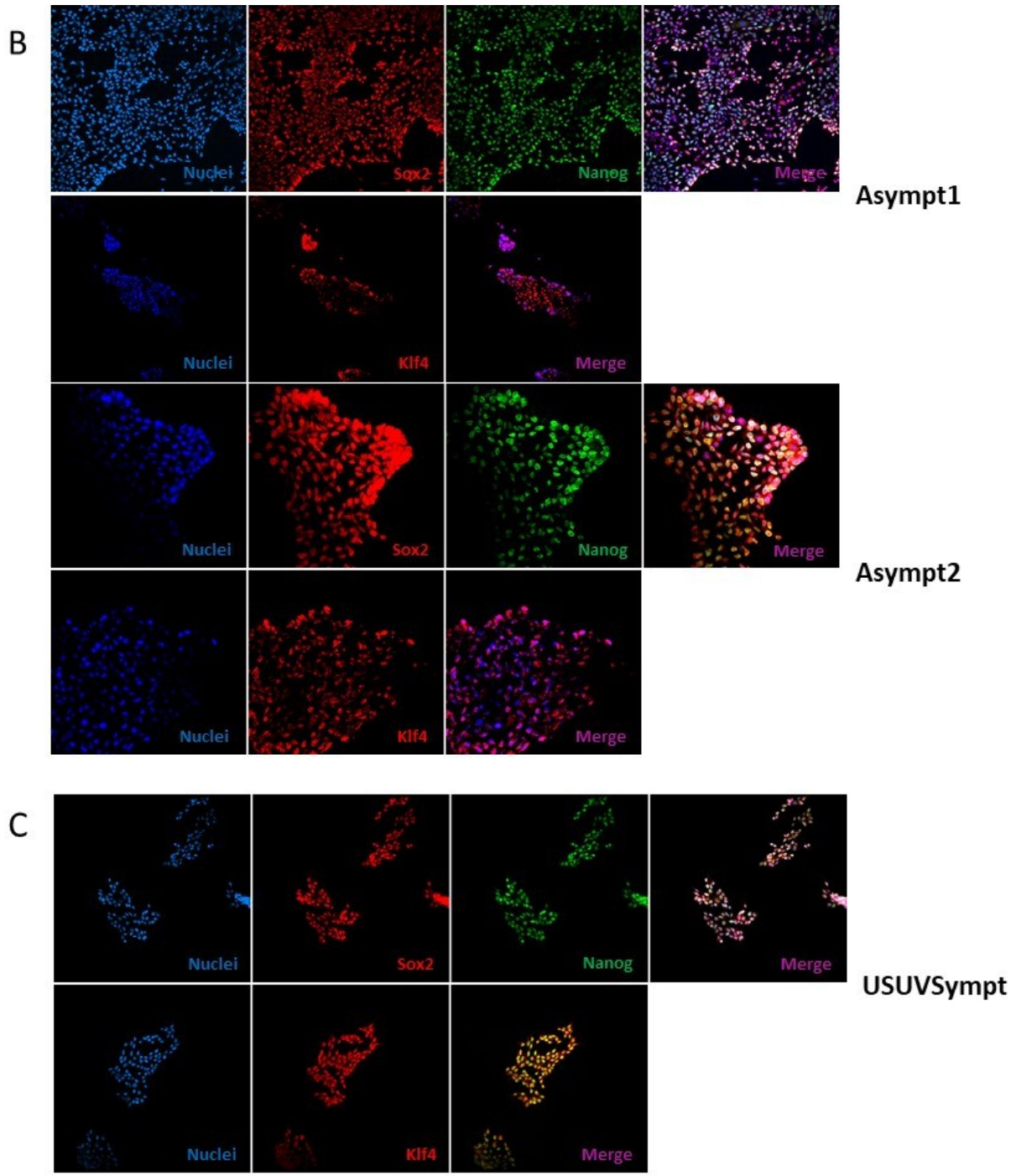

Fig 4.4 IIF analysis confirmed the expression of Sox-2, Nanog and Klf-4 on hiPSC clones derived from two WNV-infected patients with CNS disorders (cell lines WNND1 and WNND2) (**A**), from two blood donors with asymptomatic WNV infection (cell lines Asympt1 and Asympt2) (**B**) and one patient with symptomatic USUV infection (cell line USUVSympt) (**C**). hiPSCs were grown as single cells on Matrigel; nuclei were stained with DRAQ5 and images were acquired by confocal microscope at 20× magnification.

4.2.2 iPSC differentiation potential was validated by EBs test

The ability of hiPSCs to differentiate and form tissues derived from the three primordial germ layers of the embryo (ectoderm, mesoderm, and endoderm) can be shown by the EBs test (see paragraph 3.5.3). Patient-derived hiPSCs were grown in suspension for 7 days in iPS medium without b-FGF so that they form large aggregates called embryoid bodies (EBs).

During this first stage of differentiation, cells started to aggregate, to increase in dimensions and to assume a spherical shape (Fig. 4.5A). Once formed, the EBs were transferred onto 0.1% gelatine pre-coated 6-well plates with MEF medium, to favour differentiation toward a specific cell lineage (Fig. 4.5B).

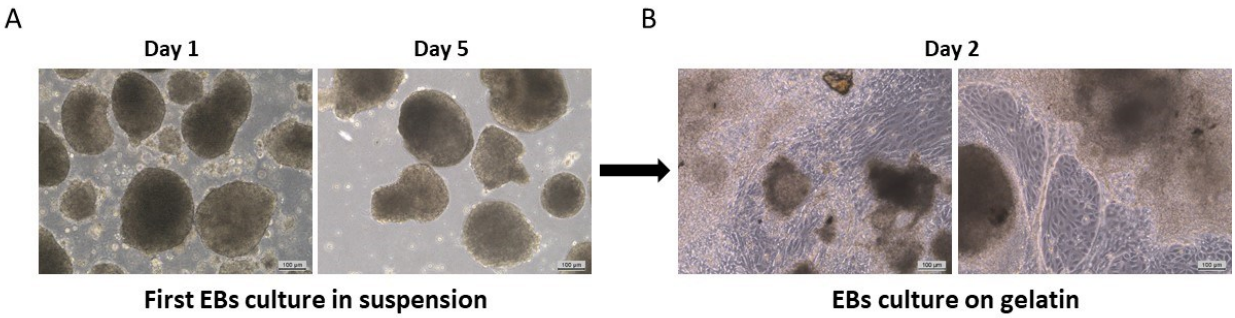

Fig 4.5 Generation of embryoid bodies (EBs) from a representative hiPSCs clone: First stage of differentiation in suspension (**A**) and EBs after adhesion on gelatine coated surfaces (**B**), (20× magnification).

After 7 days of culture on gelatine substrate, cells were harvested to verify by RT-PCR the expression of differentiation genes belonging to the three germ layers: ectoderm (*TUBB*, *PAX6*), mesoderm (*KLF1*, *GATA2*, *PECAM*, *CDH5*) and endoderm (*AFP*, *GATA4*). All the patient-derived iPSC lines expressed the differentiation markers, as shown in Fig 4.6.

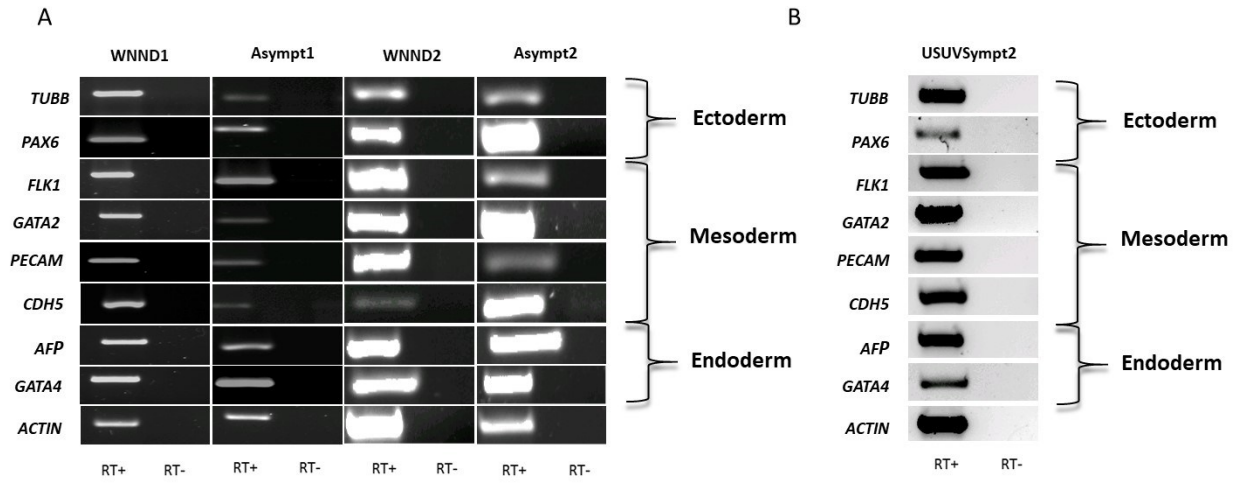

Fig 4.6 EBs test: RT-PCR products of the three germ layers markers confirmed the differentiation potential of iPSC lines derived from WNV-infected patients (**A**) and USUV-infected patient (**B**). RT: Reverse transcriptase.

4.3 Differentiation of patient-specific iPSCs into neural stem cells (NSCs)

To generate patient-specific *in vitro* models of flavivirus infection, patient-derived hiPSCs were differentiated into neural cells. When hiPSCs growing on Geltrex with StemMACs medium reached 15-25% of confluency, culture medium was switched to Neural Induction Medium

(see paragraph 3.3). Approximately 7 days after medium switch, cells with rounded immature neural morphology (i.e., NSCs) appaired and started to grow in monolayer (Fig 4.7). hiPSC-derived NSCs were ready to be expanded and the Neural Induction Medium was replaced with Neural Expansion Medium.

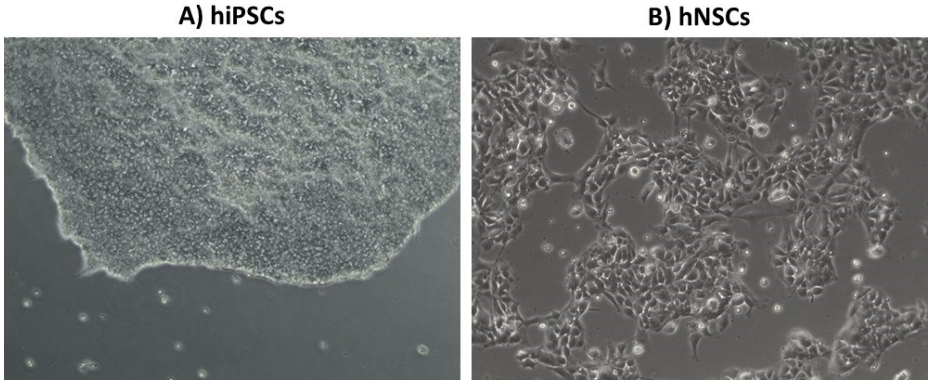

Fig 4.7 Differentiation of hiPSCs into NSCs. **A**) Representative hiPSCs cultured in a feeder-free layer and **B**) NSCs obtained at day 7 of the protocol of hiPSCs differentiation into NSCs. 10× magnification.

4.3.1 Characterization of human neural stem cells (hNSCs) generated from patient-specific iPSCs

Neural stem cells are undifferentiated multipotent precursor cells able to self-renew. NSCs generate clonally related descendants that differentiate to form neurons, astrocytes, oligodendrocytes and ependymal cells. Through symmetric cell division, NSCs maintain the stem cell population in the CNS, while asymmetric cell division produce neural progenitor daughter cell (NPC) with restricted differentiation potential to neuronal and glial lineages.
Several molecular and biochemical markers have been identified that play a crucial role in the maintenance and differentiation of NSCs. These markers include the transcription factor Pax-6 that assess the proper neural, olfactory and ocular development; the intermediate filament Nestin that is downregulated and replaced by tissue-specific filaments in differentiated cells, and the transcription factors Sox-1 and Sox-2 that are essential for maintaining self-renewal of NSCs.
The expression of these neural markers was investigated by RT-PCR analysis and IIF staining to confirm the identity of NSCs generated from patient-specific iPSCs.

4.3.1.1 Expression of NSC markers in hiPSC-derived NSCs was validated by RT-PCR analysis

The expression of neural stem cell genes was evaluated in patient-specific cells cultured on Geltrex in Neural Expansion Medium. hNSCs at passages between 4 and 8 were collected and the RNA was extracted and reverse transcribed into cDNA. Expression of the NSC markers

NESTIN, *PAX*6, *SOX1*, and *SOX2* and the iPSC marker *OCT4* was analysed by RT-PCR, which validated the identity of NSCs derived from all patient (Fig 4.8).

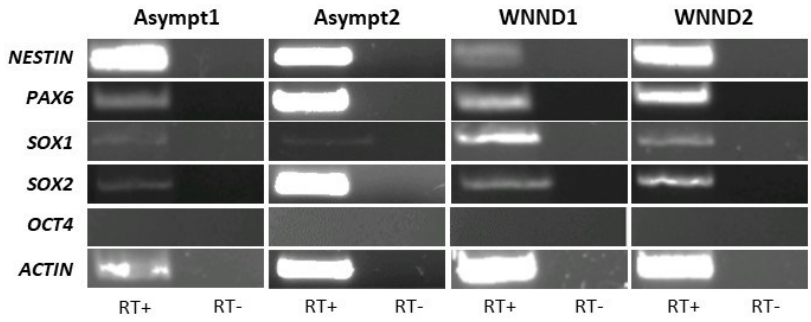

Fig 4.8 Characterization of patient-specific and hiPSC-derived NSCs: RT-PCR products of NSC markers and the pluripotency marker OCT4 analysed in NSCs derived from asymptomatic WNV-infected blood donors (Cell lines Asympt1 and Asympt2) and WNV-encephalitis patients (cell line WNND1 and WNND2). RT: Reverse transcriptase.

4.3.1.2 Expression of NSCs specific markers in hiPSC-derived NSCs was confirmed by indirect immunofluorescence (IIF) assay

Expression of neural marker genes was also confirmed at protein level by IIF analysis. Immunostaining with antibodies specific for intermediate filament protein Nestin and the transcription factor Pax-6 was observed in NSCs derived from asymptomatic blood donors (Fig 4.9A, B and C) and in those derived from WNV encephalitis patients (Fig 4.10).

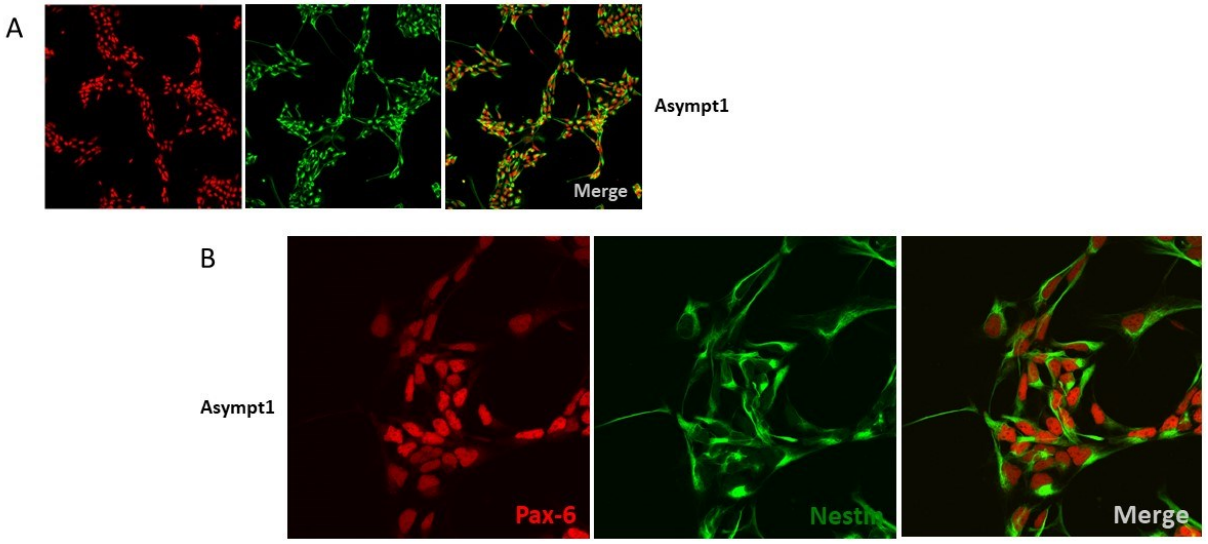

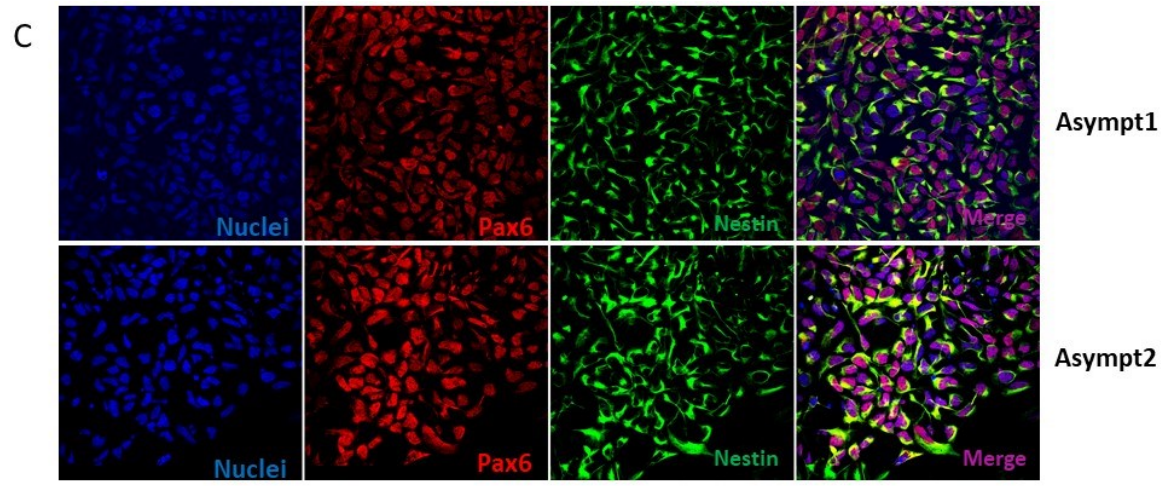

Fig 4.9 Characterization of NSCs derived from asymptomatic blood donors by IIF staining. (**A**) Expression of neural markers Nestin (green) and Pax6 (red) in NSCs derived from Asympt1 iPSC line at 40× magnification and (**B**) 60× zoom 2.5. (**C**) Expression of neural markers in NSCs derived from Asympt1 and Asympt2 iPSC lines at 60× magnification. Nuclei were stained with DAPI.

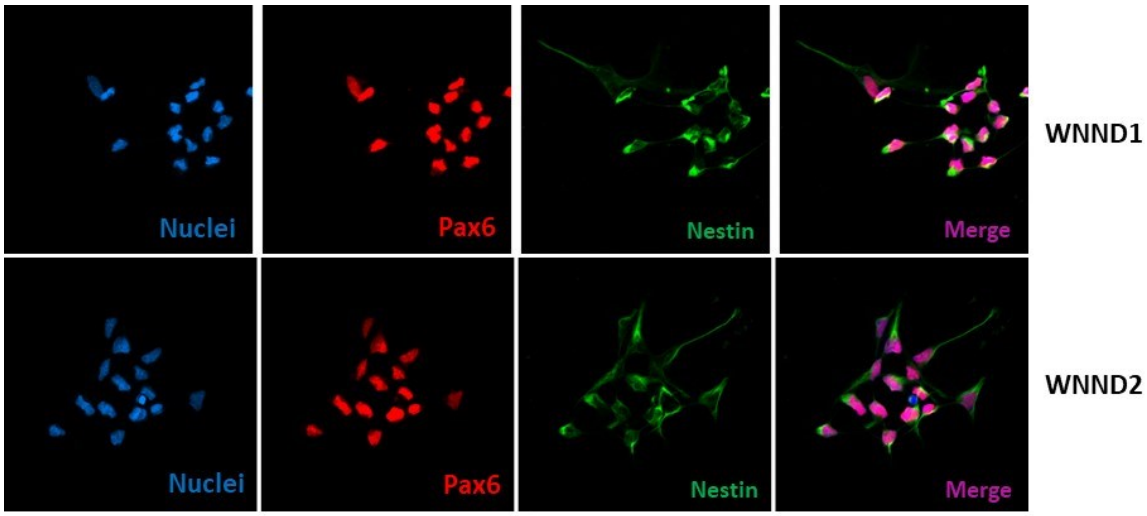

Fig 4.10 Characterization of NSCs derived from WNV-encephalitis patients by IIF staining. Expression of neural markers Nestin (green) and Pax6 (red) in NSCs derived from WNND1 and WNND2 iPSC lines at 40× magnification. Nuclei were stained with DAPI.

4.4 Evaluation and comparison of hNSC susceptibility to flavivirus infection

The reason why some flaviviruses cause severe clinical manifestations only in a small percentage of infected individuals have not been completely elucidated, but host-dependent genetic factors involved in innate antiviral immunity could play a crucial role. One of the central questions in the search for therapeutic targets for the treatment of flavivirus neurological syndromes is whether these diseases are induced by virus-mediated cytolysis, immune-pathological responses to virus infection, or a combination of both. The availability of patient-specific iPSC-derived NSCs represents a fundamental support to solve these issues and to investigate more deeply virus interaction with the human host.

4.4.1 WNV, ZIKV, and USUV productively infect patient-specific iPSC-derived NSCs

To investigate the susceptibility of patient-specific NSCs to flaviviruses, cells derived from asymptomatic blood donors and WNND-patients were infected with WNV, ZIKV and USUV at MOI 1. At 48h pi, cells were immunoassayed with pan-flavivirus antibody targeting the viral envelope (E) glycoprotein and the proportion of infected cells was examined. Cells were fixed in PFA 4%, permeabilized with Triton X-100, and blocked in BSA prior to immunostaining with the pan-flavivirus antibody.

Panels (Fig 4.11) show positive anti-E-immunostaining in NSCs derived from asymptomatic blood donors (Fig 4.11 A and B) and WNND patients (Fig 4.11 C, D and E) infected with ZIKV, WNV and USUV. Immunostaining of neural marker Pax6 was performed to verify that patient specific NSCs retained their differentiation status after infection.

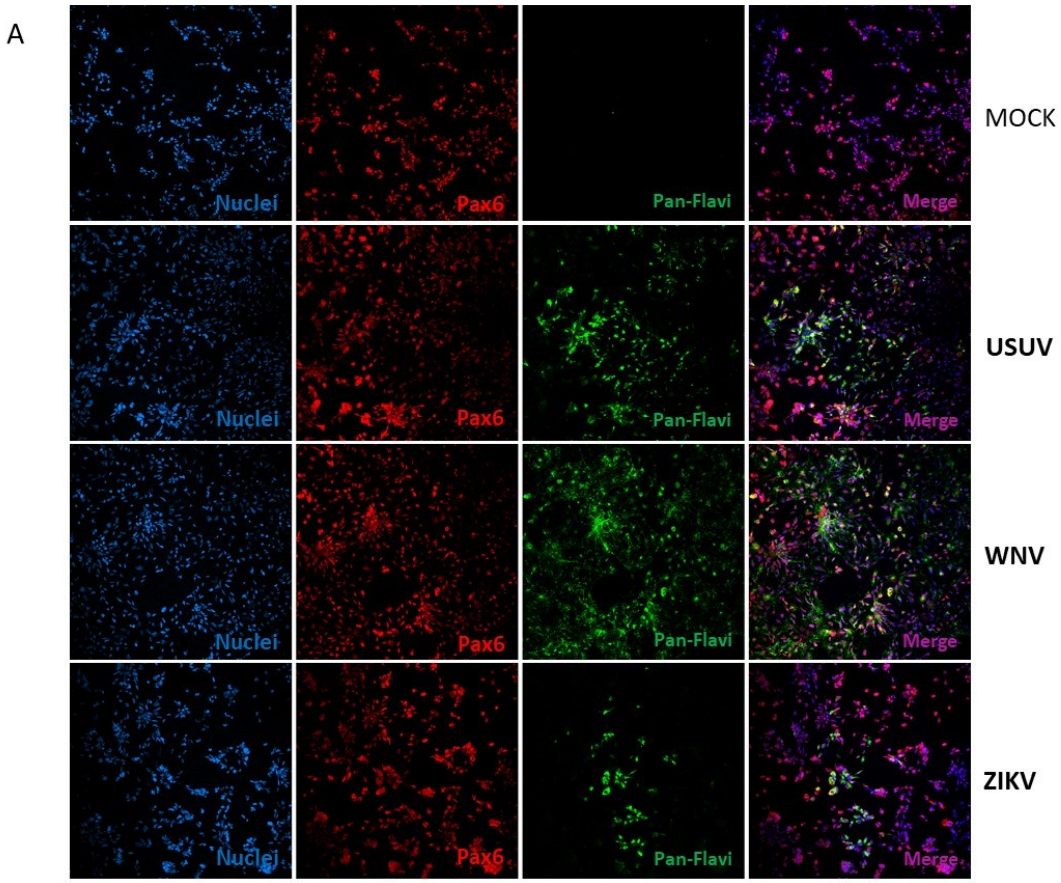

B

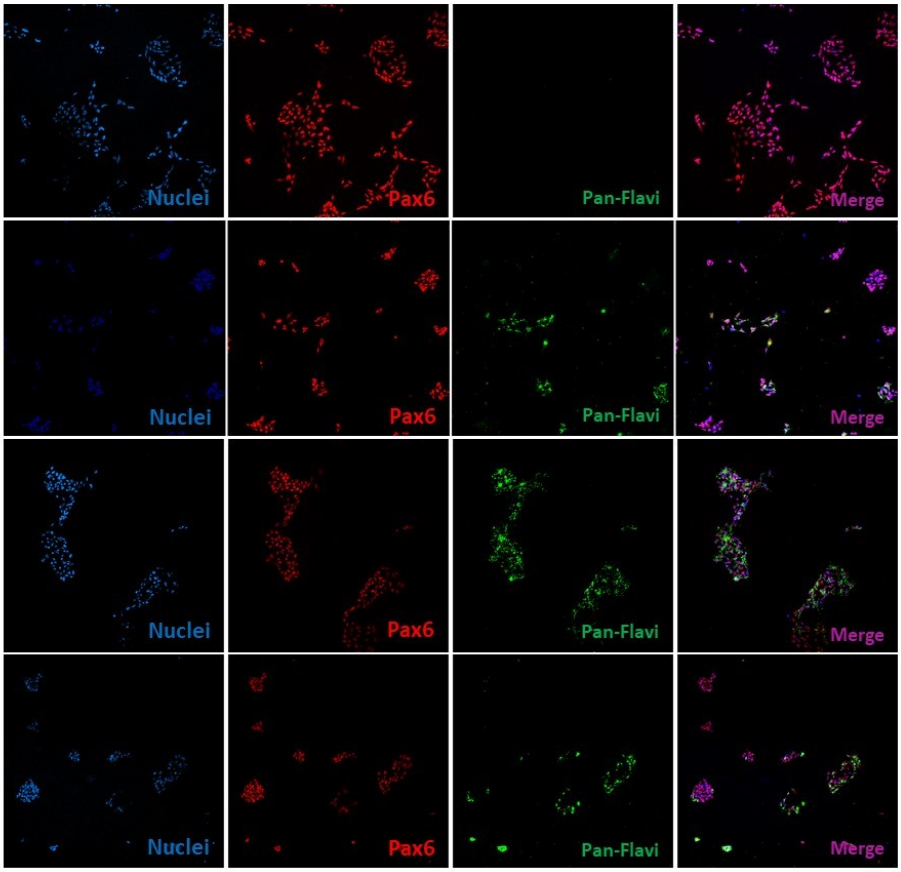
Nuclei
Pax6
Pan-Flavi
Merge
MOCK
USUV
WNV
ZIKV

C

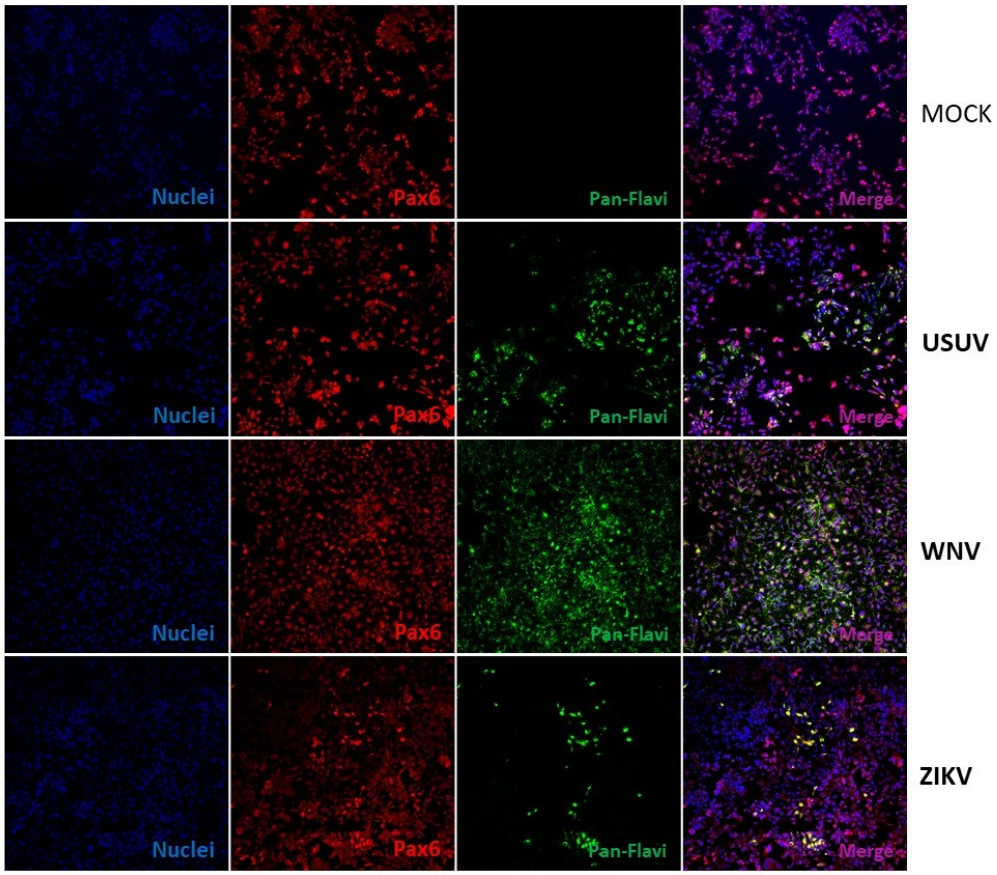
Nuclei
Pax6
Pan-Flavi
Merge
MOCK
USUV
WNV
ZIKV

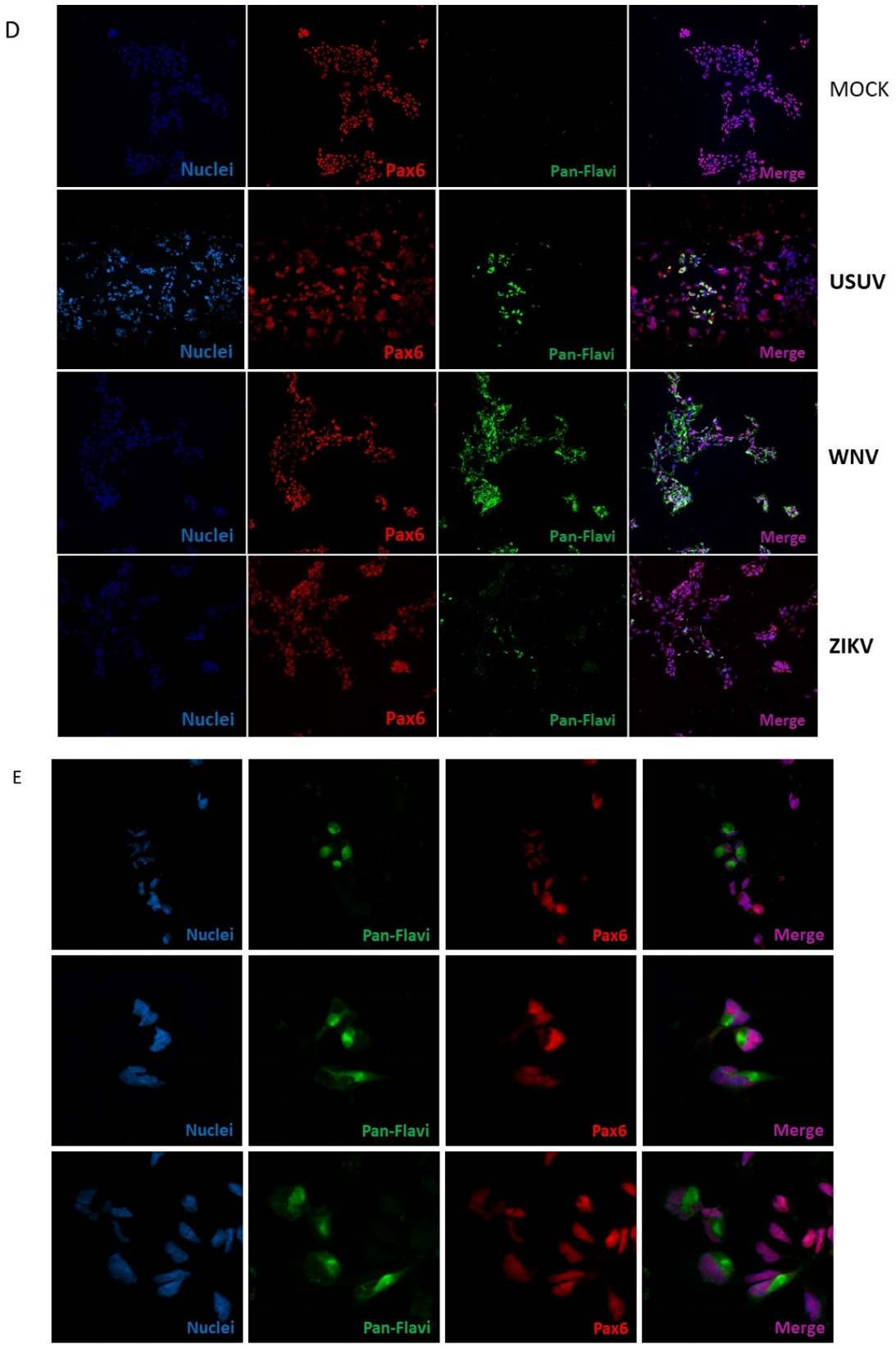

Fig 4.11: Patient-specific hiPSC-derived NSCs infected with flaviviruses. Envelope E glycoprotein (green) of WNV, ZIKV and USUV (MOI 1) and the NSC marker Pax6 (red) were stained by IIF in patient-specific NSCs at 48h pi. Asymptomatic individuals: Asympt1 cell line (**A**), and Asympt2 cell line (**B**), 20× magnification. Symptomatic patients: WNND1 cell line (**C**) and WNND2 cell line (**D**), 20× magnification. (**E**) Details of ZIKV E cytoplasmatic localization in NSC line WNND1; CROP series, from top to bottom: 20×; 20× zoom 2.5 ;60× magnification. Nuclei were stained with DRAQ5 (blue).

4.4.2 Replication kinetics of flaviviruses in patient-specific iPSC-derived NSCs

Replication kinetics of USUV, WNV and ZIKV in patient-specific NSCs were investigated in time-course experiments of infection at different MOIs (0.01, 0.1, and 1). Viral RNA load was measured by qRT-PCR in supernatants of infected cells collected every 24 h until day 5 and was confirmed by TCID50 titration assay.

4.4.2.1 Replication kinetics of flaviviruses in NSCs derived from asymptomatic blood donors

Replication kinetics of single viruses was evaluated by qRT-PCR in NSCs derived from Asympt1 (Fig 4.12) and Asympt2 (Fig 4.13) NSC lines. Infectious titre of viruses after infection with MOI 0.1 was also evaluated by standard titration in Vero cells and reported as TCID50/ml.

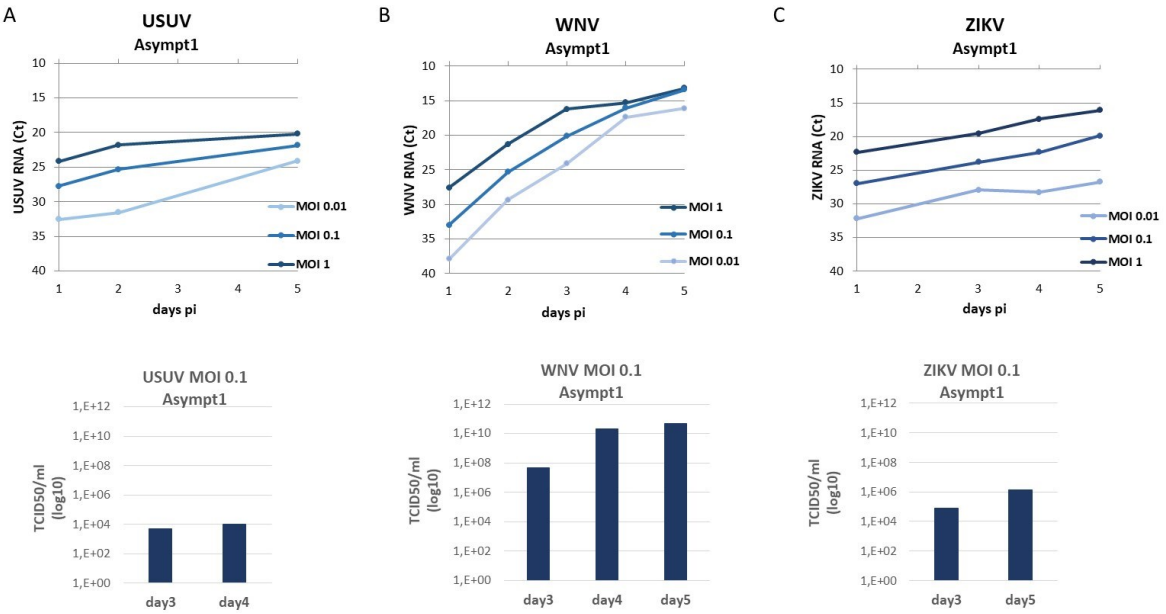

Fig 4.12 Replication kinetics and infectious titer of flaviviruses in NSCs derived from Asympt1. NSCs were infected with USUV (**A**), WNV (**B**) and ZIKV (**C**) at MOIs 0.01, 0.1 and 1. Viral RNA load was measured by qRT-PCR (upper panel) and reported as threshold cycle (Ct) value; infectious titer measured by standard titration in Vero cells grown in microtiter plates and expressed as 50% tissue culture infective doses (TCID50/ml) (lower panel).

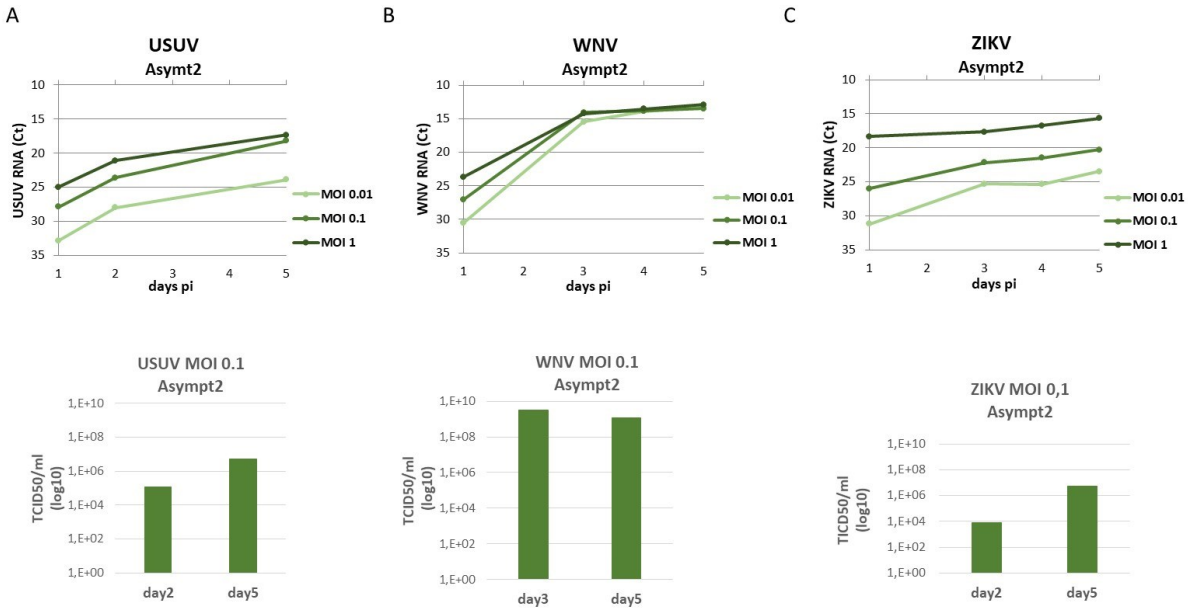

Fig 4.13 Viral replication kinetics and infectious titer in Asympt2 NSCs. NSCs were infected with USUV (**A**), WNV (**B**) and ZIKV (**C**) at MOIs 0.01, 0.1 and 1. Viral RNA load was measured by qRT-PCR (upper panel) and reported as threshold cycle (Ct); infectious titer was measured on Vero cells and expressed as TCID50/ml (lower panel).

Both cell lines showed a similar trend of viral kinetics with WNV that replicated very efficiently and rapidly reaching high viral load (Fig 4.12 B and 4.13 B), while USUV (Fig 4.12 A and 4.13 A) and ZIKV (Fig 4.12 C and 4.13 C) RNA load increased slowly during the time course experiment. Results were confirmed by infectious titer measurement on Vero cells, expressed as TCID50/ml.

4.4.2.2 Replication kinetics of flavivirus in NSCs derived from WNV encephalitis patients

The same analysis of viral replication kinetics was conducted in NSCs derived from WNND1 cell line (Fig 4.14) and WNND2 cell line (Fig 4.15).

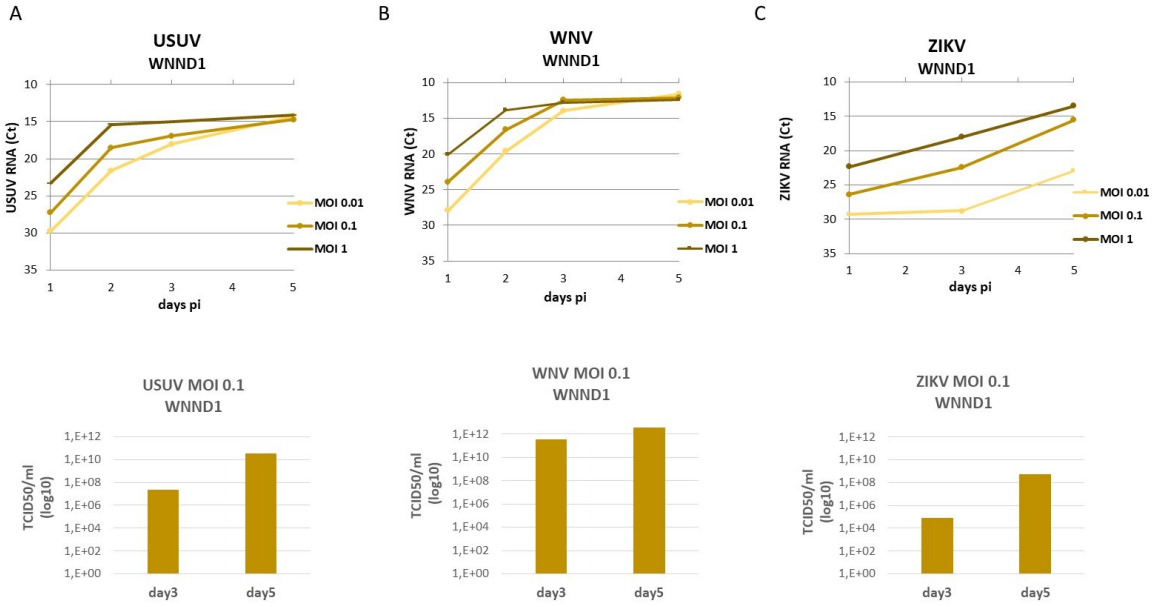

Fig 4.14 Replication kinetics and infectious titer of flavivirus in NSCs derived from WNND1 patient. NSCs were infected with USUV (**A**), WNV (**B**) and ZIKV (**C**) at MOIs 0.01, 0.1 and 1. Viral RNA load was measured by qRT-PCR (upper panel) and reported as threshold cycle (Ct), while infectious titer expressed as TCID50/ml (lower panel).

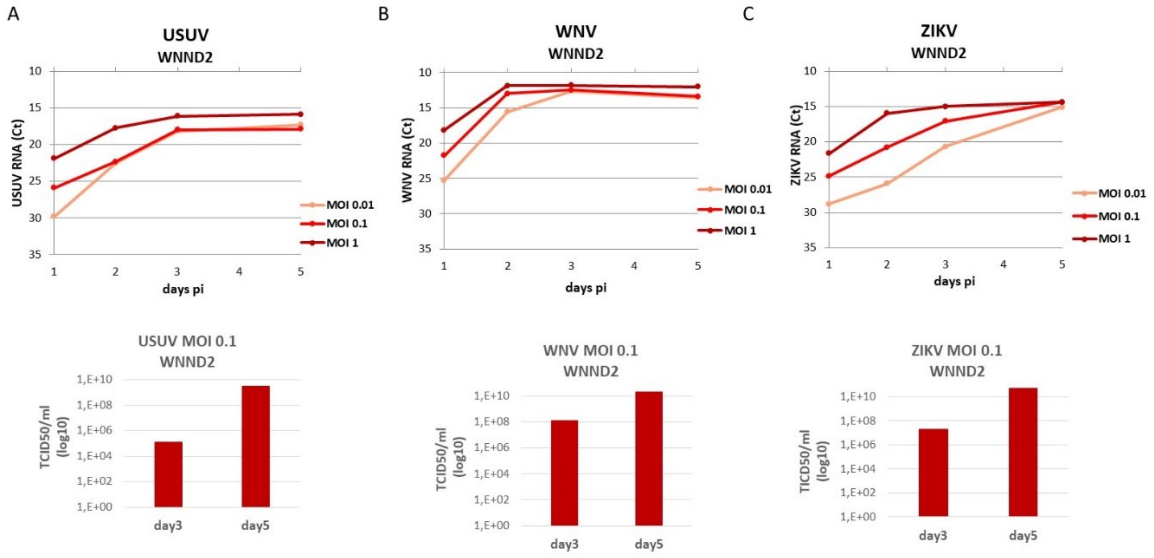

Fig 4.15 Viral replication kinetics and infectious titer in WNND2 NSCs. NSCs were infected with USUV (**A**), WNV (**B**) and ZIKV (**C**) at MOIs 0.01, 0.1 and 1. Viral RNA load was measured by qRT-PCR (upper panel) and reported as threshold cycle (Ct); infectious titer was expressed as TCID50/ml (lower panel).

Both cell lines showed a similar efficient WNV replication kinetics and high viral load was rapidly reached (Fig 4.14 B and 4.15 B). USUV replication was slower than WNV replication and more efficient in WNND1 NSCs than WNND2 NSCs. ZIKV, like USUV, replicated less efficiently than WNV.

4.4.2.3 Intra-patient comparison between replication kinetics of USUV, WNV and ZIKV

Comparison of replication kinetics of USUV, WNV and ZIKV in NSCs derived from the different iPSC lines, i.e., Asympt1 (Fig 4.16), Asympt2 (Fig 4.17), WNND1 (Fig 4.18) and WNND2 (Fig 4.19) showed that WNV replicated more efficiently than the other flaviviruses and reached rapidly high viral load, followed by a plateau.

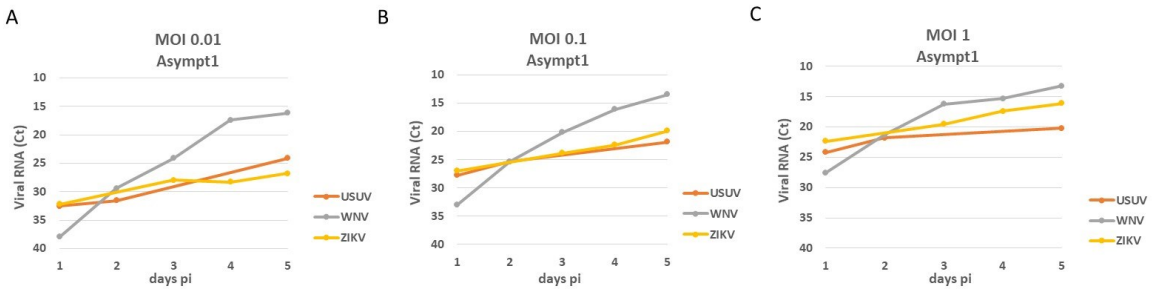

Fig 4.16 Comparison between replication kinetics of USUV, WNV, and ZIKV in Asympt1-derived NSCs. Replication kinetics of USUV, WNV and ZIKV were compared in Asympt1-derived NSCs at MOI 0.01 (**A**), 0.1 (**B**) and 1 (**C**). Viral RNA load was measured by qRT-PCR and reported as threshold cycle (Ct).

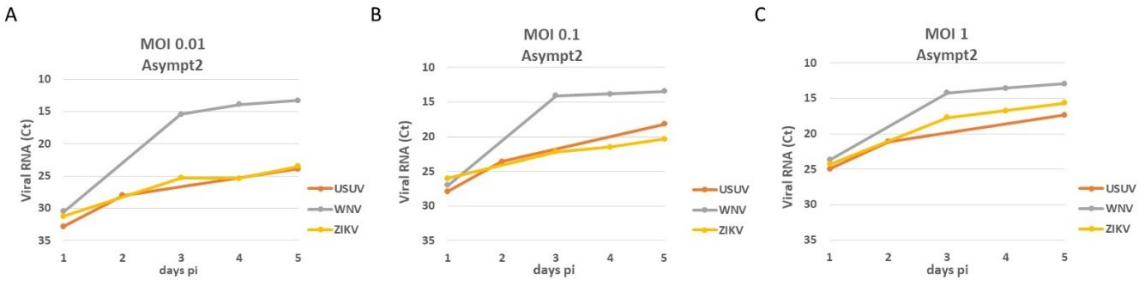

Fig 4.17 Comparison between replication kinetics of USUV, WNV and ZIKV in Asympt2-derived NSCs. Replication kinetics of USUV, WNV and ZIKV were compared in Asympt2-derived NSCs at MOI 0.01 (**A**), 0.1 (**B**) and 1 (**C**). Viral RNA load was measured by qRT-PCR and reported as threshold cycle (Ct).

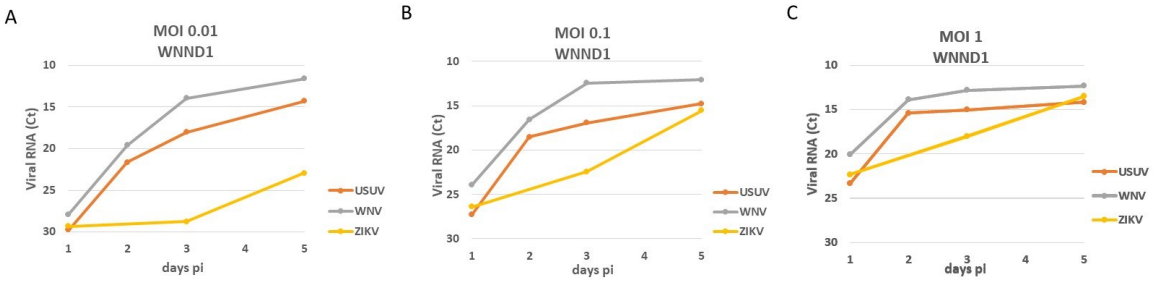

Fig 4.18 Comparison between replication kinetics of USUV, WNV and ZIKV in WNND1-derived NSCs. Replication kinetics of USUV, WNV and ZIKV were compared in patient WNND1-derived NSCs at MOI 0.01 (**A**), 0.1 (**B**) and 1 (**C**). Viral RNA load was measured by qRT-PCR and reported as threshold cycle (Ct).

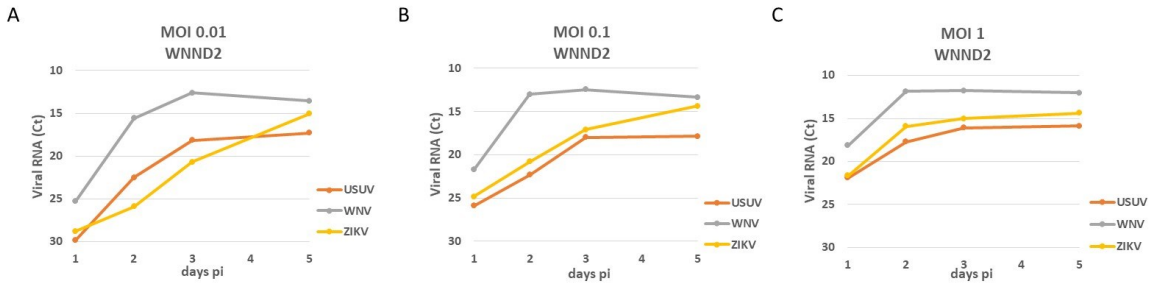

Fig 4.19 Comparison between replication kinetics of USUV, WNV and ZIKV in WNND2-derived NSCs. Replication kinetics of USUV, WNV, and ZIKV were compared in WNND2-derived NSCs at MOI 0.01 (**A**), 0.1 (**B**) and 1 (**C**). Viral RNA load was measured by qRT-PCR and reported as threshold cycle (Ct).

In particular, in Asympt1 and Asympt2-derived NSCs, WNV rapidly reached high viral load and replicated more efficiently than USUV and ZIKV, especially at MOI 0.01 and 0.1 (Fig 4.16 B and 4.17 B). USUV and ZIKV kinetics followed a similar trend and their curves almost overlapped, especially at MOIs 0.01 and 0.1. At MOI 1 all the curves became flattened and came closer, and ZIKV reached RNA load slightly higher than USUV (Fig 4.16 and 4.17).

The replicative behaviour of WNV (related to USUV and ZIKV) detected in blood donors-derived NSCs (Fig 4.16 and 4.17) appeared quite similar in WNND patients-derived NSCs (Fig 4.18 and 4.19): WNV in 2-3 days came to the highest viral RNA load before the plateau. Although the viral load of USUV and ZIKV remains lower than that of WNV, their kinetics is different to that found in Asympt1 and Asympt2 cell lines. USUV replicated more efficiently and reached viral RNA load higher than ZIKV in WNND1 patient.

4.4.2.4 Viral replication kinetics: Comparison between asymptomatic blood donors- and WNND patient-derived NSCs

To determine the presence of significant differences in host-dependent antiviral response to flavivirus infection, viral replication kinetics of ZIKV, USUV, and WNV was compared between asymptomatic blood donors- (Asympt1 and Asympt2 cell lines) and WNND patients- (WNND1 and WNND2 cell lines) derived NSCs. Viral RNA load was measured by qRT-PCR in supernatants of infected cells collected every 24 h until day 5 and infectious titer was evaluated by TCID50 titration assay performed on Vero cells with supernatant of infected cells collected at 3 days post-infection.

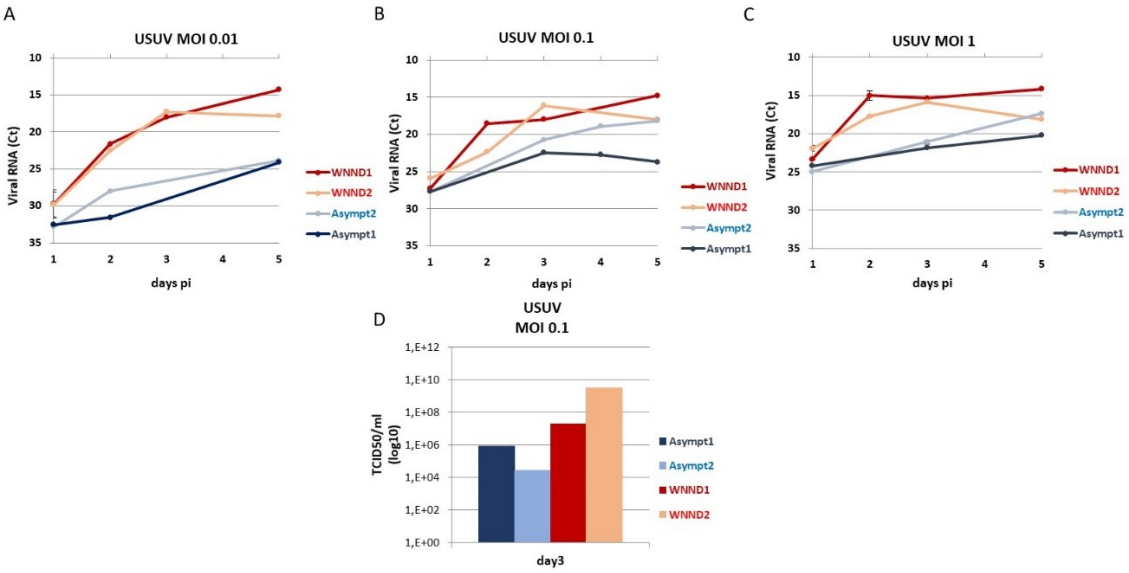

Fig 4.20 Comparison between USUV replication kinetics in NSCs derived from asymptomatic blood donors and WNND-patients. NSCs derived from asymptomatic blood donors (Asympt1 and Asymt2 cell lines) and from WNND patients (WNND1 and WNND2 cell lines) were infected with USUV and the viral replication kinetics was measured by qRT-PCR at MOI 0.01 (**A**), 0.1 (**B**) and 1 (**C**).Viral infectious titer was estimated at day 3 with supernatant of cells infected with USUV at MOI 0.1 and was expressed as TCID50/ml (**D**).

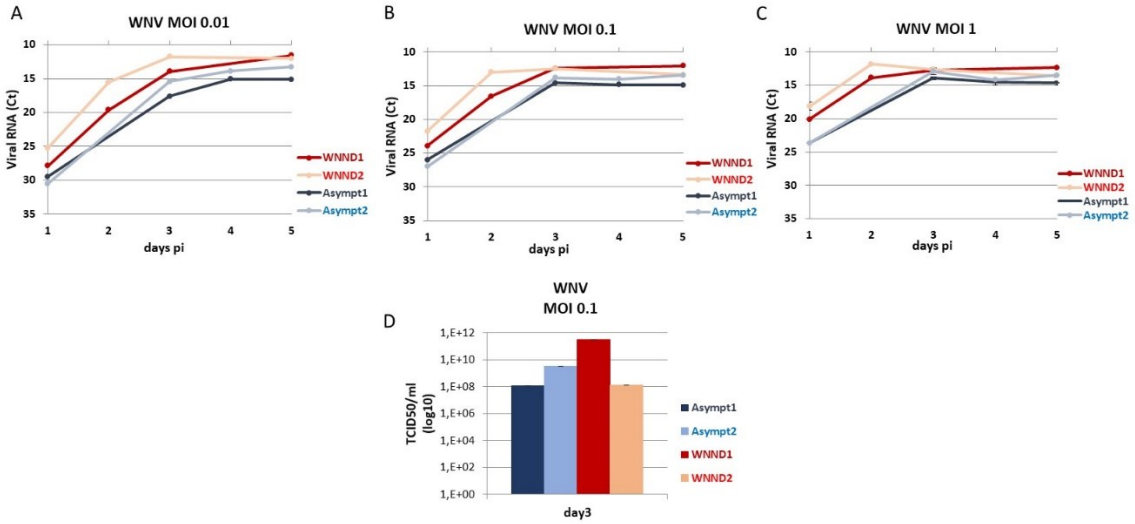

Fig 4.21 Comparison between WNV replication kinetics in NSCs derived from asymptomatic blood donors and WNND-patients. NSCs derived from asymptomatic blood donors (Asympt1 and Asymt2 cell lines) and from WNND patients (WNND1 and WNND2 cell lines) were infected with WNV and the viral replication kinetics was measured by qRT-PCR at MOI 0.01 (**A**), 0.1 (**B**) and 1 (**C**).Viral infectious titer was estimated at day 3 with supernatant of cells infected with WNV at MOI 0.1 and was expressed as TCID50/ml (**D**).

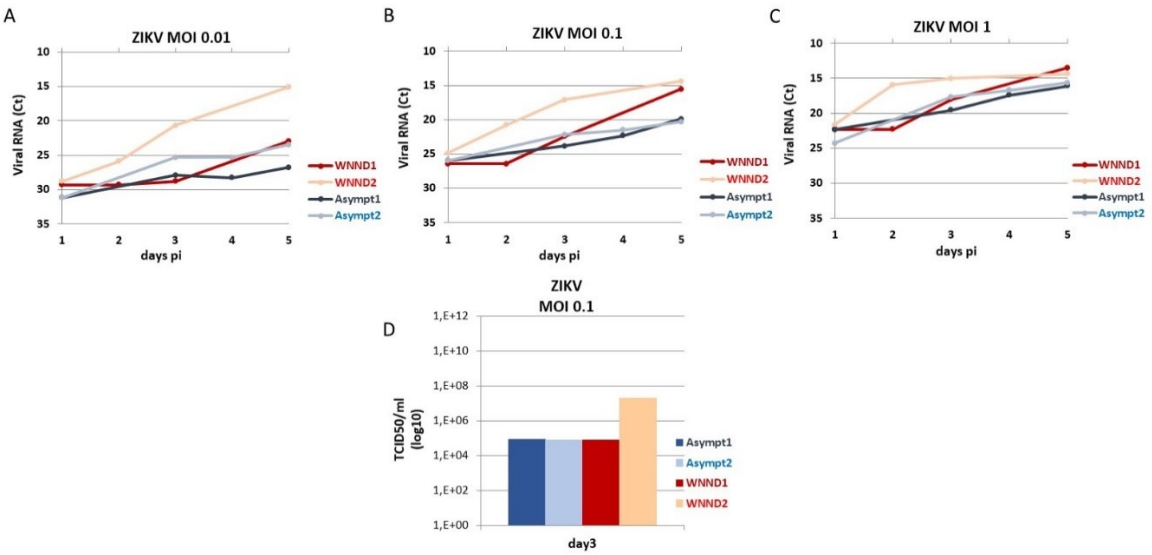

Fig 4.22 Comparison between ZIKV replication kinetics in NSCs derived from asymptomatic blood donors and WNND-patients. NSCs derived from asymptomatic blood donors (Asympt1 and Asymt2 cell lines) and from WNND patients (WNND1 and WNND2 cell lines) were infected with ZIKV and the viral replication kinetics was measured by qRT-PCR at MOI 0.01 (**A**), 0.1 (**B**) and 1 (**C**).Viral infectious titer was estimated at day 3 with supernatant of cells infected with ZIKV at MOI 0.1 and was expressed as TCID50/ml (**D**).

In NSCs derived from encephalitis patients (WNND1 and WNND2 cell lines), all the viruses replicated more efficiently and reached higher RNA loads (from 10- to 100-fold) compared to those detected in NSCs derived from asymptomatic blood donors (Asympt1 and Asympt2 cell lines) (Fig 4.19-22). However, upon ZIKV infection the difference between the two trends was less evident. At the lowest ZIKV MOI indeed, WNND1 curve overlapped with curves of Asympt1 and Asympt2 cell lines (Fig 4.22 A), while WNND2 cell line kept the highest viral titer regardless of the viral MOIs (Fig 4.22). These evidences were confirmed by TCID50 titration assay (Fig 4.19 D-4.22 D).

4.4.3 Effect of flavivirus infection on viability of patient-specific iPSC-derived NSCs

The MTT test was performed to determine NSC viability after USUV, WNV and ZIKV infection at MOI 0.1 and 1 at 96 hours and 7 days pi. WNV infection at both MOIs strongly reduced the viability of NSCs and the reduction observed after 7 days p.i. in cells derived from WNND patients (WNND1 and WNND2 cell lines) was 70% higher than those found in asymptomatic cell lines (Asympt1 and Asympt2 cell lines) (Fig 4.23 A). A similar reduction was observed after USUV infection: NSCs derived from WNND patients showed a significant higher decrease of cell viability of approximately 20% and 30% after 4 days pi with USUV MOI.0.1 and 1, respectively, and a reduction of about 25% after 7 days, when infected with both MOIs (fig 4.23 B)

The effect was less evident after ZIKV infection, but it still led to a reduction of 30% higher in WNND patients compared to the asymptomatic cell lines after 7 days pi at a MOI of 1 (Fig 4.23 C).

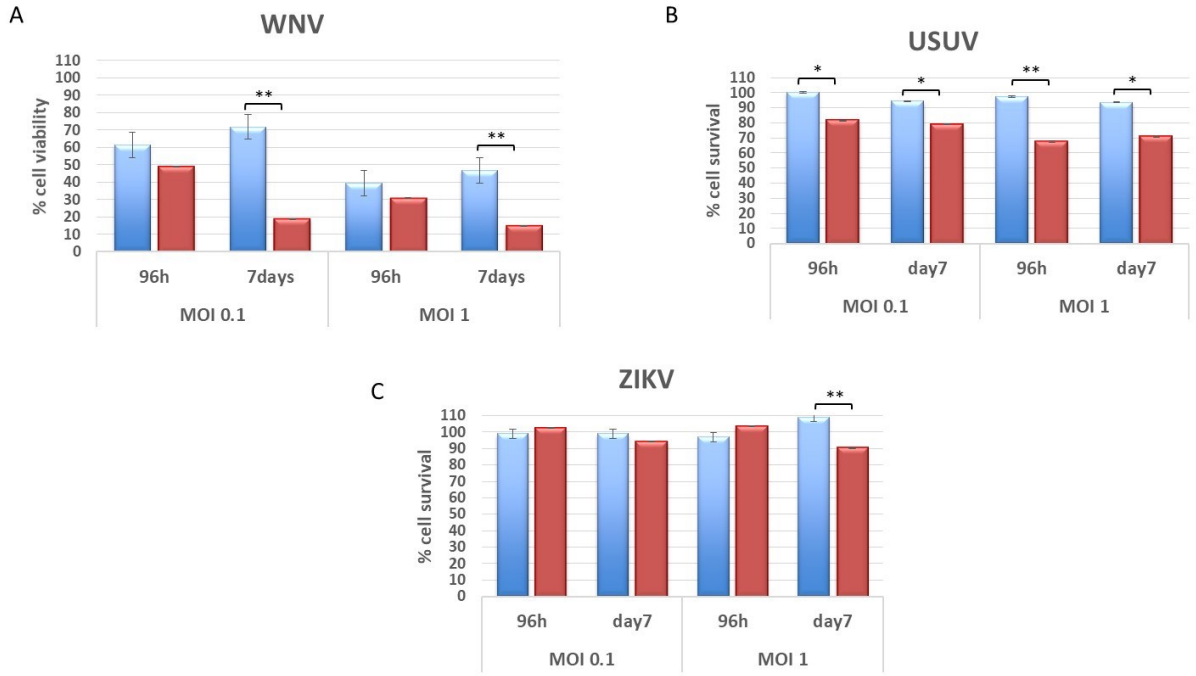

Fig 4.23 Comparison between cell viability of infected NSCs derived from asymptomatic and encephalitis patients. Cell viability of asymptomatic blood donors- and WNND patients-derived NSCs infected with WNV (**A**), USUV (**B**) and ZIKV (**C**), MOI 0.1 and 1, were compared at 96h and 7 days pi. Data are represented as mean ± SD. * p< 0.05 and ** p<0.01.

4.4.4 Effect of flavivirus infection on caspase-3 activity in patient-specific iPSC-derived NSCs

Cell mortality induced by flavivirus infection can be partly promoted by apoptotic pathway. Accordingly, cell death by apoptosis was evaluated in NSCs derived from WNND and asymptomatic patients infected with ZIKV (MOI 1) and WNV (MOI 0.01) at 96 hours pi. Briefly, collected cells were fixed with PFA 4% solution, permeabilized in 90% methanol and incubated with anti-cleaved Caspase-3 primary antibody prior to flow cytometer measurement.

Caspase assay demonstrated that at a low MOI, WNV induced a 3-fold increase of caspase 3 activity in infected-NSC derived from encephalitis patients compared to non-infected mock control and asymptomatic-derived NSCs (Fig 4.24 C). No significant differences between patients were detected instead after ZIKV infection.

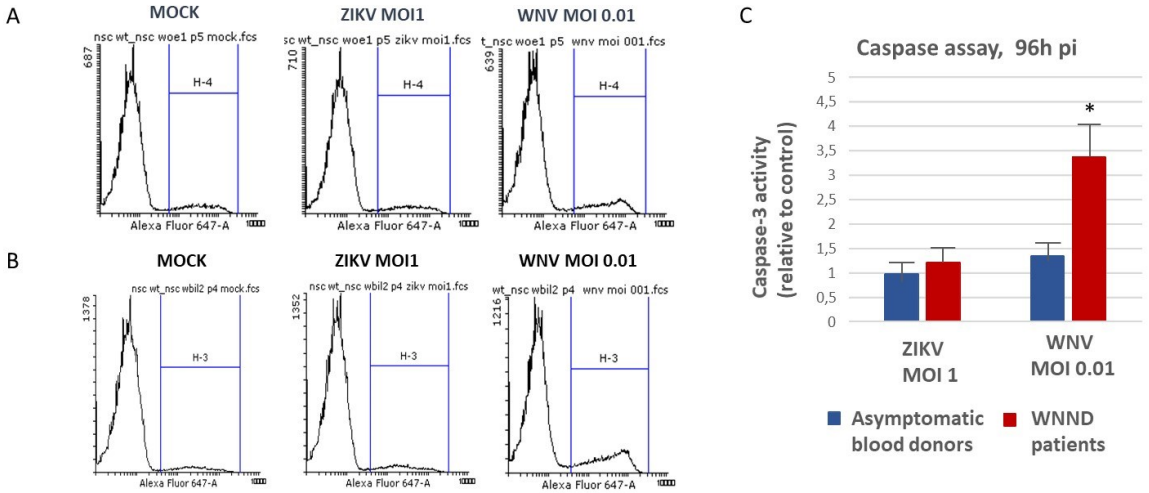

Fig 4.24 Caspase-3 activity in patient-specific iPSC-derived NSCs. Representative flow cytometry analysis for detection of activated Caspase-3 after mock, ZIKV (MOI 1) and WNV (MOI 0.01) infection (96 hpi) in NSCs derived from asymptomatic blood donor (**A**) and WNND patient (**B**). (**C**) Comparison of Caspase-3 activity detected 96 hours after ZIKV (MOI 1) and WNV (MOI 0.01) infection, between NSCs derived from asymptomatic (blue) and WNND patients (red). Data are represented as mean ± SD. * p< 0.05.

4.4.5 Effect of flavivirus infection on expression of antiviral innate immune response genes in patient-specific iPSC-derived NSCs

Host recognition of viral invasion and development of an effective antiviral innate immune response represent the first lines to survive and defence against virus infection. This response is initially mediated by detection in infected cells of non-self and pathogen-associated molecular patterns (PAMPs) by specific host PRRs such as retinoic-acid-inducible gene-I (RIG-I)-like receptors (RLRs), nucleotide-oligomerization-domain-like receptors, and Toll-like receptors (TLRs). The interaction triggers signalling cascades that induce the activation of latent TFs, including IFN regulatory factors (IRFs) and NF-kB that lead to the production of pro-inflammatory cytokines and three classes of interferons (IFNs): type I (IFN-α and IFN-β), type II (IFN-γ), and type III (IFN-λ1, IFN-λ2, and IFN-λ3). IFNs signal to neighbouring cells via distinct receptors to induce activation of the JAK-STAT pathway leading to the production of different IFN-stimulated effector genes (ISGs) that suppress viral replication, regulate cellular metabolism toward an antiviral state, and modulate the adaptive immune response.

Considering the fundamental role of the host in the interplay with viral agents and assuming that defects or variations in the modulation of antiviral innate immunity may account for differences in individual susceptibility to flavivirus infections, the modulation of several genes involved in this IFN pathway was analysed and compared by qRT-PCR on patient-specific iPSC-derived NSCs at 96 hours post-WNV, USUV, and ZIKV infection.

RNA was extracted from infected NSCs and reverse transcribed into cDNA. mRNA level of several immune response genes was analysed by qRT-PCR and the panel included: *IFIT1, IFIT2, MDA5, RIG-I, TLR2, TLR3, TLR7, TLR8, MAVS, IL-1β, CASP1, CASP3, NF-kβ, TNFα, C-GAS, IRF3, IRF7, VIPERIN, IFN-α, IFN-β, IFNλ1, IFNλ2, IFNλ3*. Results were normalized to human GAPDH and analysed using ΔΔCt method.

4.4.5.1 Antiviral innate immune response to flavivirus: Comparison between asymptomatic blood donors- and WNND patient-derived NSCs

The modulation of innate antiviral response gene expression in response to USUV and ZIKV infection at MOI 1 (Fig 4.25 A and B, respectively), and WNV infection at MOI 0.01 (Fig 4.25 C) at 96 hpi was compared in NSCs derived from WNND patients and asymptomatic blood donors.

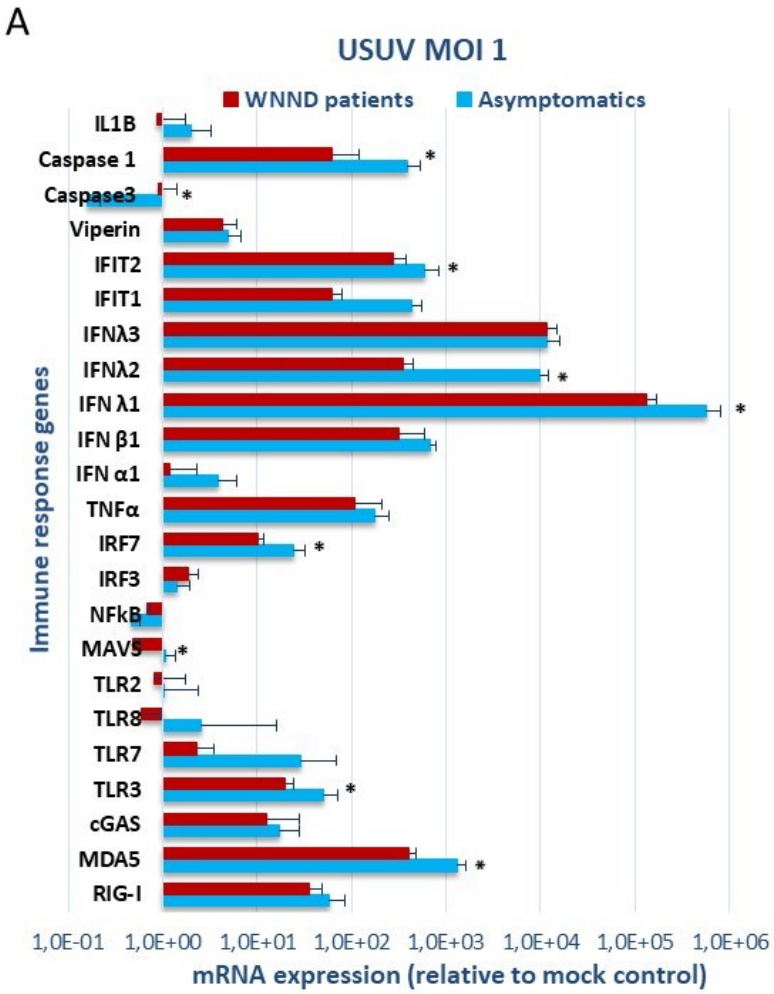

B

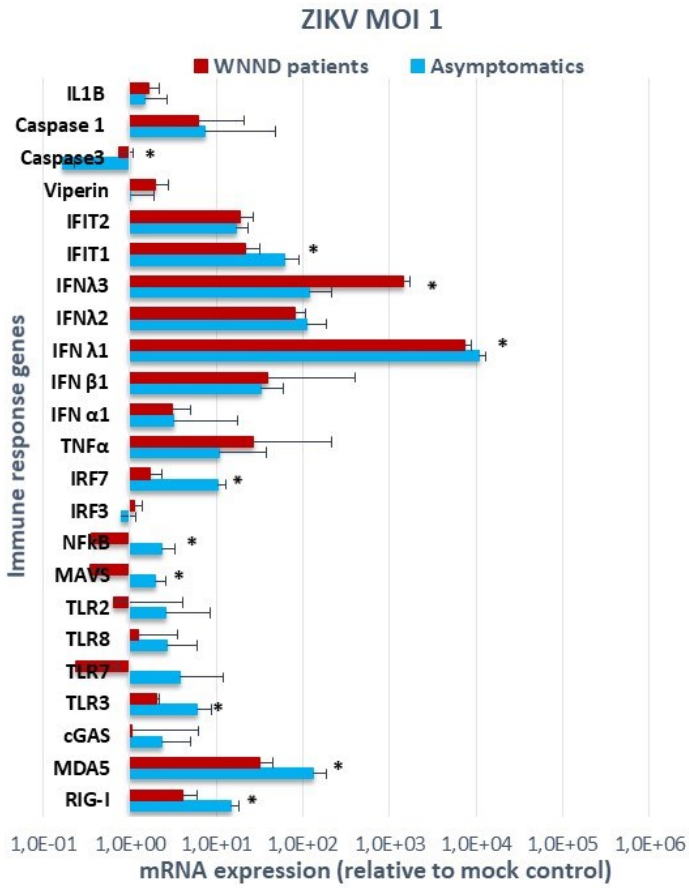
ZIKV MOI 1
WNND patients
Asymptomatics
IL1B
Caspase 1
Caspase3
Viperin
IFIT2
IFIT1
IFNλ3
IFNλ2
IFN λ1
IFN β1
IFN α1
TNFα
IRF7
IRF3
NFkB
MAVS
TLR2
TLR8
TLR7
TLR3
cGAS
MDA5
RIG-I
Immune response genes
1,0E-01 1,0E+00 1,0E+01 1,0E+02 1,0E+03 1,0E+04 1,0E+05 1,0E+06
mRNA expression (relative to mock control)

C

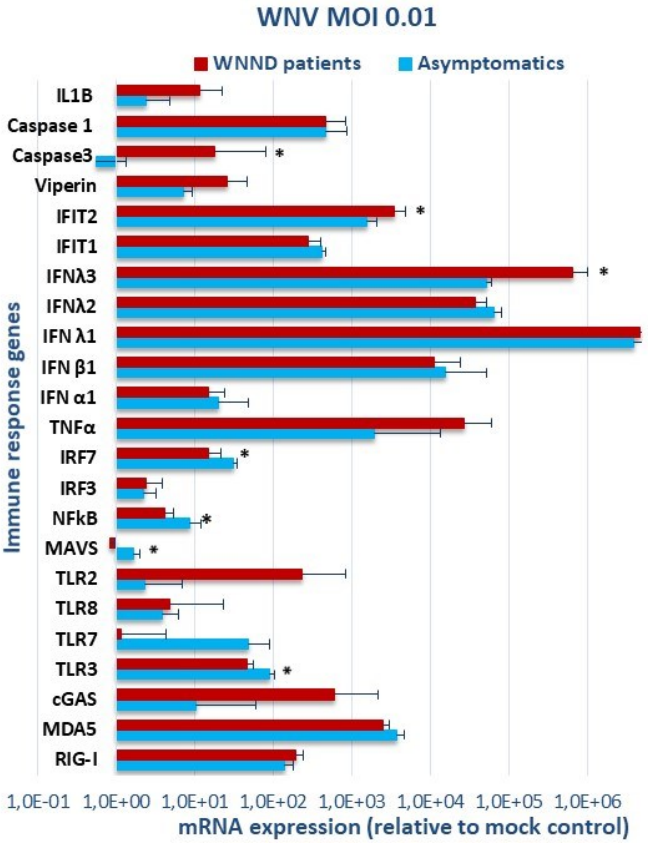
WNV MOI 0.01
WNND patients
Asymptomatics
IL1B
Caspase 1
Caspase3
Viperin
IFIT2
IFIT1
IFNλ3
IFNλ2
IFN λ1
IFN β1
IFN α1
TNFα
IRF7
IRF3
NFkB
MAVS
TLR2
TLR8
TLR7
TLR3
cGAS
MDA5
RIG-I
Immune response genes
1,0E-01 1,0E+00 1,0E+01 1,0E+02 1,0E+03 1,0E+04 1,0E+05 1,0E+06
mRNA expression (relative to mock control)

Fig 4.25 Comparison between antiviral innate immune response to flavivirus infections in asymptomatic blood donors- and WNND patients-derived NSCs. qRT-PCR analysis of genes expression in NSCs derived from iPSC of asymptomatic blood donors (mean of Asympt1 and Asympt2 cell lines) and NSCs derived from iPSCs of encephalitis patients (mean of WNND1 and WNND2 cell lines) infected with USUV at MOI 1 (**A**), ZIKV at MOI 1 (**B**) and WNV at MOI 0.01 (**C**). Cells were collected at 96 hours pi. Data are expressed as means ± SD and analysed using t-test * $p<0.05$ WNND patients vs asymptomatic blood donors.

The profile of gene expression following viral infection was similar among NSC clones derived from all study subjects. Higher mRNA levels of innate immune response genes were observed after WNV and USUV infection than ZIKV infection, in agreement with the higher infection and replication efficiency of WNV and USUV in these cells.

Comparison between WNND patients- and blood donors-derived NSCs showed a general trend towards lower levels of expression of genes in cells derived from encephalitis patients infected with all the three viruses. These genes included some upstream regulators of IFNs pathway, such as the membrane viral RNA sensor *TLR3* (3-fold lower after USUV and ZIKV infections; 2-fold lower after WNV infection), the cytoplasmatic PRR (RLRs) adaptor *MAVS* (2-fold lower in response to USUV and WNV infections; 6-fold lower after ZIKV infection) and the downstream TF, *IRF7* (2-fold lower after USUV and WNV infection, 6-fold lower after ZIKV). The expression of the gene encoding Caspase 3 was instead upregulated in WNND-derived NSCs following infection with all the three viruses (approximately 5-fold higher in response to USUV and ZIKV and even 30-fold higher in response to WNV). In response to both USUV and ZIKV infections, other genes resulted downregulated in NSCs derived from WNND patients compared to the NSC lines derived from asymptomatic donors. These genes included viral RNA sensor (RLRs) *MDA5* gene (3- and 4-fold lower after USUV and ZIKV infections, respectively), the *IFNL1* gene (4-and 1.5-fold lower after USUV and ZIKV infections, respectively) and the IFN-stimulated effector gene *IFIT1* (7-fold after USUV infection and 3-fold lower after ZIKV infection) (Fig 4.25 A and B). *IFNL2* and *NF-kB* genes appeared also downregulated in WNND patients-derived NSCs: *IFNL2* in response to USUV infection (approximately 27-fold lower) (Fig. 4.25 A), and *NF-kB* after ZIKV (6-fold lower) (Fig 4.25 B) and WNV (2-fold lower) (Fig. 4.25 C) infections.

Overall these data suggest that compared to blood donors, NSCs derived from encephalitis patients had an attenuated antiviral response to flavivirus infection.

4.4.5.2 Antiviral innate immune response to flavivirus in NSCs: Comparison between USUV and WNV infections

A further analysis was carried out to compare the NSCs antiviral innate immune profile generated in response to USUV infection with the response to WNV. WNND-patient derived NSCs (WNND1 patient cell line) was infected with USUV and WNV at MOI 1 and, at 96h pi, cells were collected and analysed for genes expression (Fig 4.26).

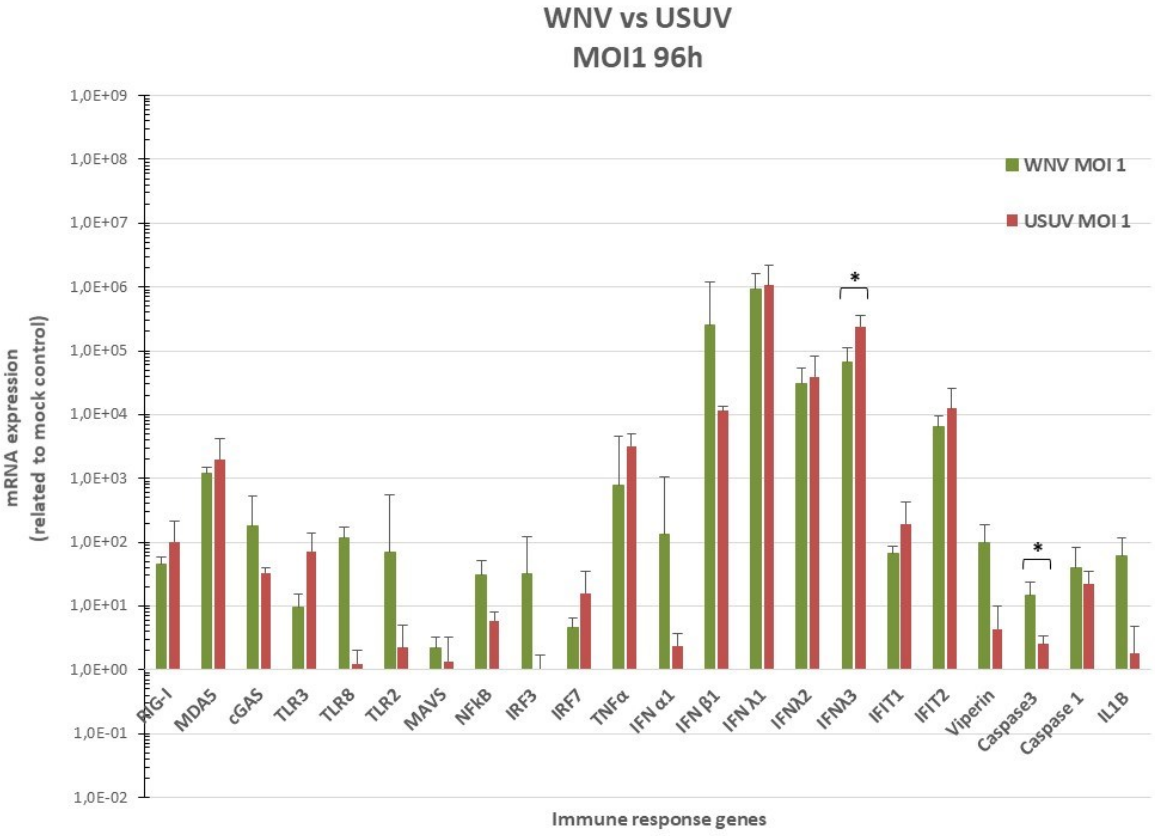

Fig 4.26 Modulation of antiviral innate immune response to USUV and WNV infections in WNND-patient derived NSCs. WNND1 patient-derived NSCs were infected with USUV and WNV at MOI 1 and mRNA levels of immune genes were analysed by qRT-PCR at 96h pi. Data are reported as means ± SD of expression values relative to mock-infected controls.

Results proposed a marginally increased innate immune response upon WNV infection compared to that of USUV, with the exception of type 3 IFN, which had significantly higher level after USUV infection (3,6-fold higher) than after WNV infection, and mRNA levels of the cellular apoptotic protease Caspase 3, which had a significant 6-fold higher value in WNV-infected than USUV-infected cells.

4.5 Exome sequencing by next generation sequencing (NGS)

To correlate the phenotypic data with host genetic background, in collaboration with the University of Helsinki, we sequenced by NGS Illumina Miseq a panel of 2,600 genes related to

antiviral response and innate immune system in iPSC clones of cases and controls. Data (median read depth: 33) were generated from iPSC WNND1 culture passage 44 (p44) and WNND2 p14 from encephalitic patients and Asympt1 p43 and Asympt2 p8 from asymptomatic WNV-infected patients. A total of 1,827 genetic alterations in WNND cases that were absent in the asymptomatic controls, specifically 1,358 in WNND1 (median read depth: 42) and 469 in WNND2 (median read depth: 31.7) were identified. Among these we filtered those alterations that affected the exonic or splicing region, 49 in WNND1 (median read depth: 37) and 33 in WNND2 (median read depth: 28) and evaluated. Sevention homozygous or heterozygous missense variants and frameshift-causing deletions were selected (16 in WNND1; 3 in WNND2; of these 2 in common between WNND1 and WNND2) and 11 were predicted as damaging to the protein function by MutationTaster computational prediction scores. MutationTaster employs a "Bayes classifier" to ultimately predict the potential pathogenicity of an alteration. This Bayes classifier calculates probabilities for the alteration to be either a disease mutation or a harmless polymorphism. For this prediction, the frequencies of all single features for known disease mutations or polymorphisms were studied in a large guidance set composed of >390,000 known disease mutations from HGMD Professional, and >6,800,000 harmless SNPs and Indel polymorphisms from the 1000 Genomes Project (TGP).

Sequencing of iPSC from the first patient (Tab 4.2) revealed that both exonic and splicing regions of the genome harbour nonsynonymous SNVs (in *ITGAX*, *PHF2*, *CEP135*, *CKAP5*, *AGPAT4*, *TRIM10* and *TRIM40* genes), and frameshift (in *PSIP1* and *IFITM5* genes), in addition to well-known polymorphisms (in *IRF4*, *SMARCA*2 and *IRF7* genes). All these alterations can potentially cause deleterious effects to the encoded protein, except for those affecting the upstream region of the *TRIM40* gene, which had no predictions.

Frequency of known polymorphisms was reported from TGP, set out in 2015, and unlike the double heterozygous variants found in IRF7 gene (rs1061502 and rs12272434), frequency of polymorphisms found in the *IRF4* gene (rs34318727) and *SMARCA2* (rs17712152) were low: 6% and 1%, respectively.

The frameshift deletion found in the *PSIP1* gene, which encodes PC4 and SFRS1 interacting protein 1 (also known as p52 or p75), was predicted to generate a premature stop codon that may activate the nonsense mediated decay process (NMD). A similar alteration was reported in the *DDX58* gene (also known as *RIG-I*) in iPSC derived from WNND2 (Table 4.3). This gene encodes a protein containing RNA helicase-DEAD box protein motifs and a caspase

recruitment domain (CARD) and acts as a cytoplasmic sensor of viral nucleic acids of both positive and negative stranded RNA viruses, including WNV and other members of the family *Flaviviridae* (Guo HY et al., 2018). Only two frequent polymorphisms were identified in common between the two patients (Table 4.4). The first harbours in the *JAK2* gene (rs2230724, frequency 62%), that encodes for a notable protein tyrosine kinase involved in a specific subset of cytokine receptor signalling pathways and it is required for responses to gamma interferon (Shuai K et al., 2003). The second was detected in the *DOCK8* gene (rs10970979, frequency 20.0%), which plays a critical role in the survival and function of several types of immune system cells, including T cells, NK cells, and B cells (Kearney CJ et al., 2017).

iPSC from patient WNND1							
Gene	**Alteration type**	**DNA changes**	**Alteration region**	**AA changes**	**Coverage**	**Frequency**	**Prediction**
PSIP1	Frameshift deletion	c.782delG	exonic	R261fs	75	1	Probably deleterious (NMD)
IFITM5	Frameshift	c.22G>A	exonic	E8K	29	0.55	Probably deleterious
ITGAX	non-synonymous SNV	c.2050G>A	exonic	G684S	30	0.5	Probably deleterious
CKAP5	non-synonymous SNV	c.4250A>C	exonic	E1417A	38	1	Probably deleterious
IRF7	rs1061502	c.574A>G	exonic	K192E	33	0.45	Polymorphism
IRF7	rs12272434	c.223-4T>A	splicing	N.D	12	0.58	Polymorphism
IRF4	rs34318727	c.634+9G>A	splicing	V216M	47	0.53	Probably deleterious
SMARCA2	rs17712152	c.2991+10G>A	splicing	G1001S	70	0.59	Probably deleterious
PHF2	non-synonymous SNV	c.205C>A	exonic	H69N	15	1	Probably deleterious
CEP135	non-synonymous SNV	c.1715A>T	exonic	E572V	15	1	Probably deleterious

TRIM10	non-synonymous SNV	c.1064T	exonic	L355P	13	0.62	Probably deleterious
TRIM40	N.D	N.D	Upstream (dist131nt)	N.D	10	1	Not known
AGPAT4	non-synonymous SNV	c.962C>T	exonic	P321L	10	1	Probably deleterious
AGPAT4	non-synonymous SNV	c.984C>A	exonic	S328R	10	1	Polymorphism
DOCK8	rs10970979	c.1034A>G	exonic	N345S	61	0.44	Polymorphism
JAK2	rs2230724	c.2490G>A	exonic	L830L	40	0.55	Polymorphism

Table 4.2 Genetic alterations identified in iPSCs derived from WNND1 patient. Homozygous and heterozygous missense variants and frameshift/deletions identified in iPSCs of WNND1 patients, by performing NGS sequencing of a panel of about 2,600 genes involved in innate immunity. The potential pathogenicity was predicted by computational scores assessed by Mutation Taster software. Frequency of known polymorphisms, according with the 2015-1000 Genomes Project, is as follows: *IRF7 rs1061502* (27%), *rs12272434* (28%); *IRF4 rs34318727* (6%); *SMARCA2 rs17712152* (1%); *DOCK8 rs10970979* (20%); *JAK2 rs2230724* (62%). N.D: not described.

iPSC from patient WNND2							
Gene	**Alteration type**	**DNA changes**	**Alteration region**	**AA changes**	**Coverage**	**Frequency**	**Prediction**
DDX58/RIG-I	Frameshift deletion	c.290delT	exonic	I97fs	33	1	Probably deleterious (NMD)
DOCK8	rs10970979	c.1034A>G	exonic	N345S	61	0.44	Polymorphism
JAK2	rs2230724	c.2490G>A	exonic	L830L	40	0.55	Polymorphism

Table 4.3 Genetic alterations identified in iPSCs derived from WNND2 patient. Homozygous frameshift deletion and heterozygous polymorphisms identified in iPSCs of WNND2 patients, by NGS sequencing of a panel of about 2,600 genes involved in innate immunity. The potential pathogenicity was predicted by Mutation Taster predication scores.

WNND1- and WNND2-derived iPSCs							
Gene	**Alteration type**	**DNA changes**	**Alteration region**	**AA changes**	**Coverage**	**Frequency**	**Prediction**
DOCK8	rs10970979	c.1034A>G	exonic	N345S	61	0.44	Polymorphism
JAK2	rs2230724	c.2490G>A	exonic	L830L	40	0.55	Polymorphism

Table 4.4 Genetic alterations identified in common between iPSCs from WNND1 and WNND2 patients. Two heterozygous polymorphisms were identified in common between WNND1- and WNND2-derived iPSCs, performing NGS sequencing. The potential pathogenicity was predicted by Mutation Taster predication scores.

5.DISCUSSION

In the present study, we developed an infection model for neurotropic viruses exploiting patient-specific hiPSC-derived neural cells. We derived iPSCs from PBMCs of two blood donors with asymptomatic WNV infection (Asympt 1 and Asympt 2) and two young patients who developed West Nile neuroinvasive disease without comorbidities or other risk factors (WNND 1 and WNND 2). Patients-specific iPSCs were differentiated into neural stem cells (NSCs) to model viral infection i*n vitro*. Infection experiments proved that this model was suitable to investigate the individual susceptibility to flaviviruses infection as the analysis of replication kinetics, cell viability and host innate immunity revealed different outcomes between neural stem cells derived from patients with WNV-related encephalitis (cases) and blood donors with asymptomatic WNV infection (controls). USUV and WNV replicated more efficiently, yielding 10 and 100-fold higher viral load and inducing 40% and 70% higher cell mortality, respectively, in NSCs derived from cases than in NSCs derived from controls. WNV induced 3-fold higher caspase 3 activity in infected NSC derived from encephalitis patients than in NSCs derived from asymptomatic donors. The increased susceptibility of patient-specific neural stem cells to neurotropic flaviviruses was also associated with blunted innate antiviral response. Despite several genes involved in the antiviral IFN pathway were significantly upregulated after USUV, ZIKV, and WNV infection (in particular, type 3 IFNs genes), the general trend indicated an attenuated response in NSCs derived from WNV encephalitis cases, which showed significantly lower mRNA levels of IFN pathway mediators, including *TLR3*, *MAVS* and *IRF7*. Sequencing analysis of a panel of genes involved in immune response identified heterozygous inactivating mutations in the *PSIP1* and *DDX58/RIG-I* genes of cases, but not in controls, and polymorphisms in other candidate genes that could play a role in disease susceptibility.

Beyond defining the mechanism of neuronal injury, patient-specific iPSCs can allow to address important questions such as the correlations between infection outcomes (neuroinvasive disease vs asymptomatic or persistent vs acute infection) and gene expression (with particular focus on innate immunity pathways) and to investigate the phenotypic effects of possible genetic anomalies or single nucleotide polymorphisms (SNPs). Some studies with a similar rationale have been reported so far: Lafaille FG *et al.* in 2012 demonstrated the high susceptibility to HSV-1 infection in neurons and oligodendrocytes differentiated from iPSCs, which were generated from patients carrying inactivating mutations in the *UNC-93B* and *TLR3* genes, confirming the linkage between herpes simplex encephalitis (HSE) in children and CNS–

intrinsic TLR3–dependent interferon immunity to HSV-1 (Lafaille FG et al., 2012). Another case study determined the phenotypic effects of compound heterozygous null mutations in the *IRF7* gene, which were associated with life-threatening influenza for the first time, in patient-specific iPSC–derived pulmonary epithelial cells, which produced reduced amounts of type I IFN and displayed increased influenza virus replication (Casanova JL and Abel L, 2013). Moreover, a recent study on neural progenitor cells (NPCs) derived from iPSCs of non-affected and congenital ZIKV syndrome (CZS)-affected twins did not identify a major locus associated with the different susceptibility to viral infection, suggesting that CZS may be a multifactorial disorder (Caires-Júnior LC et al., 2018).

Genetic defects in innate immune response genes may predispose to severe disease caused by different pathogens. Thus, in this study, we investigate patient-specific cell susceptibility not only to WNV, but also to other neurotropic flaviviruses, i.e. ZIKV and USUV. USUV appears to be less pathogenic for humans than WNV and most USUV infections are asymptomatic, with a prevalence of antibodies against USUV even higher than anti-WNV antibodies in areas where both viruses co-circulate (Pierro A et al., 2013). Considering the overlapping characteristics between USUV and WNV, the USUVsympt cell line developed in this study represents an interesting symptomatic case and despite no experiment were performed yet with this model, we speculate that its analysis will support our results and enrich the study.

The *in vitro* model allowed also comparing replication efficiency and the effects on host NSCs of the three flaviviruses. Overall, WNV, ZIKV and USUV infected and replicated efficiently in NSCs, but WNV reached rapidly higher viral load than the other flaviviruses. The replication kinetics of WNV appeared quite similar between NSCs of cases and controls and in 2-3 days reached the highest viral RNA load before the plateau. This result was quite unexpected considering that WNV, unlike ZIKV, is rarely linked to congenital malformation, including following intrauterine WNV infection (O'Leary et al., 2006). Contrary to ZIKV indeed, a few studies of WNV infection of neural stem cells (NSC) have been reported so far showing conflicting results (Liddelow SA et al., 2017; Garber C et al., 2018). Several studies in human and animal models have rather demonstrated the ability of WNV to infect and replicate, inducing severe injury, in various types of CNS resident cells, including neurons, astrocytes, and microglial cells (Shrestha B et al., 2003; Cheeran MC et al., 2005; Winkelmann ER et al., 2016). Brault JB et al. in 2016 reported productive ZIKV and WNV infection in mouse brain slices by viral titration and through immuno-staining experiments, however ZIKV revealed a

remarkable tropism for neural stem cells while WNV displayed a bias towards neurons (Brault JB et al. in 2016). A recent study, described hESCs-derived NSCs as susceptible to WNV infection, even if, in co-cultures systems of NSCs and differentiated neurons, WNV infection occurred primarily in differentiated neuronal cells (Wu X et al., 2018). Nevertheless, in previous experiments performed in our laboratory we demonstrated similarities between iPSCs-derived NSCs and differentiated neurons in their response to flavivirus infection, in terms of replication kinetics, cytopathic effects and antiviral gene expression. Thus, considering the easier *in vitro* handling of NSCs compared to neurons, we considered the NSCs an appropriate model to investigate host susceptibility to neurotropic viruses. Anyway, considering the wide-ranging neurotropism of WNV, it will be our goal to examine additional target cells exploiting the differentiation potential of the hiPSCs, including fully differentiated neurons and astrocytes, but also blood cells (Kovats S et al., 2016).

Interestingly, despite Garber C et al. found very few NSCs and intermediate neuronal progenitors permissive to WNV infection in mouse studies, they detected altered transcriptional profiling expression of genes implicated in hippocampal neurogenesis during WNND recovery and in the Wnt signaling pathway, which can impact neural progenitor cell proliferation and motility (Garber C et al., 2018). Adult neurogenesis is a highly regulated process that take place in two specific brain regions: the dentate gyrus (DG) of the hippocampus and the subventricular zone (SVZ) along the lateral ventricle. Neural stem cells within these two zones generate neuronal progenitor cells that provide a source of new neurons for neuron turnover, repair from injury, and hippocampal plasticity, which is essential for proper learning and memory. Many of the molecules that induce NPCs to proliferate and differentiate, such as CXCL12 and CXCR4, are the same recruited by the immune system to direct and regulate the extravasation of leukocytes across the blood brain barrier in response to CNS pathogens (Li M and Ransohoff RM et al., 2007). Of interest, several patients who recover from WNV encephalitis report cognitive sequelae, including memory impairments and depression (Lambert SL et al., 2016; Patel H et al., 2015). In patients with encephalitis, WNV has been hypothesized to induce resident neurons and glia to upregulate chemokines and cytokines that recruit leukocytes, and to influence proliferation, migration, and fate of NPCs. Chemokine expression patterns that are altered at perivascular spaces to promote leukocyte entry may impact the homeostasis of NPCs, which use perivascular spaces within neurogenic zones as a trophic niche and migratory scaffold (Decimo I et al., 2012). Since the effects of WNV encephalitis on adult NPC homeostasis have not been previously investigated, acquiring

mechanistic knowledge about the behaviour of NSCs upon WNV infection and within inflamed conditions may be interesting and may help guiding the development of stem cell-based therapeutics for other CNS diseases with inflammation.

USUV and ZIKV kinetics followed a similar trend of WNV and their replication curves almost overlapped, especially at lower MOIs (0.01 and 0.1). At MOI 1 instead, the viral loads came closer, with a slight increase of ZIKV compared to USUV. Despite the effect was less evident for ZIKV, all the viruses, included WNV, reduced the viability of NSCs and upregulated the expression of innate immune genes. The effect of ZIKV on neural cell viability that we obtained was in agreement with evidence reported by several studies based on human iPSC-derived NPCs, which showed attenuated growth of NPCs when infected with ZIKV (Thornton GK et al., 2010; Lancaster MA et al., 2013) and a rapidly progression to apoptotic cell death (Souza BS et al., 2016). Similar observations were also described in cultures of neurospheres and cerebral organoids (Marthiens V et al., 2013). Since NSCs are present throughout foetal development and remain confined in a few regions of the adult brain, this remarkable susceptibility of NPCs to ZIKV supports the pathological findings in humans.
Despite the interest in USUV has arisen in recent years and only a few studies aimed at analysing host range, pathogenesis and the triggered innate immune response of USUV have been performed, in accordance with our result, a previous work reported that iPSC-derived hNSCs were highly permissive to USUV infection and underwent caspase-dependent apoptosis (Salinas S et al., 2017).

The main objective of this study was to analyse and compare the different susceptibility to WNV and other flavivirus infection of iPSC-derived neural cells that recapitulate *in vitro* the divergent disease traits, which characterized the asymptomatic individuals and patients we enrolled in the study. Despite the low number of cases involved in the present study, no one else before has ever studied individual susceptibility to WNV infections using patient specific IPSCs. Until now indeed, the Collaborative Cross (CC) mouse model has represented the principal and most suitable model of WNV infection able to capture the wide heterogenicity of human responses (Graham JB et al., 2015).
Analysis of replication kinetics of WNV, USUV and ZIKV until day 5 post infection revealed higher viral RNA loads in NSCs derived from encephalitis patients, compared to those detected in NSCs derived from asymptomatic blood donors. This result is similar to the findings in the brain of CC. In fact, in a previous study conducted by Graham JB *et al.* in 2015, asymptomatic

mice quickly cleared WNV from the spleen by day 7 post infection with minimal viral escape to the CNS at early time points and only one mouse showing low levels of virus reaching the brain at day 12. Instead, the WNV loads in symptomatic RIX mice increased in CNS from day 4 to day 7 post infection (Graham JB et al., 2015). The same research group, four years later studied immune correlates of viral peripheral restriction by comparing WNV infection in "PR" mice, which could restrict WNV to the periphery and showed no signs of disease, and "NND" mice, which had no disease but WNV was present in their brain inducing CNS immunopathology. On day 4 after infection no virus was detected in the brain of NND mice but WNV viral load increased on day 7 and 12 while remained undetectable in PR mice. Both groups achieved viral clearance in the periphery by day 7, maybe in response to viral invasion of NND mice brain (Graham JB et al. 2019). We noticed, however, that after ZIKV infection the differences between the trends of asymptomatic iPSC-derived NSCs and WNND iPSC-derived NSCs was less evident, and, at the lowest MOI, ZIKV replication kinetics diverged between WNND1 and WNND2 lines. This intragroup difference was not unexpected given the low number of cases and depicts the variation within the human population, highlighting the critical role of population-based approaches in better understanding the genetic architecture that drives wide ranges of disease responses, even within individuals sharing major resistance loci.

The effect of WNV infection on NSCs viability was deleterious at day 4 and day 7 post infection and the reduction observed in WNND lines was significantly higher than those found in Asympt lines. A similar reaction, but to a lesser extent, was observed after USUV infection while the cytopathic effect was less evident after ZIKV infection probably due to the lower replicative capacity compared to the other viruses. Cell mortality induced by WNV infection can be partly promoted by apoptotic pathway (Urbanowski MD et Hobman TC, 2013) and 4 days after infection we observed an increased activity of caspase 3 in WNND lines compared to Asympt lines. Similarly, in the brain of WNV symptomatic RIX mice, Graham JB and colleagues found signs of neuropathology including parenchymal lesions characterized by combinations of tissue degeneration, apoptosis and necrosis, while no signs of inflammation or parenchymal damage was detected in asymptomatic mice (Graham JB et al., 2015).

The comparison between NSCs derived from WNND patients and asymptomatic blood donors in their modulation of innate antiviral response gene expression to USUV, ZIKV and WNV revealed that the increased susceptibility to neurotropic flaviviruses was associated with

blunted innate antiviral response. qRT-PCR analysis of the innate immune response triggered by WNV, USUV and ZIKV at 4 days after infection, revealed a similar gene expression profiles in NSCs clones among cases and controls but slightly higher upon WNV and USUV infection than ZIKV infection, in agreement with the higher infection and replication efficiency of WNV and USUV in these cells. However, the analysis reported a general trend towards lower levels of expression of genes in WNND lines compared to Asympt lines infected with all the three viruses. This evidence suggests that the decrease in antiviral activity may contribute to a higher viral load in the cells. Previous analysis of immunophenotypes after infection in mice with neuroinvasion without or with disease, demonstrated that prolonged and robust innate immune activity within the brain, probably due to a lack of peripheral virus control and viral spread to the brain, correlates with disease (Graham JB et al., 2015; 2019). However, it is possible that this immune activity may be either a driver of disease or an indicator of continued viral replication with the nervous system. Recently, Green R and colleagues studied the innate immune transcriptomic profiles of asymptomatic and symptomatic CC mice in response to WNV. They found that symptomatic F1s CC mice lacking functional Oas1b (N/N) had a lack of innate immune induction and cell migration that included monocyte migration and macrophage development, while the asymptomatic F/F F1s CC mice displayed earlier viral recognition, which appeared in IFIT1 and IFNβ1 expression (Green R et al., 2017). These observations indicated that insufficient activation of key processes, such as systemic innate immune signalling as well as intrinsic CNS antiviral and IFN responses, does not enable the host to develop a strong defence, which thus succumbs to infection in a manner linked to loss of Oas1b function. Moreover, considering the data obtained by the just mentioned *in vivo* studies, further *in vitro* comparisons of innate immune genes expression kinetics in response to virus infections will be performed to provide novel insights into the correlation between antiviral response activity and disease outcomes.

Studies with transgenic gene knockout mice have shown that innate immune responses are essential for the protection of flavivirus infection and control the diseases (Suthar MS et al., 2010; Suthar MS et al., 2013). These defences include the production of type I IFNs that induce the expression of antiviral genes and pro-inflammatory cytokines, which activate the adaptive immune response (Fig 5.1). Host factors finely regulate these signalling pathways at multiple levels starting from viral sensing and recognition to transduction and regulation of transcription (Pastorino Bet al., 2010). RLR-mediated innate immunity and IFN actions are

essential for restricting WNV replication and neuroinvasion to the CNS (Daffis S et al., 2007; 2008).

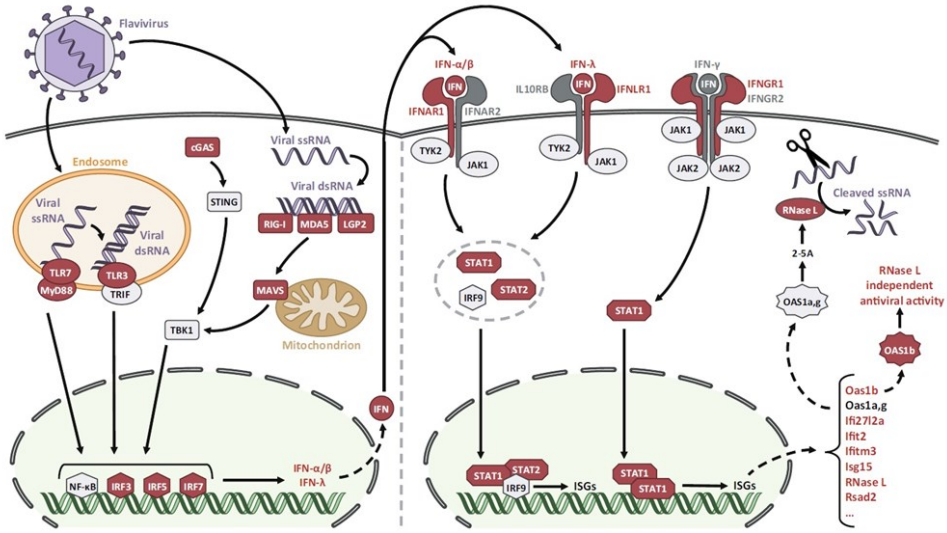

Fig 5.1 Innate immune response against flavivirus infection (Manet C et al., 2018)
Infected cells first sense the presence of viruses through the actions of host RIG-I-like receptors (RLRs), such as RIG-I and MDA5, which are expressed within the cell cytoplasm, and subsequently through endosomal Toll-like receptor 3 (TLR3) (Daffis S et al., 2008; Kawai T and Akira S, 2007). Virus recognition drives RLR signaling to downstream activation of interferon (IFN) regulatory factor 3 (IRF3) and NF-kB transcription factors for induction of type I type II, and type III IFNs transcription. Each IFN subtype (α/β, γ, λ) binds to its specific receptor (IFNAR, IFNGR, IFNLR) expressed on surrounding cells which leads to the activation of the JAK/STAT transduction pathways. STAT proteins activate the transcription of hundreds of ISGs, effector genes that confer antiviral actions, including Oas genes, some of which sense viral dsRNA and further promote viral ssRNA cleavage by activating RNase L.

In addition to the previous evidences, our analysis also proposes IFN pathway as a key regulator of susceptibility to flavivirus. Several pathway mediators indeed, resulted downregulated in WNND lines compared to the asymptomatic cell lines in response to viral infections. They included the viral sensor TLR3, the cytoplasmatic MAVS and the downstream IRF7 (Lazear HM et al., 2013b)

Toll-like receptors (TLR) are pattern recognition receptors (PRR) expressed on the cell surface or within endosomes. After recognizing double-stranded RNA associated to viral infection, TLR3 activates IRF-3/ IRF-7 and NF-KB transcriptional pathways and induce type I IFN (Fig 5.1). The role of TLR-3 in protection against WNV infections *in vitro* was largely dispensable (Fredericksen BL and Gale M Jr et al., 2006; Scholle F and Mason PW et al., 2005), by contrast, the analysis of TLR3-deficient mice has drawn contradictory results. A first study found that TLR3 (-/-) mice were more resistant to WNV infection than controls, and protected mice from lethal infection (Wang et al. 2004), while another study reported higher mortality and increased viral burden in the CNS (Daffis et al.2008a). Anyhow, discrepancies were associated

to differences in passage of the virus, and to viral dose or route of inoculation. MAVS is a mitochondrial-associated IFN-promoter stimulator that acts downstream of the cytosolic PRRs, also known as RLRs (RIG-1 and MDA5) to coordinate path leading to activation of NFkB, IRF3, IRF7 and subsequent induction of antiviral cytokines (Fig 5.1). Supporting our results, mice deficient for Mavs were high susceptible to WNV and ZIKV and showed enhanced WNV replication and dissemination, with high mortality (Suthar et al., 2010) and maintained productive ZIKV infection abrogating almost completely type I IFN induction (Ma J et al., 2018). Despite IRF-3, IRF-5, and IRF-7 seem to have redundant functions, since these three genes need to be simultaneously inactivated to induce susceptibility to DENV or ZIKV (Carlin et al., 2017; Lazear et al., 2016). IRF-7(-/-), mice infected with WNV showed increased lethality compared to congenic wild-type mice and developed early and elevated WNV burdens in both peripheral and CNS tissues. In agreement with our results, the deficiency of IRF-7 blunted the systemic type I IFN response in mice (Daffis et al. 2008b). Low level of endogenous IRF-7 are constitutively expressed and at early stage of infection, together with IRF3 and NF-kB. They are activated by TLRs or RLRs and mediate a transcriptional cascade that allows rapid ISG expression before IFN itself can be produced. However, IRF7 is an ISG induced by type 1 IFN and it is the major source of IRF7 expression in the cells (Fig 5.1).

Our results suggested that the key apoptotic regulator Caspase 3 was the only upregulated gene in WNND lines compared to Asympt lines following infection with all the three viruses, confirming the outcome of caspase activity assay. Caspase 3 is an effector caspase that has central regulator functions in apoptosis (Jänicke RU et al., 1998). Ability of WNV infection to triggers apoptotic pathway resulting in caspase 3 activation, cytochrome c release, and exposure of phosphatidylserine on the outer leaflet of the plasma membrane is now well established. It has been demonstrated in different transformed cell lines (Chu JJ and Ng ML, 2003; Parquet MC et al., 2001) and mouse ESC-derived neurons and neuroblastoma cells (Shrestha Be et al., 2003). Several other encephalitic flaviviruses induce apoptosis, including ZIKV and USUV, as experimentally demonstrated both *in vitro* and *in vivo* (Huang WC et al., 2016; Hastings AK et al., 2019; Weissenböck H et al., 2004; Salinas S et al.,2017). In brains of wild-type mice, WNV infection induced caspase 3 activation and apoptosis (Samuel MA et al., 2007). Although no significant differences in tissue viral burden or the kinetics of viral spread were detected, congenic caspase 3−/− mice were more resistant to lethal WNV infection and decreased neuronal death was observed in the cerebral cortices, brain stems, and cerebella (Samuel MA et al., 2007).

Other modulators of IFN pathway analysed in our study appeared less expressed in symptomatic WNND lines. These include the viral RNA sensor MDA5 and the effector gene IFIT1, which were less expressed in response to both USUV and ZIKV infections; IFN λ2 in response to USUV infection; and NF-kB following ZIKV and WNV infections. Mice lacking MDA5 gene were extremely susceptible to WNV infection, which led to reduced survival and elevated viral burden in the CNS, with small effects on systemic type I interferon response or viral replication in peripheral tissues. (Lazear et al. 2013). No KO mouse models have yet been developed to investigate the effect of NF-κB ablation upon ZIKV and WNV infections. Lang J and colleagues showed that ZIKV inhibited the NF-κB signalling pathway in hiPSC-derived macrophage with a mechanism to be still elucidated (Lang J et al., 2018). However, it has been reported that ZIKV NS5 is able to inhibit NF-κB signalling pathway by inducing STAT2 degradation (Kumar et al., 2016). Similarly, WNV non-structural protein NS1 was shown to inhibit the translocation of NF-kB to the nucleus, preventing IFNβ and inflammatory cytokine expression (Wilson et al., 2008).

Many ISGs have been shown to influence mouse susceptibility to WNV infection, including viperin, Ifi27l2a, Ifitm3, or Ifit2 (Cho et al. 2013; Gorman et al. 2016; Lucas et al. 2015; Szretter et al. 2011). Nevertheless, the magnitude of ISG induction does not always correlate with the strength of antiviral effects. A key example is the family of IFIT proteins (IFIT1,2,3,5). IFIT family members form a multiprotein complex in which IFIT1 sequesters viral RNAs containing 5' triphosphates. In our study, IFIT1 resulted less expressed in NSCs from cases. However, we cannot speculate any direct correlation between lower expression and disease outcome since flaviviruses use a virally-encoded 2'O-methyltransferase to specifically evade inhibition by IFIT proteins, and virulent strain of WNV, commonly used for pathogenesis studies exhibited no phenotype in IFIT1−/− primary cells or mice (Lazear HM and Diamond MS, 2015).

Type 1 (α, β) and 3 (λ1,2,3,4) IFNs overlap expression and functions but also have distinct functions: they are induced through specific pathways, are temporally regulated and bind to different receptors with specific binding affinity. Despite the notable expression of type 3 IFNs in response to USUV, we found a significant lower level of IFNλ2 mRNA expression in NSCs from cases than from controls. Interestingly, the strong IFNs induction did not prevent USUV replication, thus suggesting that USUV infection may inhibit IFN antiviral activity through a mechanism that remains to be determined. A previous study demonstrated that in DCs, USUV induced higher antiviral activities, and was more sensitive to type I and III IFNs than WNVs (Cacciotti G. et al., 2015). Overall, these data suggest that compared to blood donors, NSCs

derived from encephalitis patients had an attenuated antiviral response to flavivirus infection that may contribute to a higher viral load in these cells.

To correlate the phenotypic data with host genetic background and to identify individual genome signatures influencing protection or susceptibility to WNV, we performed exome sequencing by NGS of a panel of 2,600 genes related to antiviral response and innate immune system in iPSC clones of cases and controls. We evaluated the presence of alterations in the patients' genes that were absent in the controls. Despite data need to be fully confirmed, we found some homozygous or heterozygous missense variants and deletions, and a large portion was predicted as damaging the protein function by different computational scores. Quite interesting were the premature stop codon that may activate the nonsense mediated decay process (NMD), which we identified in the *PSIP1* gene in the first patient, and in the cytoplasmic sensor of viral nucleic acids *DDX58*, in the second patient. Both variants were in homozygosity. Lens epithelium-derived growth factor/p75 (LEDGF/p75, or PSIP1) is a transcriptional coactivator that tethers other proteins to gene bodies. LEDGF/p75 functions as a chromatin tethering factor for the pre-integration complex, and targets HIV-1 integration towards actively transcribed genomic regions. Also known as transcription co-activator p75, PC4 and SFRS1 interacting protein (PSIP1), and dense fine speckled autoantigen of 70 kD (DFS70). It is known to be a transcriptional co-activator for heat-shock and stress-related genes and plays a role as anti-apoptotic protein in diverse oncologic settings and this multifunctional protein has gained relevance in the study of cancer, autoimmunity, and eye disease (Basu A et al., 2015). It could be sensor of cellular stress and inflammation associated with environmental factors (Ochs RL et al., 2015).

DDX58, also known as retinoic acid-inducible gene I (RIG-I), is a PRR gene which plays a major role in sensing viral infection and in association with mitochondria antiviral signalling protein (MAVS/IPS1), it activates a cascade of antiviral responses including the induction of type I interferons and proinflammatory cytokines (Fig 5.1). Previous studies showed that lack of RIG-I resulted in reduced innate immune signalling and virus control in primary cells *in vitro* and increased mortality in mice, after WNV infection (Errett et al. 2013; Lazear et al. 2013). Indeed, it is well known that this protein is a target for the non-structural protein 1 (NS1) of WNV that by interacting with it, induce its degradation and thus, antagonizes the induction of IFN-β (Zhang HL et al., 2017). Jang MA and colleagues demonstrated that two human gain-of-function *DDX58* mutations cause atypical Singleton-Merten syndrome (SMS) manifesting with

variable expression of glaucoma, aortic calcification, and skeletal abnormalities without dental anomalies. RIG-I over-expression led to increased expression of IFN-β, interferon-stimulated gene 15, and chemokine (C-C motif) ligand 5 (Jang MA et al., 2015). While these variants induced an excessive production of type I IFNs and inflammatory cytokines that might be related to a predisposition to inflammatory or autoimmune diseases, we speculate that the homozygous frameshift deletion which involved the *DDX58* gene detected in our WNND2 patient may result to a decrease of mRNA expression due to activation of NMD pathway, leading to a defective negative regulation of innate IFNs response.

NMD is an RNA surveillance mechanism that operates by selectively degrading mRNA transcripts that contain premature terminated codons (PTCs) from nonsense and frameshift mutations (Nickless A et al., 2017). When nonsense or frameshift mutations were in heterozygosity, NMD may prevents the deleterious effects of a dominant-negative to haploinsufficiency by degrading mutant mRNAs before they could produce large amounts of defective protein. In contrast, in individuals who were homozygous for the same mutation, NMD could let to almost complete elimination of the gene product inducing a severe phenotype (Zarraga IG et al., 2011). However, as a molecular 'vacuum cleaner', NMD apparently limits the expression of transcripts produced by faulty or alternative splicing that also creates PTCs. Therefore, we must confirm and better characterize this result with additional expression analysis and functional studies.

Another interesting result was the double heterozygous SNIP in IRF7 gene found in iPSC of the WNND1 patient. The lack of IRF7 was previously associated to severe WNV-infection outcome (Daffis et al. 2008b) and heterozygous null mutations in human IRF7 were identified as responsible to life-threatening influenza during primary infection (Ciancanelli et al., 2017). Albeit very frequent among population, these variants harbour in a well know key transcriptional regulator of the innate immune response against RNA viruses (Ning S et al., 2011). Polymorphic alleles of specific genes may have separately little effect on the phenotype, but the total effect of the combination of these alleles could be high. Supported by previous studies (Caires-Júnior LC et al., 2018; Yudin NS et al., 2018), we speculated that a recessive or multifactorial inheritance rather than a dominant monogenic inheritance may explain the individual susceptibility to flavivirus infection.

Only two polymorphisms that are quite frequent among the population were identified in common between the two patients. Anyway, we did not expect a different result, given the small number of samples and all the possible genetic factors that may be involved in infectious

disease susceptibility. These single nucleotide polymorphisms (SNIPs) included the synonymous variant L830L in the *JAK2* gene (rs2230724) and the N345S variant in the *DOCK8* gene (rs10970979). JAK2 encodes for the protein tyrosine kinase Janus kinase 2 (JAK2), which is involved in a specific subset of cytokine receptor signalling pathways and it is required for responses to IFNγ (Shuai K et al., 2003). Several flaviviruses including WNV, Japanese encephalitis virus, ZIKV, and dengue virus, can suppress JAK/STAT signalling by inhibiting JAK phosphorylation (Guo JT et al., 2005; Lin RJ et al., 2004; Thurmond S et al., 2018; Ho LJ et al., 2005) and blocking IFN signalling. The recurrent JAK2 V617F gain-of-function mutation has been an important molecular marker for myeloproliferative neoplasms that includes polycythemia vera, essential thrombocythemia, and idiopathic myelofibrosis since its discovery in 2005 (Kralovics R et al., 2005). *DOCK8*, encoding a guanine nucleotide exchange factor, is mostly found in cells of the immune system including T cells, NK cells, and B cells and plays a critical role in their survival and function (Kearney CJ et al., 2017). Additionally, DOCK8 regulates MyD88-dependent Toll-like receptor signalling and the activation of the transcription factor STAT3 (Jabara HH et al., 2012). Loss of function mutations in *DOCK8* was responsible to Dedicator of Cytokinesis 8 (DOCK8) deficiency, which is a rare autosomal recessive primary immunodeficiency seen predominantly in consanguineous populations. The clinical features ranging from recurrent infections, allergic diseases including eczema and food allergy, autoimmunity and virally driven cancers (Aydin SE et al.,2015; Zhang Q et al., 2009).

Sequencing of iPSC from the first patient revealed other exonic and splicing regions of the genome harbouring nonsynonymous SNVs including the following genes: ITGAX, PHF2, CEP135, CKAP5, AGPAT4, TRIM10 and TRIM40; and a frameshift IFITM5 genes. Additionally, we identified two well-known polymorphisms in IRF4 and SMARCA2 genes. All these alterations can potentially cause deleterious effects to the encoded protein, except for those affecting the upstream region of the TRIM40 gene, which has no predictions.

The analysis will be completed only after having confirmed by Sanger sequencing all the mutations we identified and mentioned above. The same analysis will be performed on both iPSCs and PBMCs derived from cases and controls to exclude mutations acquired during the reprogramming. Functional studies will be carried out in order to deepen the analysis. A further investigation that we are going to perform is to analyse the genetic variations which are present in the asymptomatic WNV-infected controls but absent in WNV-infected patients, to better characterized these patients and to find, if any, some genetic variations correlated to flaviviruses infection resistance.

In conclusion, our study demonstrated that patient-specific iPSCs are useful tools to model individual susceptibility to viral infectious diseases and recapitulated *in vitro* the individual disease traits. Data showed how WNV, USUV and, to a lesser extent, ZIKV, replicated more efficiently and induced more cell death and apoptosis in NSCs derived from patients with WNV encephalitis than in cells derived from blood donors with asymptomatic infection. Notably, the increased susceptibility of patient-specific NSCs to neurotropic flaviviruses was associated with blunted innate antiviral response and the presence of inactivating mutations in candidate infectious disease susceptibility genes.

Besides the identification of the disease risk groups who might benefit from targeted vaccination and preventive therapy, detection of human predisposition genes to severe forms of infectious diseases is important also for understanding the mechanisms of pathogenesis. By improving our knowledge about the types of immune responses that can naturally confer protection from viral invasion of the nervous system, we can look for ways to generate or manipulate these protective immune responses to prevent deleterious clinical outcomes.

Human pathogens affect patient health through a complex interplay with the host, which cannot be recapitulated completely in *in vivo* mouse models. The availability of human iPSC-derived differentiated cells holds immense promise for the development of easy to handle cell systems for the investigation of interaction with the human host, viral tropism, pathogenesis, latency and reactivation. But, the greatest advantage of iPSC technology remains the possibility to generate pluripotent cells from any individual in the context of his or her own genetic identity, including individuals with rare forms of disease or those affected by complex multifactorial diseases of unknown genetic component.

6. ACKNOWLEDGMENTS

I would like to thank Dr.ssa Giovanna Desole, Dr.ssa Giulia Masi, Dr.ssa Elektra Peta, and Dr.ssa Monia Pacenti for the technical support;

Dr.ssa Marta Trevisan, my teacher and example from the beginning. I thank Marta for initiating me to the scientific world and accompanying me throughout my entire growth;

Dr. Alessandro Sinigaglia for the supervision but mostly, for the moral support and patience that has shown me during all these years. Alessandro's serenity was precious and contagious to me;

My mentor Prof.ssa Luisa Barzon, who gave me the opportunity to undertake this scientific training with extreme intellectual freedom and enthusiasm.

Without all of them I could not have learned to work with perseverance and dedication, to wear the lab coat with pride and to approach the scientific life. My PhD training has been fundamental for my personal development and has taught me to face the problems of research with tenacity and to develop a critical eye; to wait patiently for the outcome of an experiment and to welcome it with extreme enthusiasm once it arrives. At the end of this experience, a fundamental concept was strongly internalized in me: there is no research without passion.

Finally, the greatest thank goes to my family, my refuge. I would not have enriched my life with similar experiences and goals, if they had not always left me free to choose and to make mistakes, then grow and mature my person, both from a human and a professional point of view.

7. REFERENCES

Abrahams VM, Potter JA, Bhat G, Peltier MR, Saade G, Menon R. Bacterial modulation of human fetal membrane Toll-like receptor expression. Am J Reprod Immunol. 2013 Jan;69(1):33-40. doi: 10.1111/aji.12016. Epub 2012 Sep 11.

Al-Obaidi MMJ, Bahadoran A, Har LS, Mui WS, Rajarajeswaran J, Zandi K, Manikam R, Sekaran SD. Japanese encephalitis virus disrupts blood-brain barrier and modulates apoptosis proteins in THBMEC cells. Virus Res. 2017 Apr 2;233:17-28. doi: 10.1016/j.virusres.2017.02.012. Epub 2017 Mar 6.

Alonso-Palomares LA, Moreno-García M, Lanz-Mendoza H, Salazar MI. Molecular Basis for Arbovirus Transmission by Aedes aegypti Mosquitoes. Intervirology. 2018;61(6):255-264. doi: 10.1159/000499128. Epub 2019 May 13.

Annamalai AS, Pattnaik A, Sahoo BR, Muthukrishnan E, Natarajan SK, Steffen D, Vu HLX, Delhon G, Osorio FA, Petro TM, Xiang SH, Pattnaik AK. Zika Virus Encoding Nonglycosylated Envelope Protein Is Attenuated and Defective in Neuroinvasion. J Virol. 2017 Nov 14;91(23). pii: e01348-17. doi: 10.1128/JVI.01348-17. Print 2017 Dec 1.

Ashraf U, Ye J, Ruan X, Wan S, Zhu B, Cao S. Usutu virus: an emerging flavivirus in Europe. Viruses. 2015 Jan 19;7(1):219-38. doi: 10.3390/v7010219.

Aydin SE, Kilic SS, Aytekin C, Kumar A, Porras O, Renner ED, Su H, Freeman AF, Engelhardt K, Albert MH. DOCK8 Deficiency : Clinical and Immunological Phenotype and Treatment Options - a Review of 136 Patients. J Clin Immunol. 2015;35:189–198. doi: 10.1007/s10875-014-0126-0

Bardos V, Adamcova J, Dedei S, Gjini N, Rosicky B, Simkova A. Neutralizing antibodies against some neurotropic viruses determined in human sera in Albania. J Hyg Epidemiol Microbiol Immunol. 1959;3:277-82.

Barzon L, Pacenti M, Franchin E, Lavezzo E, Masi G, Squarzon L, Pagni S, Toppo S, Russo F, Cattai M, Cusinato R, Palu G. Whole genome sequencing and phylogenetic analysis of West Nile virus lineage 1 and lineage 2 from human cases of infection, Italy, August 2013. Euro Surveill. 2013 Sep 19;18(38). pii: 20591.

Barzon L, Pacenti M, Franchin E, Martello T, Lavezzo E, Squarzon L, Toppo S, Fiorin F, Marchiori G, Scotton GP, Russo F, Cattai M, Cusinato R, Palù G. Clinical and virological findings in the ongoing outbreak of West Nile virus Livenza strain in northern Italy, July to September 2012. Euro Surveill. 2012 Sep 6;17(36):20260.

Barzon L, Pacenti M, Franchin E, Pagni S, Lavezzo E, Squarzon L, Martello T, Russo F, Nicoletti L, Rezza G, Castilletti C, Capobianchi MR, Salcuni P, Cattai M, Cusinato R, Palù G. Large human outbreak of West Nile virus infection in north-eastern Italy in 2012. Viruses. 2013 Nov 22;5(11):2825-39

Barzon L, Pacenti M, Franchin E, Squarzon L, Lavezzo E, Cattai M, Cusinato R, Palù G. The complex epidemiological scenario of West Nile virus in Italy. Int J Environ Res Public Health. 2013 Sep 30;10(10):4669-89.

Barzon L, Papa A, Lavezzo E, Franchin E, Pacenti M, Sinigaglia A, Masi G, Trevisan M, Squarzon L, Toppo S, Papadopoulou E, Nowotny N, Ulbert S, Piralla A, Rovida F, Baldanti F, Percivalle E, Palù G. Phylogenetic characterization of Central/Southern European lineage 2 West Nile virus: analysis of human outbreaks in Italy and Greece, 2013-2014. Clin Microbiol Infect. 2015 Dec;21(12):1122.e1-10. doi: 10.1016/j.cmi.2015.07.018. Epub 2015 Jul 31.

Barzon L, Squarzon L, Cattai M, Franchin E, Pagni S, Cusinato R, Palu G. West Nile virus infection in Veneto region, Italy, 2008-2009. Euro Surveill. 2009 Aug 6;14(31). pii: 19289.

Barzon L. Ongoing and emerging arbovirus threats in Europe. J Clin Virol. 2018 Oct;107:38-47. doi: 10.1016/j.jcv.2018.08.007. Epub 2018 Aug 23.

Barzon, L., Pacenti, M., Franchin, E., Lavezzo, E., Trevisan, M., Sgarabotto, D., Palù, G.Infection dynamics in a traveller with persistent shedding of Zika virus RNA in semen for six months after returning from Haiti to Italy, January 2016.Euro Surveill. 2016. 21(32). doi: 10.2807/1560-7917.ES.2016.21.32.30316

Basu A, Sanchez TW, Casiano CA. DFS70/LEDGFp75: An Enigmatic Autoantigen at the Interface between Autoimmunity, AIDS, and Cancer. Front Immunol. 2015 Mar 20;6:116. doi: 10.3389/fimmu.2015.00116. eCollection 2015.

Baud D, Gubler DJ, Schaub B, Lanteri MC, Musso D. An update on Zika virus infection. Lancet. 2017 Nov 4;390(10107):2099-2109.

Bayer A, Lennemann NJ, Ouyang Y, Bramley JC, Morosky S, Marques ET Jr, Cherry S, Sadovsky Y, Coyne CB. Type III Interferons Produced by Human Placental Trophoblasts Confer Protection against Zika Virus Infection. Cell Host Microbe. 2016 May 11;19(5):705-12. doi: 10.1016/j.chom.2016.03.008. Epub 2016 Apr 5.

Bayer A, Lennemann NJ, Ouyang Y, Sadovsky E, Sheridan MA, Roberts RM, Coyne CB, Sadovsky Y. Chromosome 19 microRNAs exert antiviral activity independent from type III interferon signalling. Placenta. 2018 Jan;61:33-38. doi: 10.1016/j.placenta.2017.11.004. Epub 2017 Nov 10.

Bażanów B, Jansen van Vuren P, Szymański P, Stygar D, Frącka A, Twardoń J, Kozdrowski R, Pawęska JT. A Survey on West Nile and Usutu Viruses in Horses and Birds in Poland. Viruses. 2018 Feb 17;10(2). pii: E87. doi: 10.3390/v10020087.

Beasley DW, Barrett AD. Identification of neutralizing epitopes within structural domain III of the West Nile virus envelope protein. J. Virol. 2002; 76: 13 097– 100.

Beasley DW, Davis CT, Whiteman M, Granwehr B, Kinney RM, Barrett AD. Molecular determinants of virulence of West Nile virus in North America. Arch Virol Suppl. 2004;(18):35-41.

Beasley DW, Whiteman MC, Zhang S, Huang CY, Schneider BS, Smith DR, Gromowski GD, Higgs S, Kinney RM, Barrett AD. Envelope protein glycosylation status influences mouse neuroinvasion phenotype of genetic lineage 1 West Nile virus strains. J Virol. 2005 Jul;79(13):8339-47.

Bennett SN, Holmes EC, Chirivella M, Rodriguez DM, Beltran M, Vorndam V, Gubler DJ, McMillan WO. Selection-driven evolution of emergent dengue virus. Mol Biol Evol. 2003 Oct;20(10):1650-8. Epub 2003 Jun 27.

Best SM. Flaviviruses. Curr Biol. 2016 Dec 19;26(24):R1258-R1260. doi: 10.1016/j.cub.2016.09.029.

Bigham AW, Buckingham KJ, Husain S, Emond MJ, Bofferding KM, Gildersleeve H, Rutherford A, Astakhova NM, Perelygin AA, Busch MP, Murray KO, Sejvar JJ, Green S, Kriesel J, Brinton MA, Bamshad M. Host genetic risk factors for West Nile virus infection and disease progression. PLoS One. 2011;6(9):e24745. doi: 10.1371/journal.pone.0024745. Epub 2011 Sep 15.

Bonnevie-Nielsen V, Field LL, Lu S, Zheng DJ, Li M, Martensen PM, Nielsen TB, Beck-Nielsen H, Lau YL, Pociot F. Variation in antiviral 2',5'-oligoadenylate synthetase (2'5'AS) enzyme activity is controlled by a single-nucleotide polymorphism at a splice-acceptor site in the OAS1 gene. Am J Hum Genet. 2005 Apr;76(4):623-33. Epub 2005 Feb 24.

Bossert B, Marozin S, Conzelmann KK. Nonstructural proteins NS1 and NS2 of bovine respiratory syncytial virus block activation of interferon regulatory factor 3. J Virol. 2003 Aug; 77(16):8661-8.

Brasil P, Pereira JP Jr, Moreira ME, Ribeiro Nogueira RM, Damasceno L, Wakimoto M, Rabello RS, Valderramos SG, Halai UA, Salles TS, Zin AA, Horovitz D, Daltro P, Boechat M, Raja Gabaglia C, Carvalho

de Sequeira P, Pilotto JH, Medialdea-Carrera R, Cotrim da Cunha D, Abreu de Carvalho LM, Pone M, Machado Siqueira A, Calvet GA, Rodrigues Baião AE, Neves ES, Nassar de Carvalho PR, Hasue RH, Marschik PB, Einspieler C, Janzen C, Cherry JD, Bispo de Filippis AM, Nielsen-Saines K. Zika Virus Infection in Pregnant Women in Rio de Janeiro. N Engl J Med. 2016 Dec 15;375(24):2321-2334. Epub 2016 Mar 4.

Brault AC, Huang CY, Langevin SA, Kinney RM, Bowen RA, Ramey WN, Panella NA, Holmes EC, Powers AM, Miller BR. A single positively selected West Nile viral mutation confers increased virogenesis in American crows. Nat Genet. 2007 Sep;39(9):1162-6. Epub 2007 Aug 12.

Brault JB, Khou C, Basset J, Coquand L, Fraisier V, Frenkiel MP, Goud B1, Manuguerra JC, Pardigon N, Baffet AD. Comparative Analysis Between Flaviviruses Reveals Specific Neural Stem Cell Tropism for Zika Virus in the Mouse Developing Neocortex. EBioMedicine. 2016 Aug;10:71-6. doi: 10.1016/j.ebiom.2016.07.018. Epub 2016 Jul 16.

Brinton MA, Perelygin AA. Genetic resistance to flaviviruses. Adv Virus Res. 2003;60:43-85.

Cacciotti G, Caputo B, Selvaggi C, la Sala A, Vitiello L, Diallo D, Ceianu C, Antonelli G, Nowotny N, Scagnolari C. Variation in interferon sensitivity and induction between Usutu and West Nile (lineages 1 and 2) viruses. Virology. 2015 Nov;485:189-98. doi: 10.1016/j.virol.2015.07.015. Epub 2015 Aug 14.

Cadar D, Lühken R, van der Jeugd H, Garigliany M, Ziegler U, Keller M, Lahoreau J, Lachmann L, Becker N, Kik M, Oude Munnink BB, Bosch S, Tannich E, Linden A, Schmidt V, Koopmans MP, Rijks J, Desmecht D, Groschup MH, Reusken C, Schmidt-Chanasit J. Widespread activity of multiple lineages of Usutu virus, western Europe, 2016. Euro Surveill. 2017 Jan 26;22(4). pii: 30452. doi: 10.2807/1560-7917.ES.2017.22.4.30452.

Caires-Júnior LC, Goulart E, Melo US, Araujo BHS, Alvizi L, Soares-Schanoski A, de Oliveira DF, Kobayashi GS, Griesi-Oliveira K, Musso CM, Amaral MS, daSilva LF, Astray RM, Suárez-Patiño SF, Ventini DC, Gomes da Silva S, Yamamoto GL, Ezquina S, Naslavsky MS, Telles-Silva KA, Weinmann K, van der Linden V, van der Linden H, de Oliveira JRM, Arrais NMR, Melo A, Figueiredo T, Santos S, Meira JGC, Passos SD, de Almeida RP, Bispo AJB, Cavalheiro EA, Kalil J, Cunha-Neto E, Nakaya H, Andreata-Santos R, de Souza Ferreira LC, Verjovski-Almeida S6, Ho PL, Passos-Bueno MR, Zatz M. Discordant congenital Zika syndrome twins show differential in vitro viral susceptibility of neural progenitor cells. Nat Commun. 2018 Feb 2;9(1):475. doi: 10.1038/s41467-017-02790-9.

Calisher CH, Karabatsos N, Dalrymple JM, Shope RE, Porterfield JS, Westaway EG, Brandt WE. Antigenic relationships between flaviviruses as determined by cross-neutralization tests with polyclonal antisera. J Gen Virol. 1989; 70(Pt 1):37–43.

Camp JV, Kolodziejek J, Nowotny N. Targeted surveillance reveals native and invasive mosquito species infected with Usutu virus. Parasit Vectors. 2019 Jan 21;12(1):46. doi: 10.1186/s13071-019-3316-z.

Carlin AF, Plummer EM, Vizcarra EA, Sheets N, Joo Y, Tang W, Day J, Greenbaum J, Glass CK, Diamond MS, Shresta S. An IRF-3-, IRF-5-, and IRF-7-Independent Pathway of Dengue Viral Resistance Utilizes IRF-1 to Stimulate Type I and II Interferon Responses. Cell Rep. 2017 Nov 7;21(6):1600-1612. doi: 10.1016/j.celrep.2017.10.054.

Carpenter L, Carr C, Yang CT, Stuckey DJ, Clarke K, Watt SM. Efficient differentiation of human induced pluripotent stem cells generates cardiac cells that provide protection following myocardial infarction in the rat. Stem Cells Dev. 2012 Apr 10;21(6):977-86. doi: 10.1089/scd.2011.0075. Epub 2012 Feb 15.

Carteaux G, Maquart M, Bedet A, Contou D, Brugières P, Fourati S, Cleret de Langavant L, de Broucker T, Brun-Buisson C, Leparc-Goffart I, Mekontso Dessap A. Zika Virus Associated with Meningoencephalitis. N Engl J Med. 2016 Apr 21;374(16):1595-6. doi: 10.1056/NEJMc1602964. Epub 2016 Mar 9.

Casanova JL, Abel L. Primary immunodeficiencies: a field in its infancy. Science. 2007 Aug 3;317(5838):617-9.

Casanova JL, Abel L. The genetic theory of infectious diseases: a brief history and selected illustrations. Annu Rev Genomics Hum Genet. 2013;14:215-43. doi: 10.1146/annurev-genom-091212-153448. Epub 2013 May 29.

Cauchemez S, Besnard M, Bompard P, Dub T, Guillemette-Artur P, Eyrolle-Guignot D, Salje H, Van Kerkhove MD, Abadie V, Garel C, Fontanet A, Mallet HP. Association between Zika virus and microcephaly in French Polynesia, 2013-15: a retrospective study. Lancet. 2016 May 21;387(10033):2125-2132. doi: 10.1016/S0140-6736(16)00651-6. Epub 2016 Mar 16.

Cavrini, F., Della Pepa, M.E., Gaibani, P., Pierro, A.M., Rossini, G., Landini, M.P., Sambri, V. A rapid and specific real-time RT-PCR assay to identify Usutu virus in human plasma, serum, and cerebrospinal fluid.J. Clin.Virol.2011.50,221– 223. doi:10.1016/j.jcv.2010.11.008.

Chancey C, Grinev A, Volkova E, Rios M. The global ecology and epidemiology of West Nile virus. Biomed Res Int. 2015;2015:376230. doi: 10.1155/2015/376230. Epub 2015 Mar 19.

Chandak NH, Kashyap RS, Kabra D, Karandikar P, Saha SS, Morey SH, Purohit HJ, Taori GM, Daginawala HF. Neurological complications of Chikungunya virus infection. Neurol India. 2009 Mar-Apr;57(2):177-80. doi: 10.4103/0028-3886.51289.

Chang CY, Li JR, Ou YC, Lin SY, Wang YY, Chen WY, Hu YH, Lai CY, Chang CJ, Chen CJ. Interplay of inflammatory gene expression in pericytes following Japanese encephalitis virus infection. Brain Behav Immun. 2017 Nov;66:230-243. doi: 10.1016/j.bbi.2017.07.003. Epub 2017 Jul 6.

Chan-Tack KM, Forrest G. West nile virus meningoencephalitis and acute flaccid paralysis after infliximab treatment. J Rheumatol. 2006 Jan;33(1):191-2. Epub 2005 Dec 1.

Cheeran MC, Hu S, Sheng WS, Rashid A, Peterson PK, Lokensgard JR. Differential responses of human brain cells to West Nile virus infection. J Neurovirol. 2005 Dec;11(6):512-24.

Chen T, He X, Zhang P, Yuan Y, Lang X, Yu J, Qin Z, Li X, Zhang Q, Zhu L, Zhang B, Wu Q, Zhao W. Research advancements in the neurological presentation of flaviviruses. Rev Med Virol. 2019 Jan;29(1):e2021. doi: 10.1002/rmv.2021. Epub 2018 Dec 12.

Cho H, Shrestha B, Sen GC, Diamond MS. A role for Ifit2 in restricting West Nile virus infection in the brain. J Virol. 2013 Aug;87(15):8363-71. doi: 10.1128/JVI.01097-13. Epub 2013 Jun 5.

Chowers MY, Lang R, Nassar F, Ben-David D, Giladi M, Rubinshtein E, Itzhaki A, Mishal J, Siegman-Igra Y, Kitzes R, Pick N, Landau Z, Wolf D, Bin H, Mendelson E, Pitlik SD, Weinberger M. Clinical characteristics of the West Nile fever outbreak, Israel, 2000. Emerg Infect Dis. 2001 Jul-Aug;7(4):675-8.

Chu JJ, Ng ML. The mechanism of cell death during West Nile virus infection is dependent on initial infectious dose. J Gen Virol. 2003 Dec;84(Pt 12):3305-14.

Chung KM, Liszewski MK, Nybakken G, Davis AE, Townsend RR, Fremont DH, Atkinson JP, Diamond MS. West Nile virus nonstructural protein NS1 inhibits complement activation by binding the regulatory protein factor H. Proc Natl Acad Sci U S A. 2006 Dec 12;103(50):19111-6. Epub 2006 Nov 28.

Ciancanelli MJ, Huang SX, Luthra P, Garner H, Itan Y, Volpi S, Lafaille FG, Trouillet C, Schmolke M, Albrecht RA, Israelsson E, Lim HK, Casadio M, Hermesh T, Lorenzo L, Leung LW, Pedergnana V, Boisson B, Okada S, Picard C, Ringuier B, Troussier F, Chaussabel D, Abel L, Pellier I, Notarangelo LD, García-Sastre A, Basler CF, Geissmann F, Zhang SY, Snoeck HW, Casanova JL. Infectious disease. Life-threatening influenza and impaired interferon amplification in human IRF7 deficiency. Science. 2015 Apr 24;348(6233):448-53. doi: 10.1126/science.aaa1578. Epub 2015 Mar 26.

Cirulli ET, Goldstein DB. Uncovering the roles of rare variants in common disease through whole-genome sequencing. Nat Rev Genet. 2010 Jun;11(6):415-25. doi: 10.1038/nrg2779.

Clark DC, Brault AC, Hunsperger E. The contribution of rodent models to the pathological assessment of flaviviral infections of the central nervous system. Arch Virol. 2012 Aug;157(8):1423-40. doi: 10.1007/s00705-012-1337-4. Epub 2012 May 17.

Cleton N, Koopmans M, Reimerink J, Godeke GJ, Reusken C. Come fly with me: review of clinically important arboviruses for global travelers. J Clin Virol. 2012 Nov;55(3):191-203. doi: 10.1016/j.jcv.2012.07.004. Epub 2012 Jul 25.

Comstock GW. Tuberculosis in twins: a re-analysis of the Prophit survey. Am Rev Respir Dis. 1978 Apr;117(4):621-4.

Courtney SC, Di H, Stockman BM, Liu H, Scherbik SV, Brinton MA. Identification of novel host cell binding partners of Oas1b, the protein conferring resistance to flavivirus-induced disease in mice. J Virol. 2012 Aug;86(15):7953-63. doi: 10.1128/JVI.00333-12. Epub 2012 May 23.

Csank T, Drzewnioková P, Korytár Ľ, Major P, Gyuranecz M, Pistl J, Bakonyi T. A Serosurvey of Flavivirus Infection in Horses and Birds in Slovakia. Vector Borne Zoonotic Dis. 2018 Apr;18(4):206-213. doi: 10.1089/vbz.2017.2216. Epub 2018 Feb 13.

Daffis S, Samuel MA, Suthar MS, Gale M Jr, Diamond MS. Toll-like receptor 3 has a protective role against West Nile virus infection. J Virol. 2008 Nov;82(21):10349-58. doi: 10.1128/JVI.00935-08. Epub 2008 Aug 20.

Daffis S, Samuel MA, Suthar MS, Keller BC, Gale M Jr, Diamond MS. Interferon regulatory factor IRF-7 induces the antiviral alpha interferon response and protects against lethal West Nile virus infection. J Virol. 2008b Sep;82(17):8465-75. doi: 10.1128/JVI.00918-08. Epub 2008b Jun 18.

D'Aiuto L, Di Maio R, Heath B, Raimondi G, Milosevic J, Watson AM, Bamne M, Parks WT, Yang L, Lin B, Miki T, Mich-Basso JD, Arav-Boger R, Sibille E, Sabunciyan S, Yolken R, Nimgaonkar V. Human induced pluripotent stem cell-derived models to investigate human cytomegalovirus infection in neural cells. PLoS One. 2012;7(11):e49700. doi: 10.1371/journal.pone.0049700. Epub 2012 Nov 27.

D'Aiuto L, Prasad KM, Upton CH, Viggiano L, Milosevic J, Raimondi G, McClain L, Chowdari K, Tischfield J, Sheldon M, Moore JC, Yolken RH, Kinchington PR, Nimgaonkar VL. Persistent infection by HSV-1 is associated with changes in functional architecture of iPSC-derived neurons and brain activation patterns underlying working memory performance. Schizophr Bull. 2015 Jan;41(1):123-32. doi: 10.1093/schbul/sbu032. Epub 2014 Mar 12.

Danial-Farran N, Eghbaria S, Schwartz N, Kra-Oz Z, Bisharat N. Genetic variants associated with susceptibility of Ashkenazi Jews to West Nile virus infection. Epidemiol Infect. 2015 Mar;143(4):857-63. doi: 10.1017/S0950268814001290. Epub 2014 May 27.

Daniels BP, Jujjavarapu H, Durrant DM, Williams JL, Green RR, White JP, Lazear HM, Gale M Jr, Diamond MS, Klein RS. Regional astrocyte IFN signaling restricts pathogenesis during neurotropic viral infection. J Clin Invest. 2017 Mar 1;127(3):843-856. doi: 10.1172/JCI88720. Epub 2017 Jan 30.

De Groot AS, Saint-Aubin C, Bosma A, Sbai H, Rayner J, Martin W. Rapid determination of HLA B*07 ligands from the West Nile virus NY99 genome. Emerg Infect Dis. 2001 Jul-Aug;7(4):706-13

de Souza KP, Silva EG, de Oliveira Rocha ES, Figueiredo LB, de Almeida-Leite CM, Arantes RM, de Assis Silva Gomes J, Ferreira GP, de Oliveira JG, Kroon EG, Campos MA. Nitric oxide synthase expression correlates with death in an experimental mouse model of dengue with CNS involvement. Virol J. 2013 Aug 26;10:267. doi: 10.1186/1743-422X-10-267.

Dean M, Carrington M, Winkler C, Huttley GA, Smith MW, Allikmets R, Goedert JJ, Buchbinder SP, Vittinghoff E, Gomperts E, Donfield S, Vlahov D, Kaslow R, Saah A, Rinaldo C, Detels R, O'Brien SJ.

Genetic restriction of HIV-1 infection and progression to AIDS by a deletion allele of the CKR5 structural gene. Hemophilia Growth and Development Study, Multicenter AIDS Cohort Study, Multicenter Hemophilia Cohort Study, San Francisco City Cohort, ALIVE Study. Science. 1996 Sep 27;273(5283):1856-62.

Decimo I, Bifari F, Krampera M, Fumagalli G. Neural stem cell niches in health and diseases. Curr Pharm Des. 2012;18(13):1755-83.

Dighe SN, Ekwudu O, Dua K, Chellappan DK, Katavic PL, Collet TA. Recent update on anti-dengue drug discovery. Eur J Med Chem. 2019 Aug 15;176:431-455. doi: 10.1016/j.ejmech.2019.05.010. Epub 2019 May 12.

Dill MT, Duong FH, Vogt JE, Bibert S, Bochud PY, Terracciano L, Papassotiropoulos A, Roth V, Heim MH. Interferon-induced gene expression is a stronger predictor of treatment response than IL28B genotype in patients with hepatitis C. Gastroenterology. 2011 Mar;140(3):1021-31. doi: 10.1053/j.gastro.2010.11.039. Epub 2010 Nov 25.

Dirlikov E, Torres JV, Martines RB, Reagan-Steiner S, Pérez GV, Rivera A, Major C, Matos D, Muñoz-Jordan J, Shieh WJ, Zaki SR, Sharp TM. Postmortem Findings in Patient with Guillain-Barré Syndrome and Zika Virus Infection. Emerg Infect Dis. 2018 Jan;24(1):114-117. doi: 10.3201/eid2401.171331

Duffy MR, Chen TH, Hancock WT, Powers AM, Kool JL, Lanciotti RS, Pretrick M, Marfel M, Holzbauer S, Dubray C, Guillaumot L, Griggs A, Bel M, Lambert AJ, Laven J, Kosoy O, Panella A, Biggerstaff BJ, Fischer M, Hayes EB. Zika virus outbreak on Yap Island, Federated States of Micronesia. N Engl J Med. 2009 Jun 11;360(24):2536-43. doi: 10.1056/NEJMoa0805715.

Dumpis U, Crook D, Oksi J. Tick-borne encephalitis. Clin Infect Dis. 1999 Apr;28(4):882-90.

Egloff MP, Benarroch D, Selisko B, Romette JL, Canard B. An RNA cap (nucleoside-2'-O-)-methyltransferase in the flavivirus RNA polymerase NS5: crystal structure and functional characterization. EMBO J. 2002 Jun 3;21(11):2757-68.

Eiden M, Gil P, Ziegler U, Rakotoarivony I, Marie A, Frances B, L'Ambert G, Simonin Y, Foulongne V, Groschup MH, Gutierrez S5, Eloit M. Emergence of two Usutu virus lineages in Culex pipiens mosquitoes in the Camargue, France, 2015. Infect Genet Evol. 2018 Jul;61:151-154. doi: 10.1016/j.meegid.2018.03.020. Epub 2018 Mar 26.

Eiselleova, L. et al. Comparative study of mouse and human feeder cells for human embryonic stem cells. The International journal of developmental biology. 52, 353–363, https://doi.org/10.1387/ijdb.082590le (2008).

Engel D, Jöst H, Wink M, Börstler J, Bosch S, Garigliany MM, Jöst A, Czajka C, Lühken R, Ziegler U, Groschup MH, Pfeffer M, Becker N, Cadar D, Schmidt-Chanasit J. Reconstruction of the Evolutionary History and Dispersal of Usutu Virus, a Neglected Emerging Arbovirus in Europe and Africa. MBio. 2016 Feb 2;7(1):e01938-15. doi: 10.1128/mBio.01938-15.

Errett JS, Suthar MS, McMillan A, Diamond MS, Gale M Jr. The essential, nonredundant roles of RIG-I and MDA5 in detecting and controlling West Nile virus infection. J Virol. 2013 Nov;87(21):11416-25. doi: 10.1128/JVI.01488-13. Epub 2013 Aug 21.

Evans JD, Crown RA, Sohn JA, Seeger C. West Nile virus infection induces depletion of IFNAR1 protein levels. Viral Immunol. 2011 Aug;24(4):253-63. doi: 10.1089/vim.2010.0126.

Evans JD, Seeger C. Differential effects of mutations in NS4B on West Nile virus replication and inhibition of interferon signaling. J Virol. 2007 Nov;81(21):11809-16. Epub 2007 Aug 22

Failloux AB. [Mosquitoes as vectors of arboviruses: an endless story]. Biol Aujourdhui. 2018;212(3-4):89-99. doi: 10.1051/jbio/2018026. Epub 2019 Apr 11.

Faye O, Freire CC, Iamarino A, Faye O, de Oliveira JV, Diallo M, Zanotto PM, Sall AA. Molecular evolution of Zika virus during its emergence in the 20(th) century. PLoS Negl Trop Dis. 2014 Jan 9;8(1):e2636. doi: 10.1371/journal.pntd.0002636. eCollection 2014.

Fellay J, Shianna KV, Ge D, Colombo S, Ledergerber B, Weale M, Zhang K, Gumbs C, Castagna A, Cossarizza A, Cozzi-Lepri A, De Luca A, Easterbrook P, Francioli P, Mallal S, Martinez-Picado J, Miro JM, Obel N, Smith JP, Wyniger J, Descombes P, Antonarakis SE, Letvin NL, McMichael AJ, Haynes BF, Telenti A, Goldstein DB. A whole-genome association study of major determinants for host control of HIV-1. Science. 2007 Aug 17;317(5840):944-7. Epub 2007 Jul 19.

Ferguson NM. Challenges and opportunities in controlling mosquito-borne infections. Nature. 2018 Jul;559(7715):490-497. doi: 10.1038/s41586-018-0318-5. Epub 2018 Jul 25.

Fernandez E, Dejnirattisai W, Cao B, Scheaffer SM, Supasa P, Wongwiwat W, Esakky P, Drury A, Mongkolsapaya J, Moley KH, Mysorekar IU, Screaton GR, Diamond MS. Human antibodies to the dengue virus E-dimer epitope have therapeutic activity against Zika virus infection. Nat Immunol. 2017 Nov;18(11):1261-1269. doi: 10.1038/ni.3849. Epub 2017 Sep 25.

Foy E, Li K, Wang C, Sumpter R Jr, Ikeda M, Lemon SM, Gale M Jr. Regulation of interferon regulatory factor-3 by the hepatitis C virus serine protease Science. 2003 May 16; 300(5622):1145-8.

Fredericksen BL, Gale M Jr. West Nile virus evades activation of interferon regulatory factor 3 through RIG-I-dependent and -independent pathways without antagonizing host defense signaling. J Virol. 2006 Mar;80(6):2913-23.

Fredericksen BL, Smith M, Katze MG, Shi PY, Gale M Jr. The host response to West Nile Virus infection limits viral spread through the activation of the interferon regulatory factor 3 pathway. J Virol. 2004 Jul;78(14):7737-47.

Garber C, Vasek MJ, Vollmer LL, Sun T, Jiang X, Klein RS. Astrocytes decrease adult neurogenesis during virus-induced memory dysfunction via IL-1. Nat Immunol. 2018 Feb;19(2):151-161. doi: 10.1038/s41590-017-0021-y. Epub 2018 Jan 1.

García LL, Padilla L, Castaño JC. Inhibitors compounds of the flavivirus replication process. Virol J. 2017 May 15;14(1):95. doi: 10.1186/s12985-017-0761-1.

Gaunt MW., Sall AA., de Lamballerie X., Falconar AK., Dzhivanian TI., Gould EA. Phylogenetic relationships of flaviviruses correlate with their epidemiology, disease association and biogeography. J. Gen. Virol. 2001;82(Pt 8):1867–1876.

Ge D, Fellay J, Thompson AJ, Simon JS, Shianna KV, Urban TJ, Heinzen EL, Qiu P, Bertelsen AH, Muir AJ, Sulkowski M, McHutchison JG, Goldstein DB. Genetic variation in IL28B predicts hepatitis C treatment-induced viral clearance. Nature. 2009 Sep 17;461(7262):399-401. doi: 10.1038/nature08309. Epub 2009 Aug 16.

Glass WG, McDermott DH, Lim JK, Lekhong S, Yu SF, Frank WA, Pape J, Cheshier RC, Murphy PM. CCR5 deficiency increases risk of symptomatic West Nile virus infection J Exp Med. 2006 Jan 23;203(1):35-40. Epub 2006 Jan 17.

Go YY, Balasuriya UB, Lee CK. Zoonotic encephalitides caused by arboviruses: transmission and epidemiology of alphaviruses and flaviviruses. Clin Exp Vaccine Res. 2014 Jan;3(1):58-77. doi: 10.7774/cevr.2014.3.1.58. Epub 2013 Dec 18.

Gollins S, Porterfield J. The uncoating and infectivity of the flavivirus West Nile on interaction with cells: effects of pH and ammonium chloride. J. Gen. Virol. 1986; 67: 1941–50.

Gordon FE, Nutt CL, Cheunsuchon P, Nakayama Y, Provencher KA, Rice KA, Zhou Y, Zhang X, Klibanski A. Increased expression of angiogenic genes in the brains of mouse meg3-null embryos. Endocrinology. 2010 Jun;151(6):2443-52. doi: 10.1210/en.2009-1151. Epub 2010 Apr 14.

Gorman MJ, Poddar S, Farzan M, Diamond MS. The Interferon-Stimulated Gene Ifitm3 Restricts West Nile Virus Infection and Pathogenesis. J Virol. 2016 Aug 26;90(18):8212-25. doi: 10.1128/JVI.00581-16. Print 2016 Sep 15.

Gould E, Pettersson J, Higgs S, Charrel R, de Lamballerie X. Emerging arboviruses: Why today?. One Health. 2017 Jul 1;4:1-13. doi: 10.1016/j.onehlt.2017.06.001. eCollection 2017 Dec.

Gould EA, Solomon T. Pathogenic flaviviruses. Lancet. 2008 Feb 9;371(9611):500-9. doi: 10.1016/S0140-6736(08)60238-X.

Govero J, Esakky P, Scheaffer SM, Fernandez E, Drury A, Platt DJ, Gorman MJ, Richner JM, Caine EA, Salazar V, Moley KH, Diamond MS. Zika virus infection damages the testes in mice. Nature. 2016 Dec 15;540(7633):438-442. doi: 10.1038/nature20556. Epub 2016 Oct 31.

Graham JB, Swarts JL, Thomas S, Voss KM, Sekine A, Green R, Ireton RC, Gale M, Lund JM. Immune Correlates of Protection From West Nile Virus Neuroinvasion and Disease. J Infect Dis. 2019 Mar 15;219(7):1162-1171. doi: 10.1093/infdis/jiy623.

Graham JB, Thomas S, Swarts J, McMillan AA, Ferris MT, Suthar MS, Treuting PM, Ireton R, Gale M Jr, Lund JM. Genetic diversity in the collaborative cross model recapitulates human West Nile virus disease outcomes. MBio. 2015 May 5;6(3):e00493-15. doi: 10.1128/mBio.00493-15.

Green R, Wilkins C, Thomas S, Sekine A, Hendrick DM, Voss K, Ireton RC, Mooney M, Go JT, Choonoo G, Jeng S, de Villena FP, Ferris MT, McWeeney S, Gale M Jr. Oas1b-dependent Immune Transcriptional Profiles of West Nile Virus Infection in the Collaborative Cross. G3 (Bethesda). 2017 Jun 7;7(6):1665-1682. doi: 10.1534/g3.117.041624.

Griffin DE, Byrnes AP, Cook SH. Emergence and virulence of encephalitogenic arboviruses. Arch Virol Suppl 2004;21–33.

Gubler DJ. Dengue, Urbanization and Globalization: The Unholy Trinity of the 21(st) Century. Trop Med Health. 2011 Dec;39(4 Suppl):3-11. doi: 10.2149/tmh.2011-S05. Epub 2011 Aug 25.

Gubler DJ. The continuing spread of West Nile virus in the western hemisphere. Clin Infect Dis. 2007 Oct 15;45(8):1039-46. Epub 2007 Sep 14.

Gubler DJ. The global emergence/resurgence of arboviral diseases as public health problems. Arch Med Res. 2002 Jul-Aug;33(4):330-42.

Guo JT, Hayashi J, Seeger C. West Nile virus inhibits the signal transduction pathway of alpha interferon. J Virol. 2005 Feb;79(3):1343-50.

Hai-Bo Xing, Meng-Ting Tong, Jing Wang, Hong Hu, Chong-Ya Zhai, Chang-Xin Huang, and Da Licorresponding. Suppression of IL-6 Gene by shRNA Augments Gemcitabine Chemosensitization in Pancreatic Adenocarcinoma Cells. Biomed Res Int. 2018; 2018: 3195025. Published online 2018 Mar 6. doi: 10.1155/2018/3195025

Hastings AK, Hastings K, Uraki R, Hwang J, Gaitsch H, Dhaliwal K, Williamson E, Fikrig E. Loss of the TAM Receptor Axl Ameliorates Severe Zika Virus Pathogenesis and Reduces Apoptosis in Microglia. iScience. 2019 Mar 29;13:339-350. doi: 10.1016/j.isci.2019.03.003. Epub 2019 Mar 5.

He B, Paterson RG, Stock N, Durbin JE, Durbin RK, Goodbourn S, Randall RE, Lamb RA. Recovery of paramyxovirus simian virus 5 with a V protein lacking the conserved cysteine-rich domain: the multifunctional V protein blocks both interferon-beta induction and interferon signaling. Virology. 2002 Nov 10; 303(1):15-32

Heim MH, Moradpour D, Blum HE. Expression of hepatitis C virus proteins inhibits signal transduction through the Jak-STAT pathway J Virol. 1999 Oct; 73(10):8469-75.

Herndon CN & Jennings RG. A twin-family study of susceptibility to poliomyelitis. Am J Hum Genet. 1951 Mar;3(1):17-46.

Ho LJ, Hung LF, Weng CY, Wu WL, Chou P, Lin YL, et al. Dengue virus type 2 antagonizes IFN-alpha but not IFN-gamma antiviral effect via down-regulating Tyk2-STAT signaling in the human dendritic cell. J Immunol (2005) 174:8163–72. doi:10.4049/jimmunol.174.12.8163

Hoenen A, Liu W, Kochs G, Khromykh AA, Mackenzie JM J. West Nile virus-induced cytoplasmic membrane structures provide partial protection against the interferon-induced antiviral MxA protein. Gen Virol. 2007 Nov; 88(Pt 11):3013-7.

Hollidge BS, González-Scarano F, Soldan SS. Arboviral encephalitides: transmission, emergence, and pathogenesis. J Neuroimmune Pharmacol. 2010 Sep;5(3):428-42. doi: 10.1007/s11481-010-9234-7. Epub 2010 Jul 22.

Honda K, Yanai H, Negishi H, Asagiri M, Sato M, Mizutani T, Shimada N, Ohba Y, Takaoka A, Yoshida N, Taniguchi T. IRF-7 is the master regulator of type-I interferon-dependent immune responses. Nature. 2005 Apr 7;434(7034):772-7. Epub 2005 Mar 30.

Huang WC, Abraham R, Shim BS, Choe H, Page DT. Zika virus infection during the period of maximal brain growth causes microcephaly and corticospinal neuron apoptosis in wild type mice. Sci Rep. 2016 Oct 7;6:34793. doi: 10.1038/srep34793.

Huang YJ, Higgs S, Horne KM, Vanlandingham DL. Flavivirus-mosquito interactions. Viruses. 2014 Nov 24;6(11):4703-30. doi: 10.3390/v6114703.

Hubálek Z, Rudolf I, Nowotny N. Arboviruses pathogenic for domestic and wild animals. Adv Virus Res. 2014; 89:201-75. doi: 10.1016/B978-0-12-800172-1.00005-7.

Hunsperger EA, Roehrig JT. Temporal analyses of the neuropathogenesis of a West Nile virus infection in mice. J Neurovirol. 2006 Apr;12(2):129-39.

Imamura T, Cui L, Teng R, Johkura K, Okouchi Y, Asanuma K, Ogiwara N, Sasaki K. Embryonic stem cell-derived embryoid bodies in three-dimensional culture system form hepatocyte-like cells in vitro and in vivo. Tissue Eng. 2004 Nov-Dec;10(11-12):1716-24.

Jabara HH, McDonald DR, Janssen E, Massaad MJ, Ramesh N, Borzutzky A, Rauter I, Benson H, Schneider L, Baxi S, Recher M, Notarangelo LD, Wakim R, Dbaibo G, Dasouki M, Al-Herz W, Barlan I, Baris S, Kutukculer N, Ochs HD, Plebani A, Kanariou M, Lefranc G, Reisli I, Fitzgerald KA, Golenbock D, Manis J, Keles S, Ceja R, Chatila TA, Geha RS. DOCK8 functions as an adaptor that links TLR-MyD88 signaling to B cell activation. Nat Immunol. 2012 May 13;13(6):612-20. doi: 10.1038/ni.2305.

Jang MA, Kim EK, Now H, Nguyen NT, Kim WJ, Yoo JY, Lee J, Jeong YM, Kim CH, Kim OH, Sohn S, Nam SH, Hong Y, Lee YS, Chang SA, Jang SY, Kim JW, Lee MS, Lim SY, Sung KS, Park KT, Kim BJ, Lee JH, Kim DK, Kee C, Ki CS. Mutations in DDX58, which encodes RIG-I, cause atypical Singleton-Merten syndrome. Am J Hum Genet. 2015 Feb 5;96(2):266-74. doi: 10.1016/j.ajhg.2014.11.019. Epub 2015 Jan 22.

Jänicke RU, Sprengart ML, Wati MR, Porter AG. Caspase-3 is required for DNA fragmentation and morphological changes associated with apoptosis. J Biol Chem. 1998 Apr 17;273(16):9357-60.

Jemielity S, Wang JJ, Chan YK, Ahmed AA, Li W, Monahan S, Bu X, Farzan M, Freeman GJ, Umetsu DT, Dekruyff RH, Choe H. TIM-family proteins promote infection of multiple enveloped viruses through virion-associated phosphatidylserine. PLoS Pathog. 2013 Mar; 9(3):e1003232.

Joseph B. Prescott, Pamela R. Hall, Virginie S. Bondu-Hawkins, Chunyan Ye and Brian Hjelle. Early Innate Immune Responses to Sin Nombre Hantavirus Occur Independently of IFN Regulatory Factor 3, Characterized Pattern Recognition Receptors, and Viral Entry. J Immunol August 1, 2007, 179 (3) 1796-1802; DOI: https://doi.org/10.4049/jimmunol.179.3.1796

Karimi O, Goorhuis A, Schinkel J, Codrington J, Vreden SGS, Vermaat JS, Stijnis C, Grobusch MP. Thrombocytopenia and subcutaneous bleedings in a patient with Zika virus infection. Lancet. 2016 Mar 5;387(10022):939-940. doi: 10.1016/S0140-6736(16)00502-X. Epub 2016 Feb 20.

Kawai T, Akira S. Antiviral signaling through pattern recognition receptors. J Biochem. 2007 Feb;141(2):137-45. Epub 2006 Dec 26.

Keller BC, Fredericksen BL, Samuel MA, Mock RE, Mason PW, Diamond MS, Gale M Jr. Resistance to alpha/beta interferon is a determinant of West Nile virus replication fitness and virulence. J Virol. 2006 Oct;80(19):9424-34.

Kemenesi G, Buzás D, Zana B, Kurucz K, Krtinic B, Kepner A, Földes F, Jakab F. First genetic characterization of Usutu virus from Culex pipiens mosquitoes Serbia, 2014. Infect Genet Evol. 2018 Sep;63:58-61. doi: 10.1016/j.meegid.2018.05.012. Epub 2018 May 17.

Kenney AD, Dowdle JA, Bozzacco L, McMichael TM, St Gelais C, Panfil AR, Sun Y, Schlesinger LS, Anderson MZ, Green PL, López CB, Rosenberg BR, Wu L, Yount JS. Human Genetic Determinants of Viral Diseases. Annu Rev Genet. 2017 Nov 27;51:241-263. doi: 10.1146/annurev-genet-120116-023425. Epub 2017 Aug 30.

Khor CC, Hibberd ML. Host-pathogen interactions revealed by human genome-wide surveys. Trends Genet. 2012 May;28(5):233-43. doi: 10.1016/j.tig.2012.02.001. Epub 2012 Mar 22.

Kim S, Li L, McMurtrey CP, Hildebrand WH, Weidanz JA, Gillanders WE, Diamond MS, Hansen TH. Single-chain HLA-A2 MHC trimers that incorporate an immundominant peptide elicit protective T cell immunity against lethal West Nile virus infection. J Immunol. 2010 Apr 15;184(8):4423-30. doi: 10.4049/jimmunol.0903955. Epub 2010 Mar 8.

Kindberg E, Mickiene A, Ax C, Akerlind B, Vene S, Lindquist L, Lundkvist A, Svensson L. A deletion in the chemokine receptor 5 (CCR5) gene is associated with tickborne encephalitis. J Infect Dis. 2008 Jan 15;197(2):266-9. doi: 10.1086/524709.

Kindberg E, Vene S, Mickiene A, Lundkvist A, Lindquist L, Svensson L. A functional Toll-like receptor 3 gene (TLR3) may be a risk factor for tick-borne encephalitis virus (TBEV) infection. J Infect Dis. 2011 Feb 15;203(4):523-8. doi: 10.1093/infdis/jiq082. Epub 2011 Jan 7.

Kong KF, Delroux K, Wang X, Qian F, Arjona A, Malawista SE, Fikrig E, Montgomery RR. Dysregulation of TLR3 Impairs the Innate Immune Response to West Nile Virus in the Elderly. J Virol. 2008 Aug;82(15):7613-23. doi: 10.1128/JVI.00618-08. Epub 2008 May 28.

Korzeniewski K, Juszczak D, Zwolińska E. Zika - another threat on the epidemiological map of the world. Int Marit Health. 2016;67(1):31-7. doi: 10.5603/IMH.2016.0007.

Kovats S, Turner S, Simmons A, Powe T, Chakravarty E, Alberola-Ila J. West Nile virus-infected human dendritic cells fail to fully activate invariant natural killer T cells. Clin Exp Immunol. 2016 Nov;186(2):214-226. doi: 10.1111/cei.12850. Epub 2016 Sep 22.

Kraemer MUG, Reiner RC Jr, Brady OJ, Messina JP, Gilbert M, Pigott DM, Yi D, Johnson K, Earl L, Marczak LB, Shirude S, Davis Weaver N, Bisanzio D, Perkins TA, Lai S, Lu X, Jones P, Coelho GE, Carvalho RG, Van Bortel W, Marsboom C, Hendrickx G, Schaffner F, Moore CG, Nax HH, Bengtsson L, Wetter E, Tatem AJ, Brownstein JS, Smith DL, Lambrechts L, Cauchemez S, Linard C, Faria NR, Pybus OG, Scott TW, Liu Q, Yu H, Wint GRW, Hay SI, Golding N. Past and future spread of the arbovirus vectors Aedes aegypti and Aedes albopictus. Nat Microbiol. 2019 May;4(5):854-863. doi: 10.1038/s41564-019-0376-y. Epub 2019 Mar 4.

Kralovics R, Passamonti F, Buser AS, Teo SS, Tiedt R, Passweg JR, Tichelli A, Cazzola M, Skoda RC. A gain-of-function mutation of JAK2 in myeloproliferative disorders. N Engl J Med. 2005 Apr 28;352(17):1779-90.

Kumar A, Hou S, Airo AM, Limonta D, Mancinelli V, Branton W, Power C, Hobman TC. Zika virus inhibits type-I interferon production and downstream signaling. EMBO Rep. 2016 Dec;17(12):1766-1775. Epub 2016 Oct 24.

Kumar V, Wijmenga C, Xavier RJ. Genetics of immune-mediated disorders: from genome-wide association to molecular mechanism. Curr Opin Immunol. 2014 Dec;31:51-7. doi: 10.1016/j.coi.2014.09.007. Epub 2014 Oct 14.

Lafaille FG, Pessach IM, Zhang SY, Ciancanelli MJ, Herman M, Abhyankar A, Ying SW, Keros S, Goldstein PA, Mostoslavsky G, Ordovas-Montanes J, Jouanguy E, Plancoulaine S, Tu E, Elkabetz Y, Al-Muhsen S, Tardieu M, Schlaeger TM, Daley GQ, Abel L, Casanova JL, Studer L, Notarangelo LD. Impaired intrinsic immunity to HSV-1 in human iPSC-derived TLR3-deficient CNS cells. Nature. 2012 Nov 29;491(7426):769-73. doi: 10.1038/nature11583. Epub 2012 Oct 28

Lambert SL, Aviles D, Vehaskari VM, Ashoor IF. Severe West Nile virus meningoencephalitis in a pediatric renal transplant recipient: successful recovery and long-term neuropsychological outcome. Pediatr Transplant. 2016 Sep;20(6):836-9. doi: 10.1111/petr.12768. Epub 2016 Jul 28.

Lancaster MA, Renner M, Martin CA, Wenzel D, Bicknell LS, Hurles ME, Homfray T, Penninger JM, Jackson AP, Knoblich JA. Cerebral organoids model human brain development and microcephaly. Nature. 2013 Sep 19;501(7467):373-9. doi: 10.1038/nature12517. Epub 2013 Aug 28.

Lanciotti RS, Roehrig JT, Deubel V, Smith J, Parker M, Steele K, Crise B, Volpe KE, Crabtree MB, Scherret JH, Hall RA, MacKenzie JS, Cropp CB, Panigrahy B, Ostlund E, Schmitt B, Malkinson M, Banet C, Weissman J, Komar N, Savage HM, Stone W, McNamara T, Gubler DJ. Origin of the West Nile virus responsible for an outbreak of encephalitis in the northeastern United States. Science. 1999 Dec 17;286(5448):2333-7

Lanciotti, R.S., Kosoy, O.L., Laven, J.J., Velez, J.O., Lambert, A.J., Johnson, A.J., Stanfield, S.M., Duffy, M.R.Genetic and serologic properties of Zika virus associated with an epidemic, Yap State, Micronesia, 2007.Emerg Infect Dis. 2008.14:1232–1239

Lang J, Cheng Y, Rolfe A, Hammack C, Vera D, Kyle K, Wang J, Meissner TB, Ren Y, Cowan C, Tang H. An hPSC-Derived Tissue-Resident Macrophage Model Reveals Differential Responses of Macrophages to ZIKV and DENV Infection. Stem Cell Reports. 2018 Aug 14;11(2):348-362. doi: 10.1016/j.stemcr.2018.06.006. Epub 2018 Jul 5.

Lanteri MC, Kaidarova Z, Peterson T, Cate S, Custer B, Wu S, Agapova M, Law JP, Bielawny T, Plummer F, Tobler LH, Loeb M, Busch MP, Bramson J, Luo M, Norris PJ. Association between HLA Class I and Class II alleles and the outcome of West Nile virus infection: an exploratory study. PLoS One. 2011;6(8):e22948. doi: 10.1371/journal.pone.0022948. Epub 2011 Aug 1.

Laurent-Rolle M, Boer EF, Lubick KJ, Wolfinbarger JB, Carmody AB, Rockx B, Liu W, Ashour J, Shupert WL, Holbrook MR, Barrett AD, Mason PW, Bloom ME, García-Sastre A, Khromykh AA, Best SM. The NS5 protein of the virulent West Nile virus NY99 strain is a potent antagonist of type I interferon-mediated JAK-STAT signaling. J Virol. 2010 Apr;84(7):3503-15. doi: 10.1128/JVI.01161-09. Epub 2010 Jan 27.

Lazear HM, Diamond MS. New insights into innate immune restriction of West Nile virus infection. Curr Opin Virol. 2015 Apr;11:1-6. doi: 10.1016/j.coviro.2014.12.001. Epub 2014 Dec 31.

Lazear HM, Govero J, Smith AM, Platt DJ, Fernandez E, Miner JJ, Diamond MS. A Mouse Model of Zika Virus Pathogenesis. Cell Host Microbe. 2016 May 11;19(5):720-30. doi: 10.1016/j.chom.2016.03.010. Epub 2016 Apr 5.

Lazear HM, Lancaster A, Wilkins C, Suthar MS, Huang A, Vick SC, Clepper L, Thackray L, Brassil MM, Virgin HW, Nikolich-Zugich J, Moses AV, Gale M Jr, Früh K, Diamond MS. IRF-3, IRF-5, and IRF-7 coordinately regulate the type I IFN response in myeloid dendritic cells downstream of MAVS signaling. PLoS Pathog. 2013 Jan;9(1):e1003118. doi: 10.1371/journal.ppat.1003118. Epub 2013 Jan 3.

Lazear HM, Pinto AK, Ramos HJ, Vick SC, Shrestha B, Suthar MS, Gale M Jr, Diamond MS. Pattern recognition receptor MDA5 modulates CD8+ T cell-dependent clearance of West Nile virus from the central nervous system. J Virol. 2013b Nov;87(21):11401-15. doi: 10.1128/JVI.01403-13. Epub 2013b Aug 21.

Lee E, Leang SK, Davidson A, Lobigs M. Both E protein glycans adversely affect dengue virus infectivity but are beneficial for virion release. J Virol. 2010 May;84(10):5171-80. doi: 10.1128/JVI.01900-09. Epub 2010 Mar 10.

Lee KS, Zhou W, Scott-McKean JJ, Emmerling KL, Cai GY, Krah DL, Costa AC, Freed CR, Levin MJ. Human sensory neurons derived from induced pluripotent stem cells support varicella-zoster virus infection. PLoS One. 2012;7(12):e53010. doi: 10.1371/journal.pone.0053010. Epub 2012 Dec 28.

Lee MN, Ye C, Villani AC, Raj T, Li W, Eisenhaure TM, Imboywa SH, Chipendo PI, Ran FA, Slowikowski K, Ward LD, Raddassi K, McCabe C, Lee MH, Frohlich IY, Hafler DA, Kellis M, Raychaudhuri S, Zhang F, Stranger BE, Benoist CO, De Jager PL, Regev A, Hacohen N. Common genetic variants modulate pathogen-sensing responses in human dendritic cells. Science. 2014 Mar 7;343(6175):1246980. doi: 10.1126/science.1246980.

Lequime S, Lambrechts L. Vertical transmission of arboviruses in mosquitoes: a historical perspective. Infect Genet Evol. 2014 Dec;28:681-90. doi: 10.1016/j.meegid.2014.07.025. Epub 2014 Jul 29.

Li K, Phoo WW, Luo D. Functional interplay among the flavivirus NS3 protease, helicase, and cofactors. Virol Sin. 2014 Apr;29(2):74-85. doi: 10.1007/s12250-014-3438-6. Epub 2014 Mar 26.

Li M, Ransohoff RM. Multiple roles of chemokine CXCL12 in the central nervous system: a migration from immunology to neurobiology. Prog Neurobiol. 2008 Feb;84(2):116-31. doi: 10.1016/j.pneurobio.2007.11.003. Epub 2007 Nov 26.

Liangliang Niu, Shujie Zhang, Jihong Wu, Ling Chen and Yan Wang. Upregulation of NLRP3 Inflammasome in the Tears and Ocular Surface of Dry Eye Patients. PLoS One. 2015; 10(5): e0126277.Published online 2015 May 11. doi: 10.1371/journal.pone.0126277

Liddelow SA, Guttenplan KA, Clarke LE, Bennett FC, Bohlen CJ, Schirmer L, Bennett ML, Münch AE, Chung WS, Peterson TC, Wilton DK, Frouin A, Napier BA, Panicker N, Kumar M, Buckwalter MS, Rowitch DH, Dawson VL, Dawson TM, Stevens B8, Barres BA. Neurotoxic reactive astrocytes are induced by activated microglia. Nature. 2017 Jan 26;541(7638):481-487. doi: 10.1038/nature21029. Epub 2017 Jan 18.

Lim JK, Lisco A, McDermott DH, Huynh L, Ward JM, Johnson B, Johnson H, Pape J, Foster GA, Krysztof D, Follmann D, Stramer SL, Margolis LB, Murphy PM. Genetic variation in OAS1 is a risk factor for initial infection with West Nile virus in man. PLoS Pathog. 2009 Feb;5(2):e1000321. doi: 10.1371/journal.ppat.1000321. Epub 2009 Feb 27.

Lim JK, McDermott DH, Lisco A, Foster GA, Krysztof D, Follmann D, Stramer SL, Murphy PM. CCR5 deficiency is a risk factor for early clinical manifestations of West Nile virus infection but not for viral transmission. J Infect Dis. 2010 Jan 15;201(2):178-85. doi: 10.1086/649426.

Lim PY, Behr MJ, Chadwick CM, Shi PY, Bernard KA. Keratinocytes are cell targets of West Nile virus in vivo. J Virol. 2011 May;85(10):5197-201. doi: 10.1128/JVI.02692-10. Epub 2011 Mar 2.

Lim SM, Koraka P, Osterhaus AD, Martina BE. West Nile virus: immunity and pathogenesis. Viruses. 2011 Jun;3(6):811-28. doi: 10.3390/v3060811. Epub 2011 Jun 15.

Lin HH, Yip BS, Huang LM, Wu SC. Zika virus structural biology and progress in vaccine development. Biotechnol Adv. 2018 Jan - Feb;36(1):47-53. doi: 10.1016/j.biotechadv.2017.09.004. Epub 2017 Sep 12.

Lin RJ, Liao CL, Lin E, Lin YL. Blocking of the alpha interferon-induced Jak-Stat signaling pathway by Japanese encephalitis virus infection. J Virol (2004) 78:9285–94. doi:10.1128/JVI.78.17.9285-9294.2004

Linke S, Ellerbrok H, Niedrig M, Nitsche A, Pauli G. Detection of West Nile virus lineages 1 and 2 by real-time PCR. J Virol Methods. 146 (1-2), 355-8 (2007).

Liu R, Paxton WA, Choe S, Ceradini D, Martin SR, Horuk R, MacDonald ME, Stuhlmann H, Koup RA, Landau NR. Homozygous defect in HIV-1 coreceptor accounts for resistance of some multiply-exposed individuals to HIV-1 infection. Cell. 1996 Aug 9;86(3):367-77.

Liu WJ, Chen HB, Wang XJ, Huang H, Khromykh AA. Analysis of adaptive mutations in Kunjin virus replicon RNA reveals a novel role for the flavivirus nonstructural protein NS2A in inhibition of beta interferon promoter-driven transcription. J Virol. 2004 Nov;78(22):12225-35.

Liu WJ, Wang XJ, Clark DC, Lobigs M, Hall RA, Khromykh AA. A single amino acid substitution in the West Nile virus nonstructural protein NS2A disables its ability to inhibit alpha/beta interferon induction and attenuates virus virulence in mice. J Virol. 2006 Mar;80(5):2396-404.

Liu WJ, Wang XJ, Mokhonov VV, Shi PY, Randall R, Khromykh AA. Inhibition of interferon signaling by the New York 99 strain and Kunjin subtype of West Nile virus involves blockage of STAT1 and STAT2 activation by nonstructural proteins. J Virol. 2005 Feb;79(3):1934-42.

Livak, K.J., Scmittgen, T.D. Analysis of relative gene expression data using real-time quantitative PCR and 2(-Delta Delta C(T)) Method. Methods. 25, 402-408 (2001).

Llames, S., García-Pérez, E., Meana, Á., Larcher, F. & del Río, M. Feeder Layer Cell Actions and Applications. Tissue Engineering Part B: Reviews. 21, 345–353, https://doi.org/10.1089/ten.teb.2014.0547 (2015).

Lu G, Gong P. Crystal Structure of the full-length Japanese encephalitis virus NS5 reveals a conserved methyltransferase-polymerase interface. PLoS Pathog. 2013;9(8):e1003549. doi: 10.1371/journal.ppat.1003549. Epub 2013 Aug 8.

Lucas TM, Richner JM, Diamond MS. The Interferon-Stimulated Gene Ifi27l2a Restricts West Nile Virus Infection and Pathogenesis in a Cell-Type- and Region-Specific Manner. J Virol. 2015 Dec 23;90(5):2600-15. doi: 10.1128/JVI.02463-15.

Ma J, Ketkar H, Geng T, Lo E, Wang L, Xi J, Sun Q, Zhu Z, Cui Y, Yang L, Wang P. Zika Virus Non-structural Protein 4A Blocks the RLR-MAVS Signaling. Front Microbiol. 2018 Jun 25;9:1350. doi: 10.3389/fmicb.2018.01350. eCollection 2018.

Ma W, Li S, Ma S, Jia L, Zhang F, Zhang Y, Zhang J, Wong G, Zhang S, Lu X, Liu M, Yan J, Li W, Qin C, Han D, Qin C, Wang N, Li X, Gao GF. Zika Virus Causes Testis Damage and Leads to Male Infertility in Mice. Cell. 2017 Jan 26;168(3):542. doi: 10.1016/j.cell.2017.01.009.

Mackenzie JM, Khromykh AA, Parton RG. Cholesterol manipulation by West Nile virus perturbs the cellular immune response. Cell Host Microbe. 2007 Oct 11;2(4):229-39.

Magurano F, Remoli ME, Baggieri M, Fortuna C, Marchi A, Fiorentini C, Bucci P, Benedetti E, Ciufolini MG, Rizzo C, Piga S, Salcuni P, Rezza G, Nicoletti L. Circulation of West Nile virus lineage 1 and 2 during an outbreak in Italy. Clin Microbiol Infect. 2012 Dec;18(12):E545-7. doi: 10.1111/1469-0691.12018. Epub 2012 Sep 28.

Manarolla G, Bakonyi T, Gallazzi D, Crosta L, Weissenböck H, Dorrestein GM, Nowotny N. Usutu virus in wild birds in northern Italy. Vet Microbiol. 2010 Feb 24;141(1-2):159-63. doi: 10.1016/j.vetmic.2009.07.036. Epub 2009 Aug 8.

Manet C, Roth C, Tawfik A, Cantaert T, Sakuntabhai A, Montagutelli X. Host genetic control of mosquito-borne Flavivirus infections. Mamm Genome. 2018 Aug;29(7-8):384-407. doi: 10.1007/s00335-018-9775-2. Epub 2018 Aug 25.

Mansuy JM, Mengelle C, Pasquier C, Chapuy-Regaud S, Delobel P, Martin-Blondel G, Izopet J. Zika Virus Infection and Prolonged Viremia in Whole-Blood Specimens. Emerg Infect Dis. 2017 May;23(5):863-865. doi: 10.3201/eid2305.161631. Epub 2017 May 15.

Mansuy JM, Suberbielle E, Chapuy-Regaud S, Mengelle C, Bujan L, Marchou B, Delobel P, Gonzalez-Dunia D, Malnou CE, Izopet J, Martin-Blondel G. Zika virus in semen and spermatozoa. Lancet Infect Dis. 2016 Oct;16(10):1106-1107. doi: 10.1016/S1473-3099(16)30336-X. Epub 2016 Sep 19.

Marcello T, Grakoui A, Barba-Spaeth G, Machlin ES, Kotenko SV, MacDonald MR, Rice CM. Interferons alpha and lambda inhibit hepatitis C virus replication with distinct signal transduction and gene regulation kinetics. Gastroenterology. 2006 Dec;131(6):1887-98. Epub 2006 Oct 1.

Marchette NJ, Garcia R, Rudnick A. Isolation of Zika virus from Aedes aegypti mosquitoes in Malaysia. Am J Trop Med Hyg. 1969 May;18(3):411-5.

Marfin AA, Gubler DJ. West Nile encephalitis: an emerging disease in the United States. Clin Infect Dis. 2001 Nov 15;33(10):1713-9. Epub 2001 Oct 5.

Markoff L, Chang A, Falgout B. Processing of flavivirus structural glycoproteins: stable membrane insertion of premembrane requires the envelope signal peptide. Virology 1994; 204: 526–40.

Marthiens V, Rujano MA, Pennetier C, Tessier S, Paul-Gilloteaux P, Basto R. Centrosome amplification causes microcephaly. Nat Cell Biol. 2013 Jul;15(7):731-40. doi: 10.1038/ncb2746. Epub 2013 May 12.

Martin, M. J., Muotri, A., Gage, F. & Varki, A. Human embryonic stem cells express an immunogenic non human sialic acid. Nature medicine. 11, 228–232, https://doi.org/10.1038/nm1181 (2005).

Mashimo T, Lucas M, Simon-Chazottes D, Frenkiel MP, Montagutelli X, Ceccaldi PE, Deubel V, Guenet JL, Despres P. A nonsense mutation in the gene encoding 2'-5'-oligoadenylate synthetase/L1 isoform is associated with West Nile virus susceptibility in laboratory mice. Proc Natl Acad Sci U S A. 2002 Aug 20;99(17):11311-6. Epub 2002 Aug 19.

Mathur A, Arora KL, Chaturvedi UC. Transplacental Japanese encephalitis virus (JEV) infection in mice during consecutive pregnancies. J Gen Virol. 1982 Mar;59(Pt 1):213-7.

McCarthy MI, Abecasis GR, Cardon LR, Goldstein DB, Little J, Ioannidis JP, Hirschhorn JN. Genome-wide association studies for complex traits: consensus, uncertainty and challenges. Nat Rev Genet. 2008 May;9(5):356-69. doi: 10.1038/nrg2344.

Mengesha Tsegaye M, Beyene B2 Ayele W, Abebe A, Tareke I, Sall A, Yactayo S, Shibeshi ME, Staples E, Belay D, Lilay A, Alemu A, Alemu E, Kume A, H/Mariam A, Ronveaux O, Tefera M, Kassa W, Bekele Weyessa A, Jima D, Kebede A, Tayachew A. Sero-prevalence of yellow fever and related Flavi viruses in Ethiopia: a public health perspective. BMC Public Health. 2018 Aug 14;18(1):1011. doi: 10.1186/s12889-018-5726-9.

Mentzer AJ, O'Connor D, Pollard AJ, Hill AV. Searching for the human genetic factors standing in the way of universally effective vaccines. Philos Trans R Soc Lond B Biol Sci. 2015 Jun 19;370(1671). pii: 20140341. doi: 10.1098/rstb.2014.0341.

Miner JJ, Sene A, Richner JM, Smith AM, Santeford A, Ban N, Weger-Lucarelli J, Manzella F, Rückert C, Govero J, Noguchi KK, Ebel GD, Diamond MS, Apte RS. Zika Virus Infection in Mice Causes Panuveitis with Shedding of Virus in Tears. Cell Rep. 2016 Sep 20;16(12):3208-3218. doi: 10.1016/j.celrep.2016.08.079. Epub 2016 Sep 6.

Misch EA, Berrington WR, Vary JC Jr, Hawn TR. Leprosy and the human genome. Microbiol Mol Biol Rev. 2010 Dec;74(4):589-620. doi: 10.1128/MMBR.00025-10.

Misra UK, Kalita J. Overview: Japanese encephalitis. Prog Neurobiol. 2010 Jun;91(2):108-20. doi: 10.1016/j.pneurobio.2010.01.008. Epub 2010 Feb 2.

Moreira J, Peixoto TM, Siqueira AM, Lamas CC. Sexually acquired Zika virus: a systematic review. Clin Microbiol Infect. 2017 May;23(5):296-305. doi: 10.1016/j.cmi.2016.12.027. Epub 2017 Jan 3.

Mostashari F, Bunning ML, Kitsutani PT, Singer DA, Nash D, Cooper MJ, Katz N, Liljebjelke KA, Biggerstaff BJ, Fine AD, Layton MC, Mullin SM, Johnson AJ, Martin DA, Hayes EB, Campbell GL. Epidemic West Nile encephalitis, New York, 1999: results of a household-based seroepidemiological survey. Lancet. 2001 Jul 28;358(9278):261-4.

Mukhopadhyay S, Kuhn RJ, Rossmann MG. A structural perspective of the flavivirus life cycle. Nat Rev Microbiol. 2005;3(1):13-22.

Muñoz-Jordán JL, Laurent-Rolle M, Ashour J, Martínez-Sobrido L, Ashok M, Lipkin WI, García-Sastre A. Inhibition of alpha/beta interferon signaling by the NS4B protein of flaviviruses. J Virol. 2005 Jul;79(13):8004-13.

Murray CL, Jones CT, Rice CM. Architects of assembly: roles of Flaviviridae non-structural proteins in virion morphogenesis. Nat Rev Microbiol. 2008 Sep;6(9):699-708. doi: 10.1038/nrmicro1928.

Murray K, Baraniuk S, Resnick M, Arafat R, Kilborn C, Cain K, Shallenberger R, York TL, Martinez D, Hellums JS, Hellums D, Malkoff M, Elgawley N, McNeely W, Khuwaja SA, Tesh RB. Risk factors for encephalitis and death from West Nile virus infection. Epidemiol Infect. Epidemiol Infect. 2006 Dec;134(6):1325-32. Epub 2006 May 4.

Murray KO, Gorchakov R, Carlson AR, Berry R, Lai L, Natrajan M, Garcia MN, Correa A, Patel SM, Aagaard K, Mulligan MJ. Prolonged Detection of Zika Virus in Vaginal Secretions and Whole Blood. Emerg Infect Dis. 2017 Jan;23(1):99-101. doi: 10.3201/eid2301.161394. Epub 2017 Jan 15.

Musso D, Cao-Lormeau VM, Gubler DJ. Zika virus: following the path of dengue and chikungunya? Lancet. 2015 Jul 18;386(9990):243-4. doi: 10.1016/S0140-6736(15)61273-9.

Musso D, Gubler DJ. Zika Virus. Clin Microbiol Rev. 2016 Jul;29(3):487-524. doi: 10.1128/CMR.00072-15.

Musso D, Nilles EJ, Cao-Lormeau VM. Rapid spread of emerging Zika virus in the Pacific area. Clin Microbiol Infect. 2014 Oct;20(10):O595-6. doi: 10.1111/1469-0691.12707. Epub 2014 Aug 4.

Muylaert IR, Chambers TJ, Galler R, Rice CM. Mutagenesis of the Nlinked glycosylation sites of the yellow fever virus NS1 protein: effects on virus replication and mouse neurovirulence. Virology. 1996;222(1):159-168.

Nakajima R, Nakamura E, Harigaya T. Vasoinhibin, an N-terminal Prolactin Fragment, Directly Inhibits Cardiac Angiogenesis in Three-dimensional Heart Culture. Front Endocrinol (Lausanne). 2017 Jan 20;8:4. doi: 10.3389/fendo.2017.00004. eCollection 2017.

Nakano T, Kodama H, Honjo T. Generation of lymphohematopoietic cells from embryonic stem cells in culture. Science. 1994 Aug 19;265(5175):1098-101.

Neufeldt CJ, Cortese M, Acosta EG, Bartenschlager R. Rewiring cellular networks by members of the Flaviviridae family. Nat Rev Microbiol. 2018 Feb 12;16(3):125-142. doi: 10.1038/nrmicro.2017.170.

Ng WC, Soto-Acosta R, Bradrick SS, Garcia-Blanco MA, Ooi EE. The 5' and 3' Untranslated Regions of the Flaviviral Genome. Viruses. 2017 Jun 6;9(6). pii: E137. doi: 10.3390/v9060137.

Nickless A, Bailis JM, You Z. Control of gene expression through the nonsense-mediated RNA decay pathway. Cell Biosci. 2017 May 19;7:26. doi: 10.1186/s13578-017-0153-7. eCollection 2017.

Ning S, Pagano JS, Barber GN. IRF7: activation, regulation, modification and function. Genes Immun. 2011 Sep;12(6):399-414. doi: 10.1038/gene.2011.21. Epub 2011 Apr 14.

Ochs RL, Mahler M, Basu A, Rios-Colon L, Sanchez TW, Andrade LE, Fritzler MJ, Casiano CA. The significance of autoantibodies to DFS70/LEDGFp75 in health and disease: integrating basic science with clinical understanding. Clin Exp Med. 2016 Aug;16(3):273-93. doi: 10.1007/s10238-015-0367-0. Epub 2015 Jun 19.

O'Leary DR, Kuhn S, Kniss KL, Hinckley AF, Rasmussen SA, Pape WJ, Kightlinger LK, Beecham BD, Miller TK, Neitzel DF, Michaels SR, Campbell GL, Lanciotti RS, Hayes EB. Birth outcomes following West Nile Virus infection of pregnant women in the United States: 2003-2004. Pediatrics. 2006 Mar;117(3):e537-45.

Parquet MC, Kumatori A, Hasebe F, Morita K, Igarashi A. West Nile virus-induced bax-dependent apoptosis. FEBS Lett. 2001 Jun 29;500(1-2):17-24.

Pastorino B, Nougairède A, Wurtz N, Gould E, de Lamballerie X. Role of host cell factors in flavivirus infection: Implications for pathogenesis and development of antiviral drugs. Antiviral Res. 2010 Sep;87(3):281-94. doi: 10.1016/j.antiviral.2010.04.014. Epub 2010 May 7.

Patel H, Sander B, Nelder MP. Long-term sequelae of West Nile virus-related illness: a systematic review. Lancet Infect Dis. 2015 Aug;15(8):951-9. doi: 10.1016/S1473-3099(15)00134-6. Epub 2015 Jul 7.

Paul AM, Acharya D, Duty L, Thompson EA, Le L, Stokic DS, Leis AA, Bai F. Osteopontin facilitates West Nile virus neuroinvasion via neutrophil “Trojan horse” transport. Sci Rep. 2017 Jul 5;7(1):4722. doi: 10.1038/s41598-017-04839-7.

Perelygin AA, Scherbik SV, Zhulin IB, Stockman BM, Li Y, Brinton MA. Positional cloning of the murine flavivirus resistance gene. Proc Natl Acad Sci U S A. 2002 Jul 9;99(14):9322-7. Epub 2002 Jun 21.

Perera-Lecoin M, Meertens L, Carnec X, Amara, A. Flavivirus entry receptors: an update. Viruses (2013) 6:69–88. doi: 10.3390/v6010069

Perwitasari O, Cho H, Diamond MS, Gale M Jr. Inhibitor of κB kinase epsilon (IKK(epsilon)), STAT1, and IFIT2 proteins define novel innate immune effector pathway against West Nile virus infection. J Biol Chem. 2011 Dec 30;286(52):44412-23. doi: 10.1074/jbc.M111.285205. Epub 2011 Nov 7.

Petersen LR, Brault AC, Nasci RS. West Nile virus: review of the literature. JAMA. 2013 Jul 17;310(3):308-15. doi: 10.1001/jama.2013.8042.

Petrova E, Gracias S, Beauclair G, Tangy F, Jouvenet N. Uncovering Flavivirus Host Dependency Factors through a Genome-Wide Gain-of-Function Screen. Viruses. 2019 Jan 15;11(1). pii: E68. doi: 10.3390/v11010068.

Pettersson JH, Eldholm V, Seligman SJ, Lundkvist Å, Falconar AK, Gaunt MW, Musso D, Nougairède A, Charrel R, Gould EA, de Lamballerie X. How Did Zika Virus Emerge in the Pacific Islands and Latin America? MBio. 2016 Oct 11;7(5). pii: e01239-16. doi: 10.1128/mBio.01239-16.

Pierro A, Gaibani P, Spadafora C, Ruggeri D, Randi V, Parenti S, Finarelli AC, Rossini G, Landini MP, Sambri V. Detection of specific antibodies against West Nile and Usutu viruses in healthy blood donors in northern Italy, 2010-2011. Clin Microbiol Infect. 2013 Oct;19(10):E451-3. doi: 10.1111/1469-0691.12241. Epub 2013 May 10.

Pierson TC, Diamond MS. Degrees of maturity: the complex structure and biology of flaviviruses. Curr Opin Virol. 2012 Apr;2(2):168-75. doi: 10.1016/j.coviro.2012.02.011. Epub 2012 Mar 23.

Platt DJ, Smith AM, Arora N, Diamond MS, Coyne CB, Miner JJ. Zika virus-related neurotropic flaviviruses infect human placental explants and cause fetal demise in mice. Sci Transl Med. 2018 Jan 31;10(426). pii: eaao7090. doi: 10.1126/scitranslmed.aao7090.

Pokidysheva E, Zhang Y, Battisti AJ, Bator-Kelly CM, Chipman PR, Xiao C, Gregorio GG, Hendrickson WA, Kuhn RJ, Rossmann MG. Cryo-EM reconstruction of dengue virus in complex with the carbohydrate recognition domain of DC-SIGN. Cell. 2006 Feb 10;124(3):485-93.

Poole E, He B, Lamb RA, Randall RE, Goodbourn S. The V proteins of simian virus 5 and other paramyxoviruses inhibit induction of interferon-beta. Virology. 2002 Nov 10; 303(1):33-46.

Pulit-Penaloza JA, Scherbik SV, Brinton MA. Type 1 IFN-independent activation of a subset of interferon stimulated genes in West Nile virus Eg101-infected mouse cells. Virology. 2012 Apr 10;425(2):82-94. doi: 10.1016/j.virol.2012.01.006. Epub 2012 Feb 3.

Quicke KM, Bowen JR, Johnson EL, McDonald CE, Ma H, O'Neal JT, Rajakumar A, Wrammert J, Rimawi BH, Pulendran B, Schinazi RF, Chakraborty R, Suthar MS. Zika Virus Infects Human Placental Macrophages. Cell Host Microbe. 2016 Jul 13;20(1):83-90. doi: 10.1016/j.chom.2016.05.015. Epub 2016 May 27.

Rauch A, Kutalik Z, Descombes P, Cai T, Di Iulio J, Mueller T, Bochud M, Battegay M, Bernasconi E, Borovicka J, Colombo S, Cerny A, Dufour JF, Furrer H, Günthard HF, Heim M, Hirschel B, Malinverni R, Moradpour D, Müllhaupt B, Witteck A, Beckmann JS, Berg T, Bergmann S, Negro F, Telenti A, Bochud PY; Swiss Hepatitis C Cohort Study; Swiss HIV Cohort Study. Genetic variation in IL28B is associated with chronic hepatitis C and treatment failure: a genome-wide association study. Gastroenterology. 2010 Apr;138(4):1338-45, 1345.e1-7. doi: 10.1053/j.gastro.2009.12.056. Epub 2010 Jan 11.

Renault P, Solet JL, Sissoko D, Balleydier E, Larrieu S, Filleul L, Lassalle C, Thiria J, Rachou E, de Valk H, Ilef D, Ledrans M, Quatresous I, Quenel P, Pierre V. A major epidemic of chikungunya virus infection on Reunion Island, France, 2005-2006. Am J Trop Med Hyg. 2007 Oct;77(4):727-31.

Richard AS, Shim BS, Kwon YC, Zhang R, Otsuka Y, Schmitt K, Berri F, Diamond MS, Choe H. AXL-dependent infection of human fetal endothelial cells distinguishes Zika virus from other pathogenic flaviviruses. Proc Natl Acad Sci U S A. 2017 Feb 21;114(8):2024-2029. doi: 10.1073/pnas.1620558114. Epub 2017 Feb 6.

Riedmaier I, Tichopad A, Reiter M, Pfaffl MW, Meyer HH. Influence of testosterone and a novel SARM on gene expression in whole blood of Macaca fascicularis. J Steroid Biochem Mol Biol. 2009 Apr;114(3-5):167-73. doi: 10.1016/j.jsbmb.2009.01.019. Epub 2009 Feb 6.

Rijks JM, Kik ML, Slaterus R, Foppen R, Stroo A, IJzer J, Stahl J, Gröne A, Koopmans M, van der Jeugd HP, Reusken C. Widespread Usutu virus outbreak in birds in the Netherlands, 2016. Euro Surveill. 2016 Nov 10;21(45). pii: 30391. doi: 10.2807/1560-7917.ES.2016.21.45.30391.

Rios JJ, Fleming JG, Bryant UK, Carter CN, Huber JC, Long MT, Spencer TE, Adelson DL. OAS1 polymorphisms are associated with susceptibility to West Nile encephalitis in horses. PLoS One. 2010 May 7;5(5):e10537. doi: 10.1371/journal.pone.0010537.

Rizzo C, Vescio F, Declich S, Finarelli AC, Macini P, Mattivi A, Rossini G, Piovesan C, Barzon L, Palù G, Gobbi F, Macchi L, Pavan A, Magurano F, Ciufolini MG, Nicoletti L, Salmaso S, Rezza G. West Nile virus transmission with human cases in Italy, August - September 2009. Euro Surveill. 2009 Oct 8;14(40). pii: 19353.

Rizzoli A, Bolzoni L, Chadwick EA, Capelli G, Montarsi F, Grisenti M, de la Puente JM, Muñoz J, Figuerola J, Soriguer R, Anfora G, Di Luca M, Rosà R. Understanding West Nile virus ecology in Europe: Culex pipiens host feeding preference in a hotspot of virus emergence. Parasit Vectors. 2015 Apr 9;8:213. doi: 10.1186/s13071-015-0831-4.

Roby JA, Pijlman GP, Wilusz J, Khromykh AA. Noncoding subgenomic flavivirus RNA: multiple functions in West Nile virus pathogenesis and modulation of host responses. Viruses. 2014 Jan 27;6(2):404-27. doi: 10.3390/v6020404

Sadler AJ, Williams BR. Interferon-inducible antiviral effectors. Nat Rev Immunol. 2008 Jul;8(7):559-68. doi: 10.1038/nri2314.

Salimi H, Cain MD, Klein RS. Encephalitic Arboviruses: Emergence, Clinical Presentation, and Neuropathogenesis. Neurotherapeutics. 2016 Jul;13(3):514-34. doi: 10.1007/s13311-016-0443-5.

Salinas S, Constant O, Desmetz C, Barthelemy J, Lemaitre JM, Milhavet O, Nagot N, Foulongne V, Perrin FE, Saiz JC, Lecollinet S, Van de Perre P, Simonin Y. Deleterious effect of Usutu virus on human neural cells. PLoS Negl Trop Dis. 2017 Sep 5;11(9):e0005913. doi: 10.1371/journal.pntd.0005913. eCollection 2017 Sep.

Sambri V, Capobianchi M, Charrel R, Fyodorova M, Gaibani P, Gould E, Niedrig M, Papa A, Pierro A, Rossini G, Varani S, Vocale C, Landini MP. West Nile virus in Europe: emergence, epidemiology, diagnosis, treatment, and prevention. Clin Microbiol Infect. 2013 Aug;19(8):699-704. doi: 10.1111/1469-0691.12211. Epub 2013 Apr 17.

Samuel CE. Antiviral actions of interferons. Clin Microbiol Rev. 2001 Oct;14(4):778-809, table of contents.

Samuel MA, Diamond MS. Pathogenesis of West Nile Virus infection: a balance between virulence, innate and adaptive immunity, and viral evasion. J Virol. 2006 Oct;80(19):9349-60.

Samuel MA, Morrey JD, Diamond MS. Caspase 3-dependent cell death of neurons contributes to the pathogenesis of West Nile virus encephalitis. J Virol. 2007 Mar;81(6):2614-23. Epub 2006 Dec 27.

Sancho-Shimizu V, Perez de Diego R, Jouanguy E, Zhang SY, Casanova JL. Inborn errors of anti-viral interferon immunity in humans. Curr Opin Virol. 2011 Dec;1(6):487-96. doi: 10.1016/j.coviro.2011.10.016.

Sa-Ngiamsuntorn K, Wongkajornsilp A, Phanthong P, Borwornpinyo S, Kitiyanant N, Chantratita W, Hongeng S. A robust model of natural hepatitis C infection using hepatocyte-like cells derived from human induced pluripotent stem cells as a long-term host. Virol J. 2016 Apr 5;13:59. doi: 10.1186/s12985-016-0519-1.

Scheuch DE, Schäfer M, Eiden M, Heym EC, Ziegler U, Walther D, Schmidt-Chanasit J, Keller M, Groschup MH, Kampen H. Detection of Usutu, Sindbis, and Batai Viruses in Mosquitoes (Diptera: Culicidae) Collected in Germany, 2011‾2016. Viruses. 2018 Jul 23;10(7). pii: E389. doi: 10.3390/v10070389.

Schlaeger TM, Daheron L, Brickler TR, Entwisle S, Chan K, Cianci A, DeVine A, Ettenger A, Fitzgerald K, Godfrey M, Gupta D, McPherson J, Malwadkar P, Gupta M, Bell B, Doi A, Jung N, Li X, Lynes MS, Brookes E, Cherry AB, Demirbas D, Tsankov AM, Zon LI, Rubin LL, Feinberg AP, Meissner A, Cowan CA, Daley GQ. A comparison of non-integrating reprogramming methods. Nat Biotechnol. 2015 Jan;33(1):58-63. doi: 10.1038/nbt.3070. Epub 2014 Dec 1.

Scholle F, Mason PW. West Nile virus replication interferes with both poly(I:C)-induced interferon gene transcription and response to interferon treatment. Virology. 2005 Nov 10;342(1):77-87. Epub 2005 Aug 18.

Schuler-Faccini L, Ribeiro EM, Feitosa IM, Horovitz DD, Cavalcanti DP, Pessoa A, Doriqui MJ, Neri JI, Neto JM, Wanderley HY, Cernach M, El-Husny AS, Pone MV, Serao CL, Sanseverino MT; Brazilian Medical Genetics Society–Zika Embryopathy Task Force. Possible Association Between Zika Virus Infection and Microcephaly - Brazil, 2015. MMWR Morb Mortal Wkly Rep. 2016 Jan 29;65(3):59-62. doi: 10.15585/mmwr.mm6503e2.

Sha Q, Truong-Tran AQ, Plitt JR, Beck LA, Schleimer RP. Activation of airway epithelial cells by toll-like receptor agonists. Am J Respir Cell Mol Biol. 2004 Sep;31(3):358-64. Epub 2004 Jun 10.

Shapiro-Mendoza CK, Rice ME, Galang RR, Fulton AC, VanMaldeghem K, Prado MV, Ellis E, Anesi MS, Simeone RM, Petersen EE, Ellington SR, Jones AM, Williams T, Reagan-Steiner S, Perez-Padilla J, Deseda CC, Beron A, Tufa AJ, Rosinger A, Roth NM, Green C, Martin S, Lopez CD, deWilde L, Goodwin M, Pagano HP, Mai CT, Gould C, Zaki S, Ferrer LN, Davis MS, Lathrop E, Polen K, Cragan JD, Reynolds M, Newsome KB, Huertas MM, Bhatangar J, Quiñones AM, Nahabedian JF, Adams L, Sharp TM, Hancock WT, Rasmussen SA, Moore CA, Jamieson DJ, Munoz-Jordan JL, Garstang H, Kambui A, Masao C, Honein MA, Meaney-Delman D; Zika Pregnancy and Infant Registries Working Group. Pregnancy Outcomes After Maternal Zika Virus Infection During Pregnancy - U.S. Territories, January 1, 2016-April 25, 2017. MMWR Morb Mortal Wkly Rep. 2017 Jun 16;66(23):615-621. doi: 10.15585/mmwr.mm6623e1.

Sheridan MA, Yunusov D, Balaraman V, Alexenko AP, Yabe S, Verjovski-Almeida S, Schust DJ, Franz AW, Sadovsky Y, Ezashi T, Roberts RM. Vulnerability of primitive human placental trophoblast to Zika virus. Proc Natl Acad Sci U S A. 2017 Feb 28;114(9):E1587-E1596. doi: 10.1073/pnas.1616097114. Epub 2017 Feb 13.

Shlomai A, Schwartz RE, Ramanan V, Bhatta A, de Jong YP, Bhatia SN, Rice CM. Modeling host interactions with hepatitis B virus using primary and induced pluripotent stem cell-derived hepatocellular systems. Proc Natl Acad Sci U S A. 2014 Aug 19;111(33):12193-8. doi: 10.1073/pnas.1412631111. Epub 2014 Aug 4.

Shrestha B, Gottlieb D, Diamond MS. Infection and injury of neurons by West Nile encephalitis virus. J Virol. 2003 Dec;77(24):13203-13.

Silva JVJ Jr, Lopes TRR, Oliveira-Filho EF, Oliveira RAS, Durães-Carvalho R, Gil LHVG. Current status, challenges and perspectives in the development of vaccines against yellow fever, dengue, Zika and chikungunya viruses. Acta Trop. 2018 Jun; 182:257-263. doi: 10.1016/j.actatropica.2018.03.009. Epub 2018 Mar 15.

Simonin Y, Sillam O, Carles MJ, Gutierrez S, Gil P, Constant O, Martin MF, Girard G, Van de Perre P, Salinas S, Leparc-Goffart I, Foulongne V. Human Usutu Virus Infection with Atypical Neurologic Presentation, Montpellier, France, 2016. Emerg Infect Dis. 2018 May;24(5):875-878.

Sirohi D, Chen Z, Sun L, Klose T, Pierson TC, Rossmann MG, Kuhn RJ. The 3.8 Å resolution cryo-EM structure of Zika virus. Science. 2016 Apr 22;352(6284):467-70. doi: 10.1126/science.aaf5316. Epub 2016 Mar 31.

Sirohi D, Kuhn RJ. Zika virus structure, maturation, and receptors. J. Infect Dis. 2017;216(suppl_10):S935–S944.

Smit JM, Moesker B, Rodenhuis-Zybert I, Wilschut J. Flavivirus cell entry and membrane fusion. Viruses (2011) 3:160–71. doi: 10.3390/v3020160

Souza BS, Sampaio GL, Pereira CS, Campos GS, Sardi SI, Freitas LA, Figueira CP, Paredes BD, Nonaka CK, Azevedo CM, Rocha VP, Bandeira AC, Mendez-Otero R, Dos Santos RR, Soares MB. Zika virus infection induces mitosis abnormalities and apoptotic cell death of human neural progenitor cells. Sci Rep. 2016 Dec 23;6:39775. doi: 10.1038/srep39775.

Sterneckert JL, Reinhardt P, Schöler HR. Investigating human disease using stem cell models. Nat Rev Genet. 2014 Sep;15(9):625-39. doi: 10.1038/nrg3764. Epub 2014 Jul 29.

Stockert JC, Blázquez-Castro A, Cañete M, Horobin RW, Villanueva A. MTT assay for cell viability: Intracellular localization of the formazan product is in lipid droplets. Acta Histochem. 2012 Dec;114(8):785-96. doi: 10.1016/j.acthis.2012.01.006. Epub 2012 Feb 15.

Stockert JC, Horobin RW, Colombo LL, Blázquez-Castro A. Tetrazolium salts and formazan products in Cell Biology: Viability assessment, fluorescence imaging, and labeling perspectives. Acta Histochem. 2018 Apr;120(3):159-167. doi: 10.1016/j.acthis.2018.02.005. Epub 2018 Feb 26.

Suthar MS, Brassil MM, Blahnik G, Gale M Jr. Infectious clones of novel lineage 1 and lineage 2 West Nile virus strains WNV TX02 and WNV-Madagascar. J. J Virol. 2012 Jul;86(14):7704-9. doi: 10.1128/JVI.00401-12. Epub 2012 May 9.

Suthar MS, Diamond MS, Gale M Jr. West Nile virus infection and immunity. Nat Rev Microbiol. 2013 Feb;11(2):115-28. doi: 10.1038/nrmicro2950.

Suthar MS, Ma DY, Thomas S, Lund JM, Zhang N, Daffis S, Rudensky AY, Bevan MJ, Clark EA, Kaja MK, Diamond MS, Gale M Jr. IPS-1 is essential for the control of West Nile virus infection and immunity. PLoS Pathog. 2010 Feb 5;6(2):e1000757. doi: 10.1371/journal.ppat.1000757.

Swaminathan S, Schlaberg R, Lewis J, Hanson KE, Couturier MR. Fatal Zika Virus Infection with Secondary Nonsexual Transmission. N Engl J Med. 2016 Nov 10;375(19):1907-1909. Epub 2016 Sep 28.

Szaba FM, Tighe M, Kummer LW, Lanzer KG, Ward JM, Lanthier P, Kim IJ, Kuki A, Blackman MA, Thomas SJ, Lin JS. Zika virus infection in immunocompetent pregnant mice causes fetal damage and placental pathology in the absence of fetal infection. PLoS Pathog. 2018 Apr 10;14(4):e1006994. doi: 10.1371/journal.ppat.1006994. eCollection 2018 Apr.

Szretter KJ, Daniels BP, Cho H, Gainey MD, Yokoyama WM, Gale M Jr, Virgin HW, Klein RS, Sen GC, Diamond MS. 2'-O methylation of the viral mRNA cap by West Nile virus evades ifit1-dependent and -independent mechanisms of host restriction in vivo. PLoS Pathog. 2012;8(5):e1002698. doi: 10.1371/journal.ppat.1002698. Epub 2012 May 10.

Takahashi K, Tanabe K, Ohnuki M, Narita M, Ichisaka T, Tomoda K, Yamanaka S. Induction of pluripotent stem cells from adult human fibroblasts by defined factors. Cell. 2007 Nov 30;131(5):861-72.

Talbot, N. C., Sparks, W. O., Powell, A. M., Kahl, S. & Caperna, T. J. Quantitative and semiquantitative immunoassay of growth factors and cytokines in the conditioned medium of STO and CF-1 mouse feeder cells. In vitro cellular & developmental biology. Animal. 48, 1–11, https://doi.org/10.1007/s11626-011-9467-7 (2012).

Teng TS, Foo SS, Simamarta D, Lum FM, Teo TH, Lulla A, Yeo NK, Koh EG, Chow A, Leo YS, Merits A, Chin KC, Ng LF. Viperin restricts chikungunya virus replication and pathology. J Clin Invest. 2012 Dec;122(12):4447-60. doi: 10.1172/JCI63120. Epub 2012 Nov 19.

The International HIV Controllers Study. The major genetic determinants of HIV-1 control affect HLA class I peptide presentation. Science 330, 1551–1557 (2010).

Thornik Reimer, Matthias Schweizer and Thomas W. Jungi. Type I IFN Induction in Response to Listeria monocytogenes in Human Macrophages: Evidence for a Differential Activation of IFN Regulatory Factor 3 (IRF3). J Immunol July 15, 2007, 179 (2) 1166-1177; DOI: https://doi.org/10.4049/jimmunol.179.2.1166

Thornton GK, Woods CG. Primary microcephaly: do all roads lead to Rome? Trends Genet. 2009 Nov;25(11):501-10. doi: 10.1016/j.tig.2009.09.011. Epub 2009 Oct 21.

Thurmond S, Wang B, Song J, Hai R. Suppression of Type I Interferon Signaling by Flavivirus NS5. Viruses. 2018 Dec 14;10(12). pii: E712. doi: 10.3390/v10120712.

Trevisan M, Sinigaglia A, Desole G, Berto A, Pacenti M, Palù G,5, Barzon L. Modeling Viral Infectious Diseases and Development of Antiviral Therapies Using Human Induced Pluripotent Stem Cell-Derived Systems. Viruses. 2015 Jul 13;7(7):3835-56. doi: 10.3390/v7072800.

Tsai TF, Popovici F, Cernescu C, Campbell GL, Nedelcu NI. West Nile encephalitis epidemic in southeastern Romania. Lancet. 1998 Sep 5;352(9130):767-71.

Tsetsarkin KA, Vanlandingham DL, McGee CE, Higgs S. A single mutation in chikungunya virus affects vector specificity and epidemic potential. PLoS Pathog. 2007 Dec;3(12):e201.

Tu YF, Tsai YS, Wang LW, Wu HC, Huang CC, Ho CJ. Overweight worsens apoptosis, neuroinflammation and blood-brain barrier damage after hypoxic ischemia in neonatal brain through JNK hyperactivation. J Neuroinflammation. 2011 Apr 25;8:40. doi: 10.1186/1742-2094-8-40.

Urbanowski MD, Hobman TC. The West Nile virus capsid protein blocks apoptosis through a phosphatidylinositol 3-kinase-dependent mechanism. J Virol. 2013 Jan;87(2):872-81. doi: 10.1128/JVI.02030-12. Epub 2012 Oct 31.

Van Dijk EL, Auger H, Jaszczyszyn Y, Thermes C. Ten years of next-generation sequencing technology. Trends Genet. 2014 Sep;30(9):418-26. doi: 10.1016/j.tig.2014.07.001. Epub 2014 Aug 6.

Velandia-Romero ML, Calderón-Peláez MA, Castellanos JE. In Vitro Infection with Dengue Virus Induces Changes in the Structure and Function of the Mouse Brain Endothelium. PLoS One. 2016 Jun 23;11(6):e0157786. doi: 10.1371/journal.pone.0157786. eCollection 2016.

Villa-Diaz, L. G., Ross, A. M., Lahann, J. & Krebsbach, P. H. Concise review: The evolution of human pluripotent stem cell culture: from feeder cells to synthetic coatings. Stem cells. 31, 1–7, https://doi.org/10.1002/stem.1260 (2013).

Villordo SM, Carballeda JM, Filomatori CV, Gamarnik AV. RNA Structure Duplications and Flavivirus Host Adaptation. Trends Microbiol. 2016 Apr;24(4):270-283. doi: 10.1016/j.tim.2016.01.002. Epub 2016 Feb 3.

Wade CM, Kulbokas EJ 3rd, Kirby AW, Zody MC, Mullikin JC, Lander ES, Lindblad-Toh K, Daly MJ. The mosaic structure of variation in the laboratory mouse genome. Nature. 2002 Dec 5;420(6915):574-8.

Wang A, Thurmond S, Islas L, Hui K, Hai R. Zika virus genome biology and molecular pathogenesis. Emerg Microbes Infect. 2017 Mar 22;6(3):e13. doi: 10.1038/emi.2016.141.

Wang T, Fikrig E. Immunity to West Nile virus. Curr Opin Immunol. 2004 Aug;16(4):519-23.

Wang T, Town T, Alexopoulou L, Anderson JF, Fikrig E, Flavell RA. Toll-like receptor 3 mediates West Nile virus entry into the brain causing lethal encephalitis. Nat Med. 2004 Dec;10(12):1366-73. Epub 2004 Nov 21.

Weaver SC, Reisen WK. Present and future arboviral threats. Antiviral Res. 2010 Feb;85(2):328-45. doi: 10.1016/j.antiviral.2009.10.008. Epub 2009 Oct 24.

Webster LT. MICROBIC VIRULENCE AND HOST SUSCEPTIBILITY IN MOUSE TYPHOID INFECTION. J Exp Med. 1923 Jan 31;37(2):231-68.

Webster Marketon JI, Corry J, Teng MN. The respiratory syncytial virus (RSV) nonstructural proteins mediate RSV suppression of glucocorticoid receptor transactivation. Virology. 2014 Jan 20;449:62-9. doi: 10.1016/j.virol.2013.11.014. Epub 2013 Nov 26.

Weissenböck H, Bakonyi T, Rossi G, Mani P, Nowotny N. Usutu virus, Italy, 1996. Emerg Infect Dis. 2013 Feb;19(2):274-7. doi: 10.3201/eid1902.121191.

Weissenböck H, Kolodziejek J, Url A, Lussy H, Rebel-Bauder B, Nowotny N. Emergence of Usutu virus, an African mosquito-borne flavivirus of the Japanese encephalitis virus group, central Europe. Emerg Infect Dis. 2002 Jul;8(7):652-6.

Welte T, Reagan K, Fang H, Machain-Williams C, Zheng X, Mendell N, Chang GJ, Wu P, Blair CD, Wang T. Toll-like receptor 7-induced immune response to cutaneous West Nile virus infection. J Gen Virol. 2009 Nov;90(Pt 11):2660-8. doi: 10.1099/vir.0.011783-0. Epub 2009 Jul 29.

Wilder-Smith A, Gubler DJ, Weaver SC, Monath TP, Heymann DL, Scott TW. Epidemic arboviral diseases: priorities for research and public health. Lancet Infect Dis. 2017 Mar;17(3):e101-e106. doi: 10.1016/S1473-3099(16)30518-7. Epub 2016 Dec 21.

Wilson JR, de Sessions PF, Leon MA, Scholle F. West Nile virus nonstructural protein 1 inhibits TLR3 signal transduction. J Virol. 2008 Sep;82(17):8262-71. doi: 10.1128/JVI.00226-08. Epub 2008 Jun 18.

Wu SJ, Grouard-Vogel G, Sun W, Mascola JR, Brachtel E, Putvatana R, Louder MK, Filgueira L, Marovich MA, Wong HK, Blauvelt A, Murphy GS, Robb ML, Innes BL, Birx DL, Hayes CG, Frankel SS. Human skin Langerhans cells are targets of dengue virus infection. Nat Med. 2000 Jul;6(7):816-20.

Wu X, Dao Thi VL, Huang Y, Billerbeck E, Saha D, Hoffmann HH, Wang Y, Silva LAV, Sarbanes S, Sun T, Andrus L, Yu Y, Quirk C, Li M, MacDonald MR, Schneider WM, An X, Rosenberg BR, Rice CM. Intrinsic Immunity Shapes Viral Resistance of Stem Cells. Cell. 2018 Jan 25;172(3):423-438.e25. doi: 10.1016/j.cell.2017.11.018. Epub 2017 Dec 14.

Xu, C. et al. Feeder-free growth of undifferentiated human embryonic stem cells. Nature biotechnology. 19, 971–974, https://doi. org/10.1038/nbt1001-971 (2001).

Yakub I, Lillibridge KM, Moran A, Gonzalez OY, Belmont J, Gibbs RA, Tweardy DJ. Single nucleotide polymorphisms in genes for 2'-5'-oligoadenylate synthetase and RNase L inpatients hospitalized with West Nile virus infection. J Infect Dis. 2005 Nov 15;192(10):1741-8. Epub 2005 Oct 12.

Yang, W., Mills, J.A., Sullivan, S., Liu, Y., French, D.L., Gadue, P. iPSC Reprogramming from Human Peripheral Blood Using Sendai Virus Mediated Gene Transfer. StemBook [Internet]; 2012 Jun 10.

Yu J, Vodyanik MA, Smuga-Otto K, Antosiewicz-Bourget J, Frane JL, Tian S, Nie J, Jonsdottir GA, Ruotti V, Stewart R, Slukvin II, Thomson JA. Induced pluripotent stem cell lines derived from human somatic cells. Science. 2007 Dec 21;318(5858):1917-20. Epub 2007 Nov 20.

Yu L, Nomaguchi M, Padmanabhan R, Markoff L. Specific requirements for elements of the 5' and 3' terminal regions in flavivirus RNA synthesis and viral replication. Virology. 2008 Apr 25;374(1):170-85. doi: 10.1016/j.virol.2007.12.035. Epub 2008 Jan 29.

Yudin NS, Barkhash AV, Maksimov VN, Ignatieva EV, Romaschenko AG. Human Genetic Predisposition to Diseases Caused by Viruses from Flaviviridae Family. Mol Biol (Mosk). 2018 Mar-Apr;52(2):190-209. doi: 10.7868/S0026898418020039

Yugen Zhang, Laxmi Yeruva, Anthony Marinov, Daniel Prantner, Priscilla B. Wyrick, Vladimir Lupashin and Uma M. Nagarajan. The DNA Sensor, Cyclic GMP–AMP Synthase, Is Essential for Induction of IFN-β during Chlamydia trachomatis Infection. J Immunol September 1, 2014, 193 (5) 2394-2404; DOI: https://doi.org/10.4049/jimmunol.1302718

Yuki N. Infectious origins of, and molecular mimicry in, Guillain-Barré and Fisher syndromes. Lancet Infect Dis. 2001 Aug;1(1):29-37.

Yu-Lin Hsu, Mei-Yi Wang, Ling-Jun Ho and Jenn-Haung Laia. Dengue virus infection induces interferon-lambda1 to facilitate cell migration. Sci Rep. 2016; 6: 24530. Published online 2016 Jul 26. doi: 10.1038/srep24530

Yu-Lin Hsu, Shao-Fu Shi, Wan-Lin Wu, Ling-Jun Ho, Jenn-Haung Lai. Protective Roles of Interferon-Induced Protein with Tetratricopeptide Repeats 3 (IFIT3) in Dengue Virus Infection of Human Lung Epithelial Cells. PLoS One. 2013 Nov 4;8(11):e79518. doi: 10.1371/journal.pone.0079518. eCollection 2013.

Yunfei Qin, Qingxiang Li, Shuo Tian, Weihong Xie Jun Cui and Rong-Fu Wang. TRIM9 short isoform preferentially promotes DNA and RNA virus-induced production of type I interferon by recruiting GSK3β to TBK1. Cell Res. 2016 May; 26(5): 613–628. Published online 2016 Feb 26. doi: 10.1038/cr.2016.27

Zannoli S, Sambri V. West Nile Virus and Usutu Virus Co-Circulation in Europe: Epidemiology and Implications. Microorganisms. 2019 Jun 26;7(7). pii: E184. doi: 10.3390/microorganisms7070184.

Zarraga IG, Zhang L, Stump MR, Gong Q, Vincent GM, Zhou Z. Nonsense-mediated mRNA decay caused by a frameshift mutation in a large kindred of type 2 long QT syndrome. Heart Rhythm. 2011 Aug;8(8):1200-6. doi: 10.1016/j.hrthm.2011.03.039. Epub 2011 Mar 15.

Zhang HL, Ye HQ, Liu SQ, Deng CL, Li XD, Shi PY, Zhang B. West Nile Virus NS1 Antagonizes Interferon Beta Production by Targeting RIG-I and MDA5. J Virol. 2017 Aug 24;91(18). pii: e02396-16. doi: 10.1128/JVI.02396-16. Print 2017 Sep 15.

Zhang Q, Davis JC, Lamborn IT, Freeman AF, Jing H, Favreau AJ, Matthews HF, Davis J, Turner ML, Uzel G, Holland SM, Su HC. Combined immunodeficiency associated with DOCK8 mutations. N Engl J Med. 2009;361:2046–2055. doi: 10.1056/NEJMoa0905506.

Zhang SY, Herman M, Ciancanelli MJ, Pérez de Diego R, Sancho-Shimizu V, Abel L, Casanova JL. TLR3 immunity to infection in mice and humans. Curr Opin Immunol. 2013 Feb;25(1):19-33. doi: 10.1016/j.coi.2012.11.001. Epub 2013 Jan 3.

Zhang SY, Jouanguy E, Ugolini S, Smahi A, Elain G, Romero P, Segal D, Sancho-Shimizu V, Lorenzo L, Puel A, Picard C, Chapgier A, Plancoulaine S, Titeux M, Cognet C, von Bernuth H, Ku CL, Casrouge A, Zhang XX, Barreiro L, Leonard J, Hamilton C, Lebon P, Héron B, Vallée L, Quintana-Murci L, Hovnanian A, Rozenberg F, Vivier E, Geissmann F, Tardieu M, Abel L, Casanova JL. TLR3 deficiency in patients with herpes simplex encephalitis. Science. 2007 Sep 14;317(5844):1522-7.

Zong C, Kimura Y, Kinoshita K, Takasu S, Zhang X, Sakurai T, Sekido Y, Ichihara S, Endo G, Ichihara G. Exposure to 1,2-Dichloropropane Upregulates the Expression of Activation-Induced Cytidine Deaminase (AID) in Human Cholangiocytes Co-Cultured With Macrophages. Toxicol Sci. 2019 Mar 1;168(1):137-148. doi: 10.1093/toxsci/kfy280.